SUPPORTING INFORMATION for

Modeling the Atmospheric Transport and Deposition of PCDD/F to the Great Lakes

Mark D. Cohen*, Roland R. Draxler, Richard Artz
NOAA Air Resources Laboratory, Silver Spring MD

Barry Commoner, Paul Bartlett, Paul Cooney, Kim Couchot, Alan Dickar, Holger Eisl, Catherine Hill, James Quigley, Joyce E. Rosenthal[1]
Center for the Biology of Natural Systems, Queens College, Flushing, NY

David Niemi, Dominique Ratté, Marc Deslauriers
Pollution Data Branch, Environment Canada, Hull, Quebec, Canada

Rachelle Laurin
Ontario Ministry of the Environment, Toronto, Ontario, Canada

Larissa Mathewson-Brake
Ontario Ministry of Natural Resources, Peterborough, Ontario, Canada

John McDonald
International Joint Commission, Windsor, Ontario, Canada

---

* Corresponding Author:
NOAA Air Resources Laboratory
1315 East West Highway
Room 3316, R/ARL
Silver Spring, MD, 20910, USA
mark.cohen@noaa.gov
301-713-0295 x122
fax: 301-713-0119

1. Current Affiliation: Division of Environmental Health Sciences, Mailman School of Public Health, Columbia University

(This supporting information is 99 pages long, and contains 55 (+1) figures, and 4 tables.)

Table of Contents

List of Tables in Supplementary Information

List of Figures in Supplementary Information

10. A. Effect of the maximum number of puffs allowed in the simulation on the 1996 deposition to the Great Lakes arising from a hypothetical, continuous source of 2378-TCDD at San Francisco, California. The default maximum was 1000 puffs.

10. B. Effect of the puff emissions frequency on the 1996 deposition to the Great Lakes arising from a hypothetical, continuous source of 2378-TCDD near the center of the modeling domain. The default emissions frequency was 1 puff every 7 hours.

11. Effect of the source height on the 1996 deposition to the Great Lakes arising from a hypothetical, continuous source of 2378-TCDD at Milwaukee, Wisconsin, on the shore of Lake Michigan. The default source height was 50 meters.

12. Summary of sensitivity analyses for factors other than the dry deposition methodology or emissions (see text for abbreviations).

13. Deposition amount and flux of 23478 PeCDF in successive, concentric, annular 200-km-radius-increment regions away from a continuous 1996 year-long source at the center of the modeling domain. The deposition amount has been divided by the total amount emitted in the simulation to give the fraction of the emissions deposited in any given concentric region. The deposition flux for each region has been normalized to correspond to an emissions rate of 1 gram/year.

14. Deposition amount and flux of 2378 TCDF in successive, concentric, annular 200-km-radius-increment regions away from a continuous 1996 year-long source at the center of the modeling domain. The deposition amount has been divided by the total amount emitted in the simulation to give the fraction of the emissions deposited in any given concentric region. The deposition flux for each region has been normalized to correspond to an emissions rate of 1 gram/year.

15. Deposition amount and flux of OCDD in successive, concentric, annular 200-km-radius-increment regions away from a continuous 1996 year-long source at the center of the modeling domain. The deposition amount has been divided by the total amount emitted in the simulation to give the fraction of the emissions deposited in any given concentric region. The deposition flux for each region has been normalized to correspond to an emissions rate of 1 gram/year.

16. Average congener emissions profile for the entire U.S./Canadian dioxin emissions inventory (used for making transfer coefficient example maps in Figure 9 of the main body of the paper).

17. Relative contribution of the seventeen 2,3,7,8-substituted PCDD/F congeners to the overall model-predicted deposition to Lake Superior.

18. Relative contribution of the seventeen 2378-substituted PCDD/F congeners to the overall model-predicted deposition to Lake Michigan.

19. Relative contribution of the seventeen 2378-substituted PCDD/F congeners to the overall model-predicted deposition to Lake Huron.

20. Relative contribution of the seventeen 2378-substituted PCDD/F congeners to the overall model-predicted deposition to Lake Erie.

21. Relative contribution of the seventeen 2378-substituted PCDD/F congeners to the overall model-predicted deposition to Lake Ontario.

22. Comparison of model predictions with 2-day ambient measurements of total PCDD/F (TEQ) at rural and semi-rural locations in Canada.

23. Comparison of model predictions with ambient measurements at month-long sample sites: TCDD.

24. Comparison of model predictions with ambient measurements at month-long sample sites: PeCDD.

25. Comparison of model predictions with ambient measurements at month-long sample sites: HxCDD.

26. Comparison of model predictions with ambient measurements at month-long sample sites: HpCDD.

27. Comparison of model predictions with ambient measurements at month-long sample sites: OCDD.

28. Comparison of model predictions with ambient measurements at month-long sample sites: TCDF.

29. Comparison of model predictions with ambient measurements at month-long sample sites: PeCDF.

30. Comparison of model predictions with ambient measurements at month-long sample sites: HxCDF.

31. Comparison of model predictions with ambient measurements at month-long sample sites: HpCDF.

32. Comparison of model predictions with ambient measurements at month-long sample sites: OCDF.

33. Errors associated with different interpolation schemes in predicting explicitly simulated transfer coefficients to the Great Lakes.

34. Influence of different spatial interpolation methodologies on the total estimated 1996

dioxin deposition to the Great Lakes (g TEQ/year).

35. Effect of fate simulation variations on total predicted deposition of PCDD/F to the Great Lakes.

36. Effect of fate simulation variations on the relative dioxin contributions of different source sectors to Lake Huron

37. Mid-range estimate of the contributions to 1996 atmospheric deposition of dioxin to Lake Michigan.

38. Mid-range estimate of the contributions to 1996 atmospheric deposition of dioxin to Lake Huron.

39. Mid-range estimate of the contributions to 1996 atmospheric deposition of dioxin to Lake Erie.

40. Mid-range estimate of the contributions to 1996 atmospheric deposition of dioxin to Lake Ontario.

41. Percent of total 1996 emissions and deposition of dioxin arising from within different distance ranges from Lake Huron.

42. Percent of total 1996 emissions and deposition of dioxin arising from within different distance ranges from Lake Erie.

43. Percent of total 1996 emissions and deposition of dioxin arising from within different distance ranges from Lake Ontario.

44. Percent of total 1996 emissions and deposition of dioxin arising from within different distance ranges from each of the Great Lakes.

45. 1996 air emissions and atmospheric deposition contributions to the Great Lakes from within and outside the overall Great Lakes watershed from air emissions sources in the United States and Canada.

46. Fraction of estimated 1996 PCDD/F atmospheric deposition contributions to Lake Michigan from U.S. and Canadian sources arising from different source categories.

47. Fraction of estimated 1996 PCDD/F atmospheric deposition contributions to Lake Huron from U.S. and Canadian sources arising from different source categories.

48. Fraction of estimated 1996 PCDD/F atmospheric deposition contributions to Lake Erie from U.S. and Canadian sources arising from different source categories.

49. Fraction of estimated 1996 PCDD/F atmospheric deposition contributions to Lake

Ontario from U.S. and Canadian sources arising from different source categories.

50. Contribution of different source sectors to atmospheric deposition of dioxin in the Great Lakes [(pg TEQ deposition / km2) / (person - year)]. Each country's annual deposition flux contribution amount normalized by their total population; "incin" = waste incineration; "metals" = metallurgical processing; "fuel" = fuel combustion.

51. Model-estimated total 1996 deposition for different PCDD/F homologue groups to Lake Superior.

52. Model-estimated total 1996 deposition for different PCDD/F homologue groups to Lake Michigan.

53. Model-estimated total 1996 deposition for different PCDD/F homologue groups to Lake Huron.

54. Model-estimated total 1996 deposition for different PCDD/F homologue groups to Lake Erie.

55. Model-estimated total 1996 deposition for different PCDD/F homologue groups to Lake Ontario.

1. Emissions Inventory

Table 2 of the main paper gives a summary of a comparison between the inventory used in this modeling work, and two recent U.S. EPA inventories for atmospheric emissions of PCDD/F. In Table 1 below, a more detailed comparison is provided.

Table 1. Comparison of Different U.S. Atmospheric PCDD/F Emissions Inventories

Source Category	1996: This Study			1995 EPA (Sept 2000 version)			1995 EPA (April 1998 version)			
	g TEQ/yr			g TEQ/yr for these Confidence Ratings		Con-fidence Rating	g TEQ/yr			Con-fidence Rating
	lower	central	higher	A,B,C	D		lower	central	higher	
WASTE INCINERATION	**588**	**1861**	**5884**	**1768**	**< 1**		**648**	**1589 + *0.1***	**3998**	
Municipal Waste Incin	404	1278	4040	1250		B	492	1100	2460	H/M
Tire Combustion				0.11		C	~ 0	~ 0	~ 0	M/L
Hazardous Waste Incin	7.2	22.7	72	5.8		B	2.6	5.7	12.8	H/M
Boilers/Industrial Furnaces				0.39		C	0.12	0.38	1.2	M/L
Medical Waste/Pathological Incin	171	541	1710	488		C	151	477	1510	L/L
Crematoria				9.1		C	0.07	0.24	0.75	H/L
Sewage Sludge Incin	3.7	11.8	37.4	14.8		B	2.7	6.0	13.4	H/M
Pulp and Paper Mill Sludge Incin	2.4	7.8	24.8	Included in Industrial Wood Combustion			Included in Industrial Wood Combustion			
Biogas Combustion	not included				< 1	D	~ 0.1 (very uncertain)			

Source Category	Table 1. Comparison of Different U.S. Atmospheric PCDD/F Emissions Inventories									
	1996: This Study			1995 EPA (Sept 2000 version)			1995 EPA (April 1998 version)			
	g TEQ/yr			g TEQ/yr for these Confidence Ratings		Con-fidence Rating	g TEQ/yr			Con-fidence Rating
	lower	central	higher	A,B,C	D		lower	central	higher	
POWER / ENERGY GENERATION	**54**	**172**	**542**	**202**	**76**		**81**	**214 + *20***	**581**	
Vehicle Fuel Combustion										
Leaded	not included			2.0		C	not included			
Unleaded	1.8	5.6	17.8	5.6		C	2.0	6.3	20	H/L
Diesel	17.6	55.5	175	33.5		C	10.6	33.5	106	H/L
Wood Combustion										
Residential	21.7	68.7	217	62.8		C	19.8	62.8	198	H/L
Industrial	a			27.6		B	13.0	29.1	65.0	H/M
Coal Combustion:										
Utility Boilers	12.5	39.5	125	60.1		B	32.6	72.8	163	H/M
Residential	not included				30	D	Residential: ~ 10 (very uncertain) (Industrial included in Utility Category above)			
Commercial/Industrial	not included				40	D				
Oil Combustion										
Industrial/Utility	not included			10.7		C	2.9	9.3	29.0	H/L
Residential	0.75	2.4	7.5		6	D	~ 10			Very uncertain

Source Category	Table 1. Comparison of Different U.S. Atmospheric PCDD/F Emissions Inventories									
	1996: This Study			1995 EPA (Sept 2000 version)			1995 EPA (April 1998 version)			
	g TEQ/yr			g TEQ/yr for these Confidence Ratings		Con-fidence Rating	g TEQ/yr			Con-fidence Rating
	lower	central	higher	A,B,C	D		lower	central	higher	
OTHER HIGH TEMPERATURE SOURCES	**137**	**433**	**1368**	**183**	**7**		**55**	**174 + *10***	**548**	
Cement Kilns Burning Hazardous Waste	131	413	1306	156.1		C	48.4	153	484	H/M
Lightweight Aggregate Kilns Burning Hazardous Waste				3.3		C				
Cement Kilns (non hazardous waste burning)	5.5	17.3	54.6	17.8		C	5.6	17.8	56.3	H/L
Asphalt Mixing Plants	not included				7	D	~ 10 (very uncertain)			
Petroleum Refining Catalyst Generation	not included			2.21		C	not included			
Cigarette Combustion	not included			0.8		C	0.25	0.81	2.5	H/L
Carbon Reactivation Furnaces	not included			0.08		C	~ 0	~ 0	~ 0	
Kraft Recovery Boilers	0.71	2.23	7.1	2.3		B	1.0	2.3	5.0	H/M

Source Category		Table 1. Comparison of Different U.S. Atmospheric PCDD/F Emissions Inventories									
		1996: This Study			1995 EPA (Sept 2000 version)			1995 EPA (April 1998 version)			
		g TEQ/yr			g TEQ/yr for these Confidence Ratings		Con-fidence Rating	g TEQ/yr			Con-fidence Rating
		lower	central	higher	A,B,C	D		lower	central	higher	
MINIMALLY CONTROLLED OR UNCONTROLLED COMBUSTION		**71**	**225**	**713**	**628**	**1257**		**65**	**208 + *2020***	**645**	
	Backyard Barrel burning	71	225	713	628		C	~ 1000 (very uncertain)			
	Combustion of Landfill Gas	not included				7	D	~ 10 (very uncertain)			
	Landfill Fires	not included				1000	D	~ 1000 (very uncertain)			
	Accidental Fires: Structural	not included				> 20	D	not included			
	Accidental Fires: Vehicles	not included				30	D	~ 10 (very uncertain)			
	Forest and Brush Fires	not included				200	D	64.5	208	645	L/L

Table 1. Comparison of Different U.S. Atmospheric PCDD/F Emissions Inventories

Source Category	1996: This Study			1995 EPA (Sept 2000 version)			1995 EPA (April 1998 version)			
	g TEQ/yr			g TEQ/yr for these Confidence Ratings		Con-fidence Rating	g TEQ/yr			Con-fidence Rating
	lower	central	higher	A,B,C	D		lower	central	higher	
METALLURGICAL PROCESSES	**188**	**596**	**1900**	**330**	**82**		**177**	**560 + *130***	**1767**	
Ferrous Metal Smelting and Refining										
Sintering Plants	89	281	887	28		B	~ 100 (very uncertain)			
Coke Production	not included				7	D	~ 10 (very uncertain)			
Electric Arc Furnaces	6.2	21.7	76		40	D	~ 10 (very uncertain)			
Foundries	0.04	0.4	12.8		20	D	~ 10 (very uncertain)			
Non-Ferrous Metal Smelting/Refining										
Primary Copper	not included			0.5		B	not included			
Secondary Aluminum	28	89	282	29.1		C	5.4	17.0	53.8	H/L
Secondary Copper Smelters	63	198	625	271		C	171	541	1710	H/L
Secondary Copper Refiners	1.8	5.6	17.8				not included			
Secondary Lead	not included			1.72		B	0.73	1.63	3.65	M/M
Primary Magnesium	not included				15	D	not included			
Drum and Barrel Reclamation	not included			0.08		C	not included			

Source Category	Table 1. Comparison of Different U.S. Atmospheric PCDD/F Emissions Inventories									
	1996: This Study			1995 EPA (Sept 2000 version)			1995 EPA (April 1998 version)			
	g TEQ/yr			g TEQ/yr for these Confidence Ratings		Con-fidence Rating	g TEQ/yr			Con-fidence Rating
	lower	central	higher	A,B,C	D		lower	central	higher	
CHEMICAL MANUFACTURING / PROCESSING SOURCES	**0**	**0**	**0**	**11.2**			**0**	**0**	**0**	
Ethylene Dichloride / Vinyl Chloride	not included			11.2		B	not included			

Source Category	Table 1. Comparison of Different U.S. Atmospheric PCDD/F Emissions Inventories									
	1996: This Study			1995 EPA (Sept 2000 version)			1995 EPA (April 1998 version)			
	g TEQ/yr			g TEQ/yr for these Confidence Ratings		Con-fidence Rating	g TEQ/yr			Con-fidence Rating
	lower	central	higher	A,B,C	D		lower	central	higher	
"Quantified Sources"	**1039**	**3286**	**10408**	**3111**			**1026**	**2745**	**7539**	
Sources too uncertain to "include" in main inventory but for which order of magnitude estimates have been made					***1434***			***2180***		
Total Emissions in Inventory	**1038**	**3286**	**10407**	***4546***				***4925***		

a. Some industrial wood combustion included in Hazardous Waste Incineration; and industrial wood combustion in Pulp/Paper Mill Sludge and Wood Residue Incineration (included by EPA in industrial wood combustion category) was included as its own category.

EPA REPORTS serving as sources for the above data:

USEPA, *The Inventory of Sources of Dioxin in the United States*. External Review Draft. EPA/600/P-98/002Aa, April 1998, Office of Research & Development, Washington D.C., April, 1998

USEPA. *Exposure and Human Health Reassessment of 2,3,7,8-TCDD and Related Compounds. Part 1: Estimating Exposure to Dioxin-Like Compounds. Vol. II: Sources of Dioxin-Like Compounds in the United States*. Draft Final Report. EPA/600/P-00/001Bb, Office of Research & Development, Washington D.C., September, 2000.

2. Modeling Single Congeners from Single Sources

A. Vapor-Particle Partitioning Formulation

We used the conventional Junge (1977) formulation of the vapor/particle phenomenon:

$$F_p = c\ S_t / (p(T) + cS_t) \quad (1)$$

in which F_p is the fraction of the total mass of the species absorbed to the particle phase (dimensionless), S_t is the total surface area of particles, per unit volume of air (cm^2/cm^3), p(T) = the saturation vapor pressure of the species of interest (atm), at the ambient temperature (T), and c is an empirical constant, estimated by Junge to be approximately 1.7×10^{-4} atm-cm.

While the most thermodynamically stable form of all PCDD/F's at ambient temperatures is a solid, we have followed the suggestion of Bidleman (1988) in using the "non-equilibrium" or subcooled liquid phase as that which is relevant to the equilibrium partitioning of such compounds between the vapor phase and the atmospheric aerosol. This subcooled liquid vapor pressure is related to the solid's vapor pressure by:

$$\ln (P_l/P_s) = \Delta S_f\ (T_m - T) / RT \quad (2)$$

in which P_l is the subcooled liquid vapor pressure (atm) at temperature T, P_s = solid vapor pressure (atm) at temperature T, ΔS_f is the entropy of fusion (atm m^3/mole deg K) (approximately equal to 6.79 R), T_m is the melting temperature of the solid compound (deg K), T is the ambient temperature (deg K), and R is the gas constant (atm m^3/mole deg K) (Bidleman, 1988). An alternative approach to estimate the subcooled vapor pressure is that suggested by Hites, based on gas-chromatography retention times (Hites, 1998, and references therein). The solid vapor pressure at the temperature of interest can be estimated from the reported solid vapor pressure at a standard temperature with the Clausius-Clapeyron equation using the enthalpy of vaporization, according to the following equation:

$$\ln (P^s_1 / P^s_2) = (\Delta H / R)\ (1/T_2 - 1/T_1) \quad (3)$$

in which P^s_1 is the solid vapor pressure (atm) at temperature T_1, P^s_2 is the solid vapor pressure (atm) at temperature T_2, ΔH is the enthalpy of vaporization (J/mole), R is the gas constant (J/mole degK [=] (atm m^3/mole deg K), T_2 is temperature 1 (deg K), and $T_1$is temperature 2 (deg K). With Trouton's Rule, the enthalpy of vaporization can be approximately estimated by the following relation: $\Delta H / T_{boil}$ = 84 J/(mol degK) (MacKay *et al.*, 1986).

Atmospheric PCDD/F has been assumed to be "exchangable", i.e., that it is freely exchanged between the vapor and particle phases. To the extent that a portion of the material was "locked-up" within particles and was not available for exchange, this assumption would be in error. There is some experimental evidence which suggests that atmospheric PCDD/F is exchangeable. Eitzer and Hites (1989ab) measured the amounts of vapor-phase and particulate-phase PCDD/F in the atmosphere of Bloomington, Indiana and found that while there was no temperature-related effect on the total concentration of PCDD/F in the atmosphere, the

proportions in the two phases were dependent on the ambient temperature at the time of the measurement. Furthermore, in agreement with theory, it was found that the vapor/particle partitioning of each of the congeners was, in general, critically dependent on each congener's subcooled liquid vapor pressure (Eitzer and Hites, 1989b).

Example calculations of the estimated vapor/particle partitioning characteristics of selected PCDD/F congeners are presented in Figure 1. The aerosol surface area used in these calculations is 3.5e-06 cm2/cm3, equivalent to "Background + Local Sources" (Bidleman, 1988).

Thibodeaux and coworkers (1991) have extended the adsorption-based theory of vapor/particle partitioning of semivolatile organic compounds (SOC) to include the effect of the competition of water vapor for adsorption sites on an atmospheric particle before deliquesence. The effect of moisture was shown to reduce the fraction of the SOC that is predicted to be adsorbed to atmospheric particles. However, the effect of moisture on the vapor/particle partitioning behavior of atmospheric PCDD/F was not considered in this modeling.

B. Physical-Chemical Properties Used in Modeling.

In Table 2, below, the relevant, available physical-chemical properties of selected PCDD/F congeners are presented, based primarily on data compiled from Mackay and coworkers (1992) and the U.S. EPA (1994).

Figure 1. Estimated vapor/particle partitioning characteristics of selected PCDD/F congeners

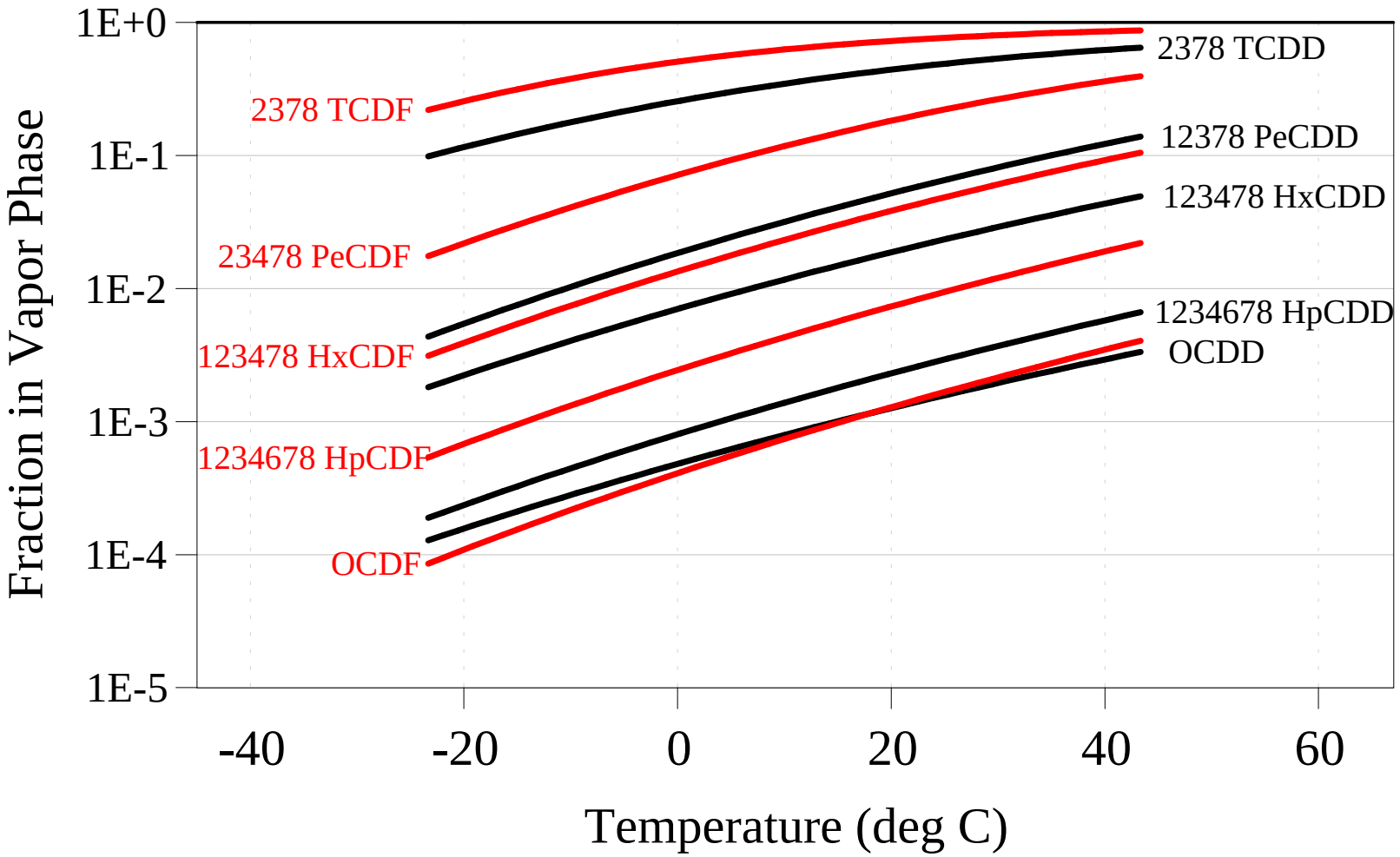

The aerosol surface area used in these calculations is 3.5e-06 cm2/cm3, equivalent to "Background + Local Sources".

Table 2. Physical-Chemical Properties of PCDD/F

congener	cas	code	vapor pressure (Pa) at 298.15 K		T_{melt} (^oK)	T_{boil} (^oK)	henry's law (atm m3/mol)	*	fracpart 290 under "medium" conditions (g)	OH rxn rate at 298.15 ^oK (cm3/ molec-sec) (h)	TEF WHO humans/ mammals (i)
2378 TCDD	001746-01-6	tcdd	9.9E-008	b	578.15	719.65	3.3E-005	a	58.8%	2.0E-012	1
12378 PeCDD	040321-76-4	5D01	8.8E-008	a	468.15	737.85	2.6E-006	c	95.5%	1.7E-012	1
123478 HxCDD	039227-28-6	6D01	5.1E-009	a	546.15	760.85	1.1E-005	a	98.4%	1.2E-012	0.1
123678 HxCDD	057653-85-7	6D02	5.1E-009	a	546.15	760.85	1.1E-005	d	98.4%	1.4E-012	0.1
123789 HxCDD	019408-74-3	6D03	5.1E-009	a	546.15	760.85	1.1E-005	d	98.4%	1.4E-012	0.1
1234678 HpCDD	035822-46-9	7D01	7.5E-010	a	538.15	780.35	1.3E-005	a	99.8%	9.2E-013	0.01
OCDD	003268-87-9	OCDD	1.1E-010	a	595.15	783.15	6.8E-006	a	99.9%	4.2E-013	0.0001
2378 TCDF	051207-31-9	tcdf	2.0E-006	a	500.15	711.45	1.4E-005	a	30.2%	1.6E-013	0.1
12378 PeCDF	057117-41-6	5F01	3.5E-007	a	469.15	737.85	5.0E-006	e	84.0%	7.5E-014	0.05
23478 PeCDF	057117-31-4	pcdf	3.5E-007	a	469.15	737.85	5.0E-006	a	84.0%	7.5E-014	0.5
123478 HxCDF	070648-26-9	6F01	3.2E-008	a	498.65	760.85	1.4E-005	a	96.7%	3.0E-013	0.1
123678 HxCDF	057117-44-9	6F02	3.5E-008	a	505.15	760.85	7.3E-006	a	95.8%	3.6E-013	0.1
123789 HxCDF	072918-21-9	6F03	3.4E-008	a	501.90	760.85	1.1E-005	f	96.3%	3.4E-014	0.1
234678 HxCDF	060851-34-5	6F04	3.4E-008	a	501.90	760.85	1.1E-005	f	96.3%	3.0E-013	0.1
1234678 HpCDF	067562-39-4	7F01	4.7E-009	a	509.15	780.35	1.4E-005	a	99.4%	1.5E-014	0.01
1234789 HpCDF	055673-89-7	7F02	6.2E-009	a	494.15	780.35	1.4E-005	a	99.4%	1.5E-014	0.01
OCDF	039001-02-0	OCDF	5.0E-010	a	531.15	810.15	1.9E-006	a	99.9%	6.9E-015	0.0001

NOTES:

* Reference for Tmelt, Tboil, and Henry's Law Constant; a. Mackay (1992); b. USEPA (1994); c. Using value for 12347 PeCDD; d. Using value for 123478 HxCDD; e. Using value for 23478 PeCDF; f. Using average of values for 123478 HxCDF and 123678 HxCDF; g. fraction estimated to be associated with particles at 290 K, aerosol surface area = 3.5×10^{-6} cm^2/cm^2 air;
h. Estimated from AOPWIN (Meylan and Howard, 1993, 1996ab); i. Van den Berg *et al.*, 1998.

C. Particle Size Distribution and Particle Concentration

A typical particle size distribution was chosen, corresponding to the average distribution found in a comprehensive 1969 study of Pasadena, California aerosol (Whitby, 1975). Figure 2 shows the properties of this size distribution.

Assuming the above particle size distribution consists of spherical particles with a density of 2 g/cm^3 , the selected surface area of $3.5x10^{-6}$ cm^2/cm^3 is equivalent to an atmospheric particulate mass concentration of 39 $\mu g/m^3$. About 90% of the mass of the above distribution has a diameter of less than 10 μm; i.e., the PM-10 concentration associated with the above distribution and concentration is approximately 35 $\mu g/m^3$. This is an overestimate, as many actual aerosol particles are likely to have a somewhat higher surface area than a hypothetical spherical particle of equivalent mass. Consistent with this, the model value is comparable to but slightly higher than the average measured values in the U.S. in 1996: the average PM-10 concentration measured at 119 rural sites was 19 $\mu g/m^3$, while the average measured at 760 urban and suburban sites was 26 $\mu g/m^3$ (USEPA 1988).

A sensitivity analysis was performed in which the particle size distribution was kept constant, but, the overall particle concentration was varied over a factor of ten on either side of the nominal value used. As can be seen in Figure 3, the influence of this variation was minimal on the model-estimated transfer coefficients for 2378-TCDD from a test source location (near the center of the modeling domain, at latitude = 40 and longitude = 95) to each of the Great Lakes. The particle concentration was varied over two orders of magnitude, and the model estimated deposition varied only by about a factor of two. It would seem that for atmospheric PCDD/F, it is important to capture the essential vapor/particle partitioning phenomena, and its associated effects on pollutant transformation and deposition – as has been attempted in a simplified way here – but, it may not be as important to know the precise details of the atmospheric particulate.

Figure 2. Particle Size Distribution Used in Modeling

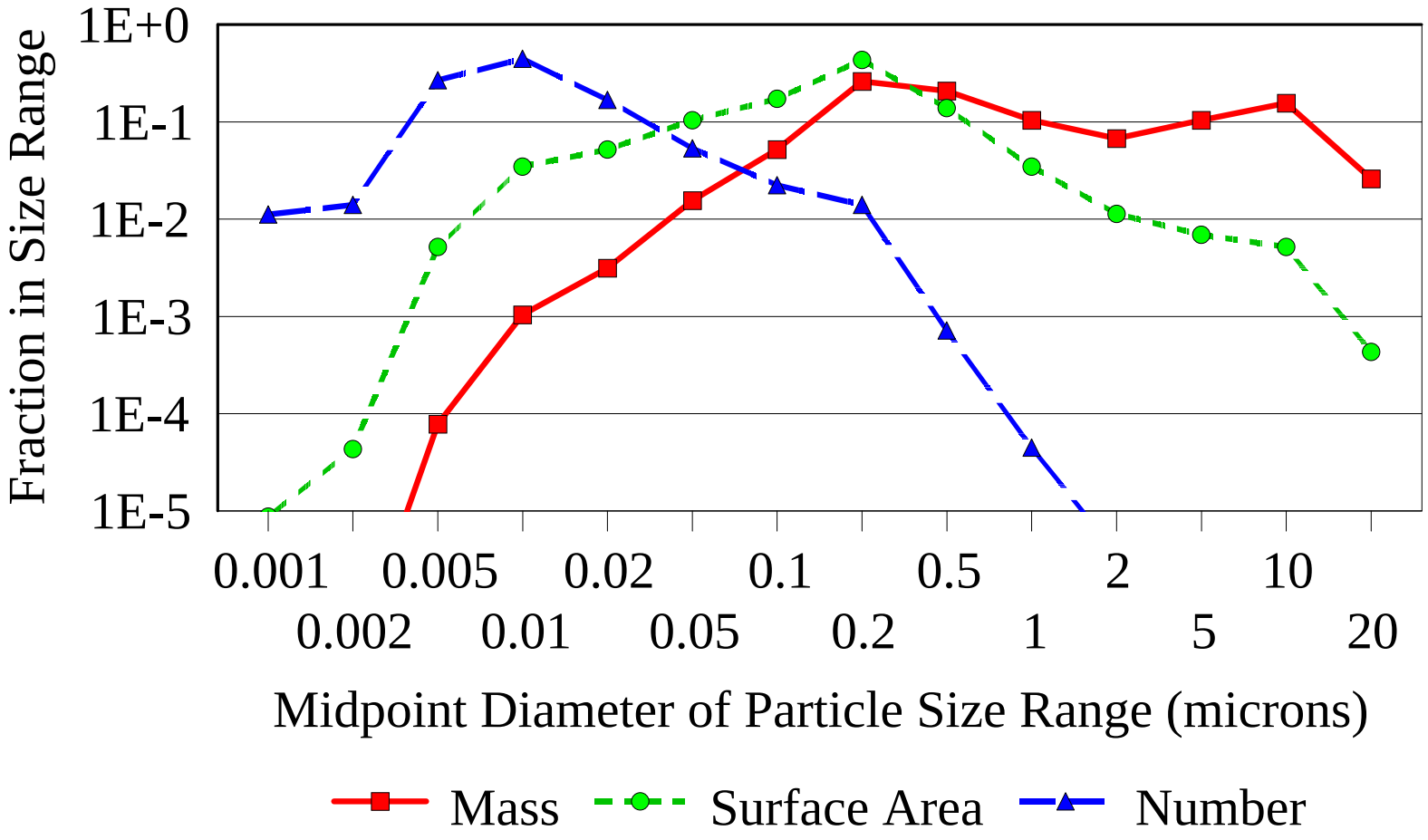

Figure 3. Example of Results of Particle Concentration Sensitivity Analysis
(Continuous Year Long Source of 2,3,7,8-TCDD at Center of Modeling Domain)

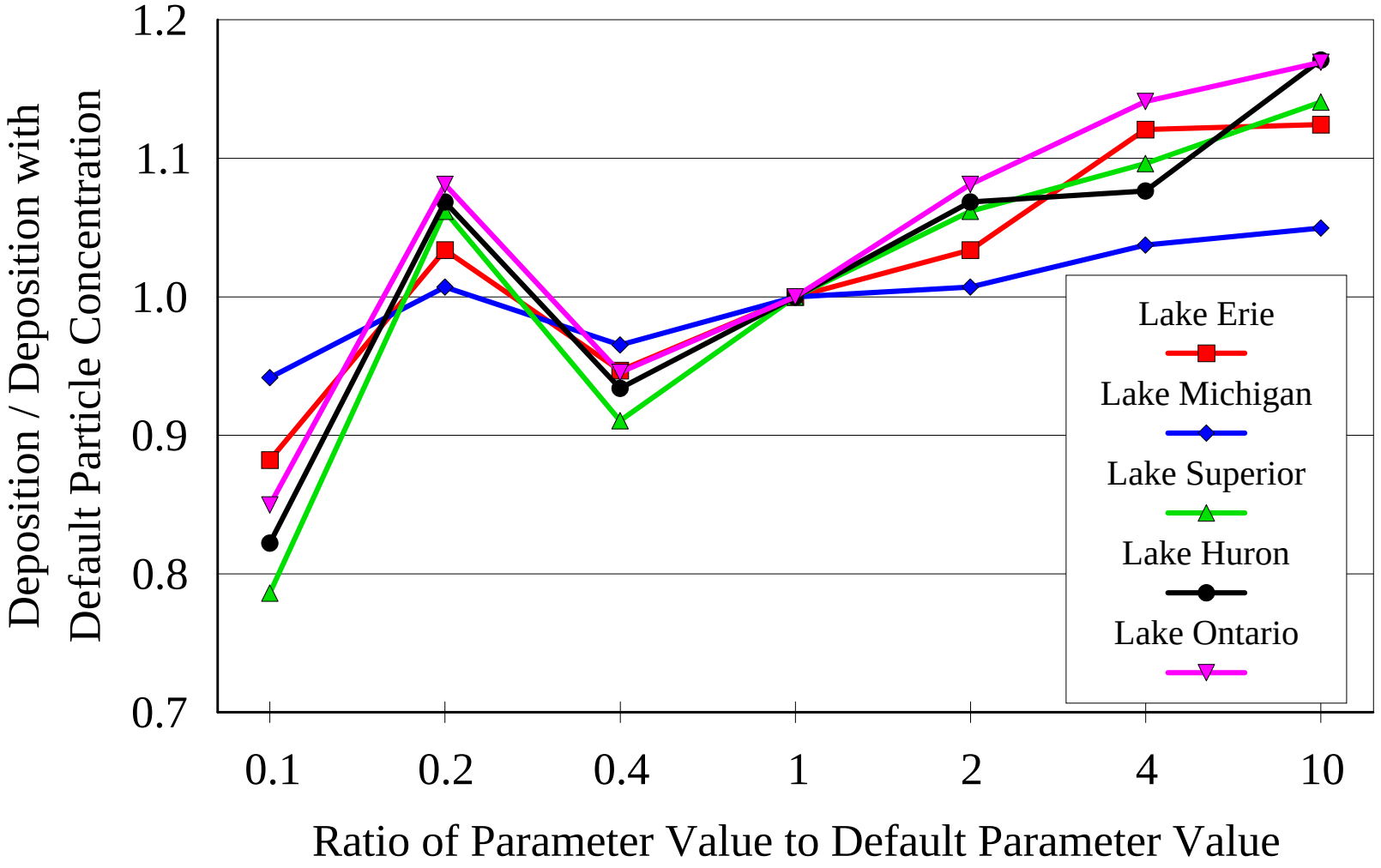

D. Photolysis

There is a great deal of uncertainty regarding the rate of photolysis of atmospheric PCDD/F congeners. Based on the experimental results of Koester and Hites (1992a) and others, it is generally believed that photolysis of particle-associated PCDD/F in the atmosphere is an insignificant loss process. Unfortunately, there appear to be no measurements of vapor-phase photolysis under typical atmospheric conditions, due to the difficulty of making such measurements for PCDD/F.

Significant levels of solar radiation at wavelengths less than about 300 nm do not generally reach the lower atmosphere or the earth surface due to absorption in the atmosphere, and the flux between ~300-320 nm is relatively low due to absorption by ozone. The UV absorption characteristics of the three most volatile 2378-substituted congeners – 2378-TCDD (Crosby *et al.*, 1973), 2378-TCDF, and 2,3,4,7,8-PeCDF (Tysklind *et al.*, 1993) – all show a maximum absorbence at ~300 nm with a broad peak that has dropped off dramatically by ~320 nm. Thus, the overlap of these congeners of wavelengths at which significant absorption occurs and those at which significant radiation is present in the lower troposphere is relatively small. This would suggest that photolysis of these compounds would be somewhat limited. In addition to this inherent limitation, a significant portion of even these more volatile congeners is expected to associated with the particle phase in the atmosphere at any given time, and would thus – as noted above – be much less vulnerable to photolytic transformation (Koester and Hites, 1992a).

Atkinson and coworkers (Atkinson, 1991; Kwok *et al.*, 1994, 1995) have considered available theoretical and experimental evidence and have suggested that photolysis (a) *may* be somewhat important for vapor-phase tetrachloro-dibenzo-p-dioxins (TCDD's), although less important than reaction with hydroxyl radical; (b) is probably not important for pentachloro-dibenzo-p-dioxins (PeCDD's); and (c) because OH radical reactions are predicted to be slower with PCDF's than with PCDD's, photolysis may be relatively more important for PCDF's.

Kwok and co-workers investigated the gas-phase atmospheric chemistry of dibenzo-p-dioxin and dibenzofuran (the unchlorinated, parent molecules of PCDD/F) (1994) and 1-chlorodibenzo-*p*-dioxin (1995). Under the spectral and light-intensity conditions used in this work, no evidence of gas-phase photolysis was found. However, the light source used in these experiments had a different spectral intensity than solar irradiation , and thus these results may not be directly relevant to ambient conditions (Atkinson *et al.*, 1989). Photolysis rates for different PCDD/F congeners appear to decrease, generally, with increasing numbers of chlorines (Sivils et al., 1994; Choudry and Webster, 1989), and so, photolysis of tetra-octa CDD/F's would also expected to be relatively insignificant, based on these findings.

There have a been a number of studies of PCDD/F photolysis in organic solvents and water, but the results of these studies cannot be directly extrapolated to the atmosphere due to the involvement of the solvent itself in the photolytic process. Moreover, photolysis of PCDD/F in solution can vary dramatically depending on the solvent used (Dung *et al.*, 1994). For example, 2378-TCDD photolyzes much faster than 1234-TCDD in a n-Hexadecane solution (Nestrick *et al.*, 1980), but, 2378-TCDD appears to degrade much slower than 1234-TCDD in the vapor phase (Sivils *et al.*, 1994).

Sivils and coworkers (1995) found that photolysis in the gas phase occurred more easily for compounds with chlorines in the *peri* position. For compounds with no chlorines in the *peri* position, e.g., 2378-TCDD, vapor-phase photolysis was relatively slow.

Given a lack of data, it is difficult to make quantitative estimates of the half-lives of vapor-phase PCDD/F molecules with respect to photolysis. Based on experimental measurements, Dulin and colleagues (1986) estimated the half-life of 2378-TCDD *in water* to be on the order of 4-5 days in the summer at a 40^{o} latitude. These results are relatively consistent with the estimates of Choudry and Webster (1989) for aquatic 1237-TCDD (~ 2 days in summer; annual average ~ 9 days). As noted above, extrapolation of solution-phase photolysis rates to the vapor phase is not straightforward, as the processes occurring in solution can be dramatically different than photolytic phenomena in the vapor phase. Nevertheless, as assumed by Atkinson (1991), the vapor-phase half-life of 2378-TCDD relative to photolysis *may* be similar to that in the aqueous phase; if so, the rate of photolytic destruction of vapor-phase 2378-TCDD would be of the same order as the destruction due to reaction with hydroxyl radical.

Because detailed information on the wavelength-dependent vapor-phase absorption cross-sections and quantum efficiencies for vapor-phase photolysis are not known for PCDD/F congeners, it is not possible to predict the rate of photolytic destruction or chemical reaction of a vapor-phase PCDD/F congener at any given location in the atmosphere with great accuracy at the present time, *even* if details about the concentrations of reactants and electromagnetic spectrum were known at that location.

In the simulations performed here, a maximum photolysis rate corresponding to a half-life of 2 days was used for any PCDD/F congener in the vapor phase, and a maximum rate corresponding to a 10-day half-life was used for congeners in the particle phase. In the simulations, the photolysis rate at any given time and location was estimated by assuming the rate was proportional to the surface radiation intensity. In this estimation procedure, the maximum decay rate was multiplied by the ratio of the model-estimated surface radiation flux to that of the maximum surface-level solar flux.

A series of sensitivity simulations were performed to investigate the influence of variations in the assumed photolysis rate on the fate and transport of PCDD/F congeners. Of the 17 toxic 2378-substituted congeners, the largest effects were seen with 2378-TCDF and 2378-TCDD, an expected result given the greater tendency of these congeners to exist in the vapor phase. An example of these results for 2378-TCDD is shown in Figure 4, for a continuous year-long release from the center of the modeling domain. It can be seen for variations of this vapor-phase half-life of up to a factor of 10 on either side of the default value – e.g., the maximum rate was changed from a value corresponding to a half-life of 0.2 days to 20 days – the changes in the estimated deposition to the Great Lakes is less than a factor of 2. Thus even though this phenomenon is very uncertain, the overall effect of this uncertainty on the model-predicted deposition appears to be relatively small.

Figure 4. Example of Results of Vapor-Phase Photolysis Sensitivity Analysis
(Continuous Year Long Source of 2,3,7,8-TCDD at Center of Modeling Domain)

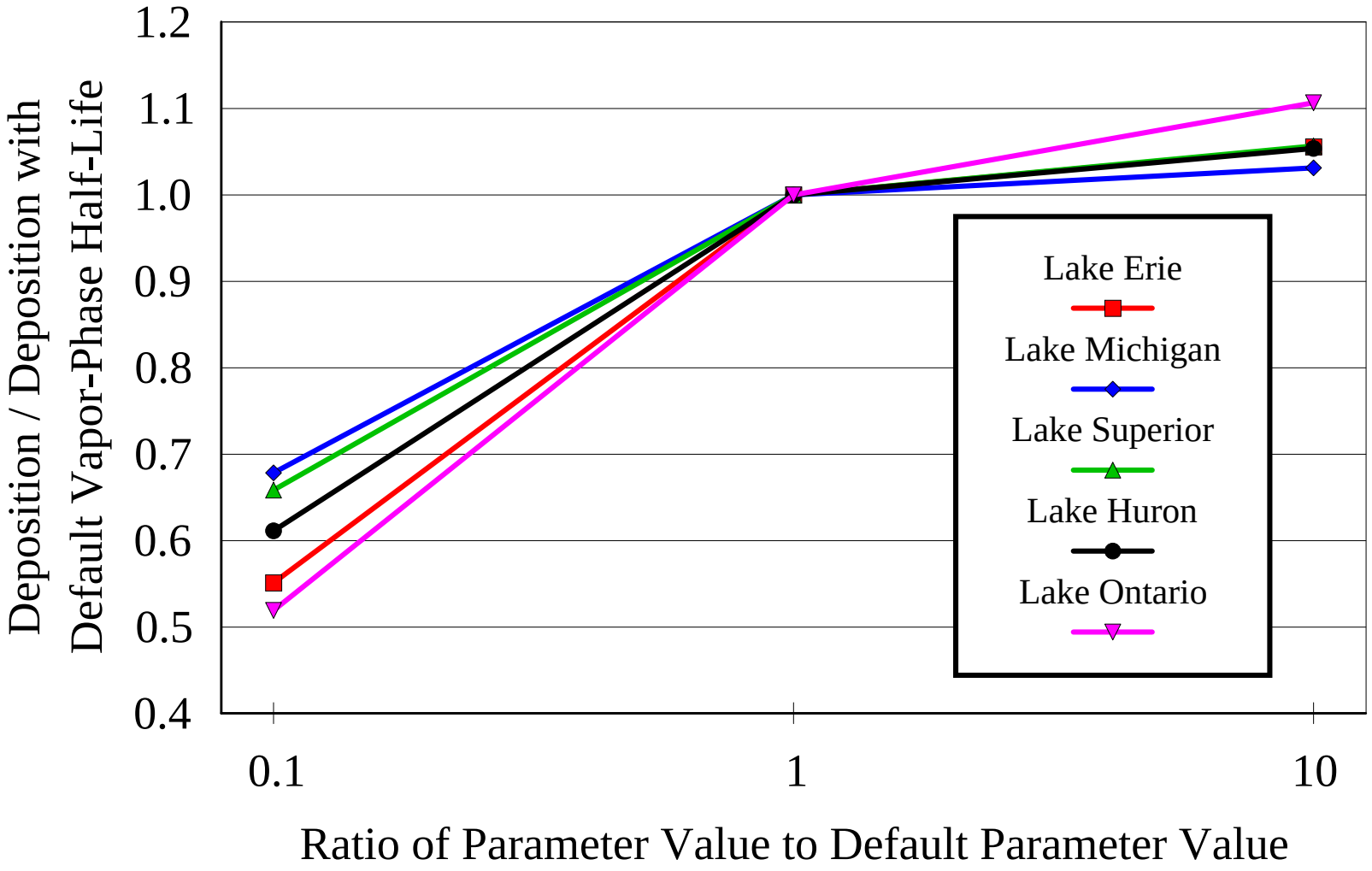

E. Dry Deposition

In this modeling analysis, the dry deposition of vapor-phase and particle-phase pollutant is estimated as the product of a deposition velocity and the relevant atmospheric concentration [e.g., (m sec^{-1}) (g m^{-3}) = g m^{-2} sec^{-1}]. The deposition velocity is generally characterized as being inversely related to various "resistances" to mass transfer that tend to retard the deposition, following the general formulation of Hicks and colleagues (1987):

$$V_d = [R_a + R_b + R_c + R_a R_b V_g]^{-1} + V_g \quad (4)$$

in which R_a is the aerodynamic resistance to mass transfer of gases and particles, R_b is the resistance of the quasi-laminar sublayer, R_c is the resistance of the "canopy" layer, i.e., the overall resistance at the ground, reflecting the characteristics of a particular land-surface, and V_g is the gravitational settling velocity (zero for gases).

Because the air motion must essentially stop at any immobile surface, there is generally a small layer of air, the *quasi-laminar sublayer*, with minimal turbulence near any such surface. Turbulent diffusion is assumed to be negligible in this layer, and consequently, movement of gases and particles can be somewhat limited. The resistance to deposition due to this layer, R_b, is often characterized as the sum of the following two factors: a diffusional component – applicable to both particles and gases – and an impaction component for particles. There is substantial convergence in the literature on the most appropriate way to characterize R_b for gases, but there are significant differences in the way that this resistance is characterized for particles, especially for deposition to water surfaces.

The method used here is essentially that used the *HYSPLIT_4* modeling system (Draxler and Hess, 1997). However, a few modifications were made to this system for the purposes of this simulation, and these changes will be briefly described. First, for dry deposition of particles and gases to water surfaces, the approach of Slinn and Slinn (1980) was used. In this methodology, the deposition resistance in the quasi-laminar sublayer over water is relatively significant. A methodology with such a characteristic was selected based on the recent experimental results of Larsen and colleagues (1995). In the use of this method, we have used the following near-surface particle- growth estimation approach (Williams, 1982), assuming 99% humidity in the surface layer, in which D_p is the diameter of the particle above the surface layer:

$$D_p^{\text{surface layer}} = 4.5\ D_p^{\ 1.04} \quad (5)$$

In a second modification, the formulation for R_b for deposition of particles to land surfaces has been changed to the following, based on the approach of Slinn (1977):

$$R_b^{-1} = 0.5\ \kappa\ u_* \left(Sc^{-0.67} + 10^{\ -3/St}\right) \quad (6)$$

where κ is Von Karman's constant (~0.4), u_* is the friction velocity, the Schmidt Number *Sc*, is the ratio of the kinematic viscosity of air (γ) to the particle diffusivity. The Stokes Number *St* in equation 6 is defined as $St = V_g\ u_*^2 / g\ \gamma$, where *g* is the acceleration of gravity.

The *HYSPLIT_4* model uses the canopy resistance formulation of Wesely (1989), as originally presented in conjunction with the Regional Acid Deposition Model (Chang, 1990), and this formulation has been used in this analysis. In the use of this method, a value of the surface reactivity parameter f_o must be chosen for every gaseous species being modeled. In an effort to evaluate the most likely value of f_o for PCDD/F, we compared the model's deposition velocity predictions for gaseous deposition to vegetation with the experimental results for 2378-TCDD of McCrady and colleagues (1993, 1994). This experiment was not designed to develop estimates of f_o, and so there is significant uncertainty in the use of these results for this purpose. Nevertheless, it appeared that the experimental results could only be matched with this dry deposition formulation if the surface reactivity was set to a high value (~ 1). We had initially assumed that f_o would be relatively low for PCDD/F, reflecting the relative *chemical* inertness of PCDD/F in comparison with gases such as ozone. We interpret this finding as being reflective of the ability of PCDD/F to be adsorbed into plant tissue. In the lack of any other additional data that could be used for screening purposes such as that above, we used a value of $f_o = 1$ for all surfaces for PCDD/F, reasoning that gaseous PCDD/F would be relatively "sticky" to many surfaces.

In addition, the Wesely algorithm utilizes a series of scaling resistances, based on measurements of the dry deposition of sulfur dioxide and ozone. In some cases the scaling resistances are set to very high values ("9999"), to indicate that a particular pathway for deposition is to be ignored. It was found that because many of the physical chemical properties of PCDD/F are somewhat different than those for sulfur dioxide and ozone, these high "cut-off" resistance values had to be increased by many orders of magnitude so that the particular pathways were indeed cut off.

Given that the overall objective of this project was the estimation of loading of PCDD/F to the Great Lakes, it was important to ensure that the estimation methodology used for prediction of dry deposition to water surfaces was reasonable. Empirical estimation methods for vapor-phase transfer of organics to water surfaces have been recently reviewed (Schwarzenbach *et al.*, 1993) and used for the modeling of PCB vapor transfer to Lakes Michigan (Achman *et al.*, 1993) and Superior (Hornbuckle *et al.*, 1994). Georgi (1986) presented a methodology for modeling particle and vapor-phase dry deposition to a range of surfaces, including water bodies. These approaches – applied to PCDD/F – were compared to the estimates of the methodology used here, and the various methods gave very similar results.

As described in the main body of this paper, the dry deposition of vapor-phase PCDD/F to land and water surfaces has been assumed to be uni-directional, i.e., revolatilization (the so-called *grasshopper* effect) is not considered to be a significant. A brief description of the terrestrial issue is given there. With deposition to water bodies, PCDD/F is believed to partition overwhelmingly to suspended matter (which slowly sinks to the bottom). This makes it generally unavailable for revolatilization – the revolatilization process from water depends on (un-ionized) molecules that are freely dissolved. Thus, it is generally believed that essentially all of the PCDD/F deposited to water bodies ends up in the sediment, and deposition rates to water bodies are frequently estimated by analyzing sediments (e.g., Cleverly et al., 1996).

F. Alternative Dry Deposition Methods.

There is substantial uncertainty in the estimation of the dry deposition of vapor and particle phase pollutants, including PCDD/F, and different approaches can give rather disparate estimates. In light of this, a variety of approaches were used in this analysis, and the results were compared in order to evaluate the influence of this uncertainty on the overall fate and transport simulation.

Six different dry deposition systems were examined, including the default method described above, as summarized in Table 3. The hygroscopic growth correction is very approximate, as different types of particles will have different hygroscopic characteristics, and, equilibrium water uptake may not always be achieved due to mass transfer limitations (Zufall *et al.*, 1998). Because of this uncertainty, method *A′* was examined to see the influence of this factor on the overall modeling results. Method *B* was that used in earlier modeling work for dioxin (Cohen *et al.*, 1995, 1997; Commoner *et al.*, 1998) and atrazine (Cohen *et al.*, 1997). A recent study (Scire *et al.*, 1993) found that method *C*, based on the formulation in the Acid Deposition and Oxidant Model (ADOM), appeared to be the algorithm which most closely matched the experimental observations for particle deposition to land surfaces, although the study did not examine particle deposition to water surfaces or gaseous deposition. In method *C*, the quasi-laminar sublayer resistance for small particles depositing to terrestrial surfaces is relatively insignificant – due to a different functional dependence on the Stokes number – and thus, the predicted deposition velocities are significantly greater than in methods *A* or *B*. Method *D* utilizes the methodology proposed by Williams (1982) for particles depositing to water bodies. Finally, method *E* is the that currently used in the basic version of *HYSPLIT_4*, when the resistance-based dry deposition calculation is invoked (Draxler and Hess, 1997). In this methodology, it is assumed that there is essentially no quasi-laminar sublayer near a water surface, because of the continual disturbances of the surface, and thus that the resistance to small particle deposition due to this layer is not significant. Method E also utilizes a different functional dependence on the Stokes number in the formulation of particle deposition to land and vegetative surfaces, based on the work of Peters and Eiden (1992), and the importance of the sublayer resistance is greater than that for method *C* but less than that for method *A* or *B*.

Each of the above methodologies was used to simulate the fate and transport of continuous emissions of 2378-TCDD and OCDD for 1996 from hypothetical sources in Milwaukee, WI, the center of the modeling domain, and San Francisco, CA to deposition in Lake Michigan. This set of simulations was chosen to examine a range of congener physical-chemical properties, and a range of relative proximity to a given lake – Milwaukee is on the shore; the center of the modeling domain is 650 km from the lake, and San Francisco is about 3000 km from the lake. As an example of the results of these simulations, the deposition to Lake Michigan relative to the default simulation value is shown in Figure 5. It can be seen that there is little difference between method *A′* and the default method. Methods *B* and *D* give results within about 50% (and in most cases within 20%) of the default methodology, while methods *C* and *E* give somewhat more disparate relative depositions. The increase relative deposition to the lake with method *E* would be expected given the low quasi-laminar sublayer resistance assumed with this method.

In Figure 6, the effect of dry deposition methodology on the fraction of emissions of 2,3,7,8-TCDD accounted for in different fate pathways is shown

Table 3. Alternative Dry Deposition Methodologies Used in this Modeling Analysis

Dry Deposition Method		Water Surfaces		Land or Vegetative Surfaces	
		Particles	Vapor	Particles	Vapor
		(if no entry in table, then use of default methodology is implied)			
A	default				
A′	default with no RH correction	no correction for hygroscopic growth of particle near water surface			
B	modified HYSPLIT_3 resistance methodology	Same as A for land/vegetative surfaces, except that exponent on *Sc* in R_b formulation is -0.5, instead of -0.67			
C	ADOM-II for particles	same as B, with addition of 0.01 cm/sec phoretic velocity component	same as B	different functional dependence on *St* in R_b formulation; addition of 0.01 cm/sec phoretic velocity component; exponent on *Sc*: - 0.5 for z0 < 10cm, and -0.7 for z0 > 10 cm	
D	Williams (1982) for particles depositing to water	Williams (1982)	same as B		
E	HYSPLIT_4 resistance methodology	similar to B, except that R_b set to 10 sec/m (a relatively low value)	same as B	a different functional dependence on *St* in R_b formulation	essentially the same as A

Figure 5. Variations in simulated 1996 deposition of 2,3,7,8-TCDD and OCDD to Lake Michigan with alternative dry deposition methodologies. "TCDD" = 2,3,7,8-TCDD; "Milw" indicates source in Milwaukee, WI; "center" indicates source at center of modeling domain; "SF" indicates source in San Francisco, CA.

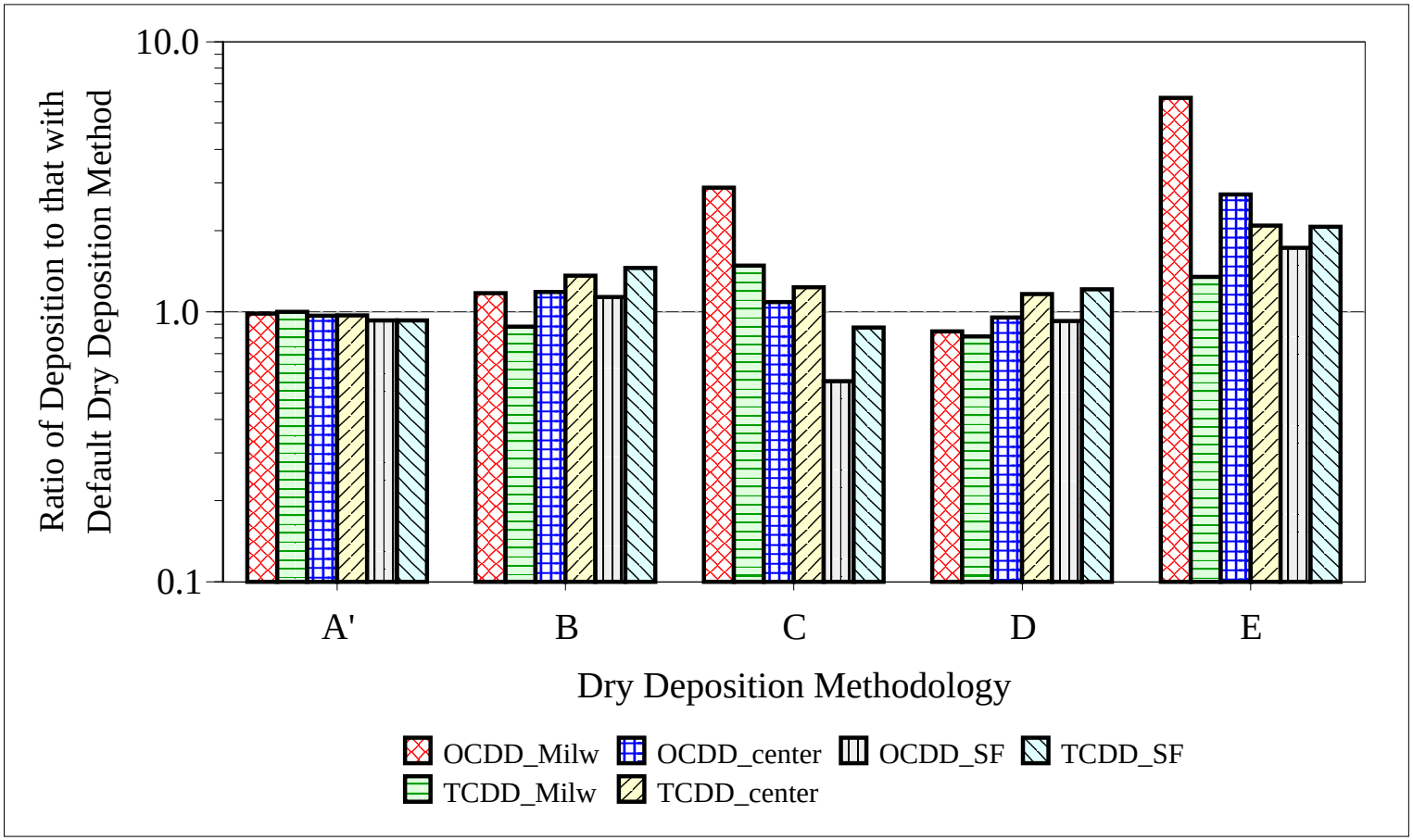

Figure 6. Effect of dry deposition methodology on the fraction of emissions 2,3,7,8-TCDD accounted for in different fate pathways anywhere in the modeling domain for a year-long continuous source near the center of the domain.

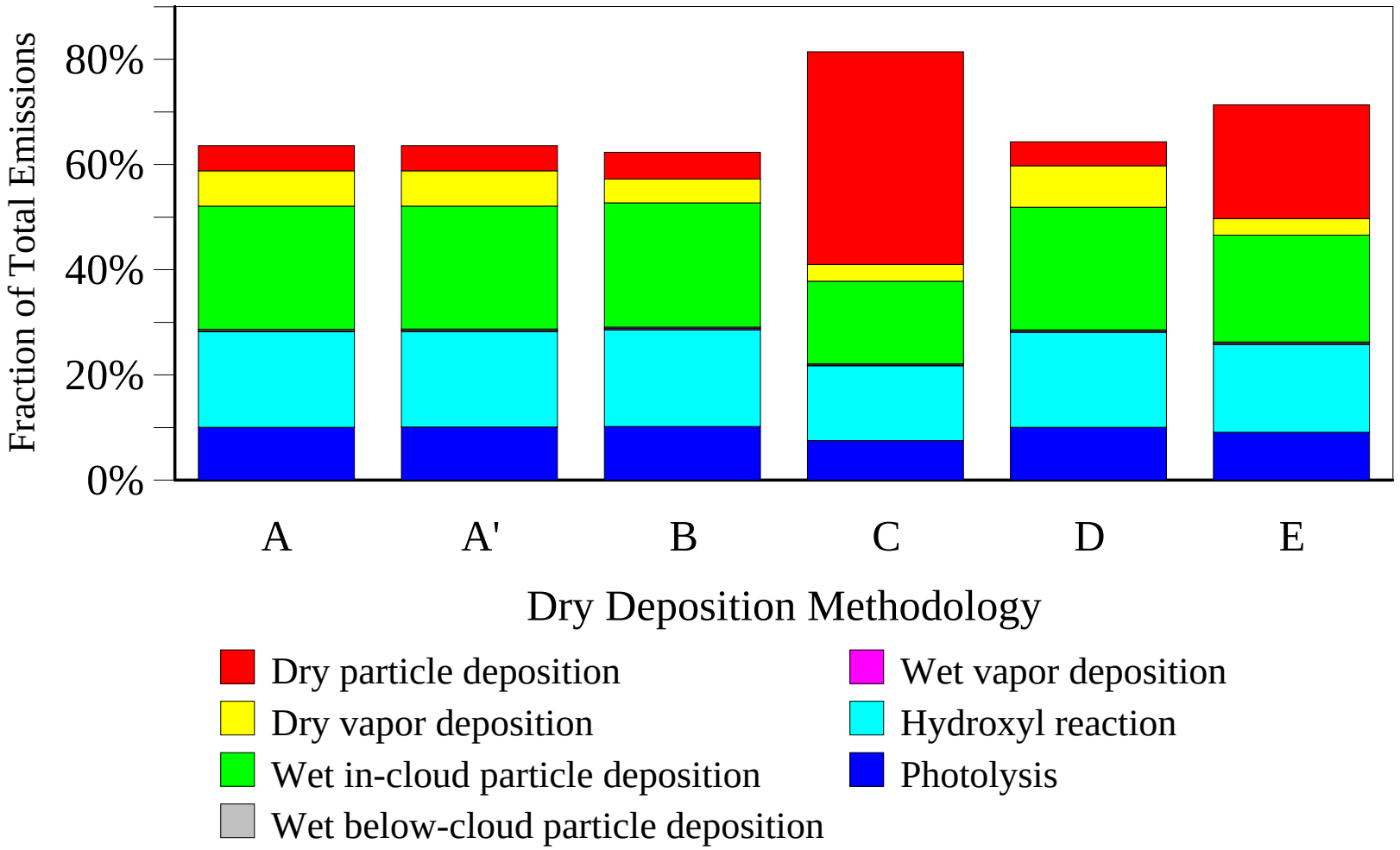

G. Wet Deposition

Wet deposition in the *HYSPLIT* model is simulated as three different phenomena: (a) in-cloud particle washout; (b) below-cloud particle scavenging; and (c) vapor-phase wet deposition, based on the review by Hicks (1986). In the simulations performed here, using a comparable methodology to that utilized in the regular *HYSPLIT* model (Draxler and Hess, 1997), below-cloud particle scavenging was an insignificant removal mechanism. Similarly, vapor-phase wet deposition was insignificant for all PCDD/F congeners simulated, due to the very low water solubility of these compounds. In the interest of brevity, therefore, these mechanisms will not be discussed further here. However, in-cloud particle washout was found to be an important fate process, and will be discussed briefly here.

Measurement-based studies of a variety of particle-associated inorganic pollutants have yielded volume-based washout ratios (units of grams of pollutant per m^3 of precipitation/ grams of pollutant per m^3 of air) on the order of 80,000 - 800,000, with an average value of about 320,000 (Lindberg, 1982). All particle-based pollutants would presumably exhibit the same washout ratio, although differences arise because of different pollutant-specific particle size distributions and particle thermodynamic characteristics. It is likely that the rain-out phenomenon is too complex to be characterized by a single washout ratio. There is strong evidence, for example, that the in-cloud rainout must depend at least on the intensity and duration of the precipitation (Tsai et al., 1991). A parameterization of this type was used, for example, by Voldner and Schroeder (1989) in their modeling of the wet deposition of toxaphene during long-range atmospheric transport to the Great Lakes. However, given the uncertainty in the rainfall intensity characterization in the meteorological data that were used in this study, it was decided that a simple washout ratio approach was a reasonable approximation.

There are no direct measurement of PCDD/F in-cloud particle washout. However, Eitzer and Hites (1989) reported measurements of PCDD/F in the atmosphere of Bloomington, IN, and Koester and Hites (1992b) reported on measurements of PCDD/F in the atmosphere of Bloomington and Indianapolis, IN. These studies measured atmospheric concentrations of both vapor-phase and particle-associated PCDD/F, and, both particle-associated and dissolved PCDD/F in rain water. From the particle-associated concentrations in air and rain water, a particle-phase washout ratio can be estimated. The washout ratios estimated from these data are presented in Figure 7.

It should be noted that these washout ratios do not correspond directly to the washout ratio in the *HYSPLIT* model formulation. First, these measured washout ratios include both in-cloud and below-cloud scavenging of particles, and so, they are overestimates of the value for in-cloud scavenging alone. Below-cloud scavenging of particles is generally considered a less efficient removal process, and so this factor is not believed to be overly significant. Second, the air measurements were taken at essentially ground level, and may not be representative of the air concentrations of PCDD/F in the rain cloud. Finally, the measured washout ratios are estimates from long-term average concentrations in air and rain, and the averaging period for the air concentrations is different from that of the rain concentrations.

Nevertheless, based on these data, we chose a value of 40,000 for the washout ratio for in-cloud scavenging of particle-associated atmospheric PCDD/F in this modeling. This is somewhat less than the "default" value used in *HYSPLIT* for particle-bound pollutants, as discussed above. Obviously, the value of this parameter is highly uncertain, and there is clearly a need for additional measurements. In light of this, this phenomenon was the subject of numerous sensitivity analyses throughout this study. As an example, the influence of variations in this parameter on the simulated deposition to Lake Michigan is presented in Figure 8. It can be seen that even though the parameter was varied up to a factor of 4 on either side of the default value (of 40,000), the deposition only varied by at most 60%.

H. Deposition Accounting Using a Puff Area Overlap Method

The *HYSPLIT* program is normally configured to allow the estimation of the atmospheric concentration or deposition flux at any point in the model domain. This was an appropriate configuration for the model, which was designed to estimate concentrations and deposition at points of interest. In this project, we were concerned with the estimation of deposition to large regions, i.e., the Great Lakes. We discovered that it was not practical to attempt to estimate the deposition to the Lakes by estimating the deposition at series of evenly spaced points in the Lakes, assuming that the estimated flux was representative of the region surrounding the points, and then summing up over the entire set of points for a given lake. The spatial gradient in the deposition flux was large near the source, and this required an impractically fine grid of points to allow for an accurate mass balance in the deposition estimation procedure.

We modified *HYSPLIT* so that deposition was estimated for a particular puff to a particular region by considering the spatial overlap between the puff and the region. We divided each of the Great Lakes into approximately 20 regions. If the horizontal extent of a puff at a given time step was completely within a given region, then all of the puff's deposition was allocated to that region. However, if the puff overlapped two or more regions, then the deposition to each of the relevant regions was estimated from the fractional overlap. This procedure allowed for deposition estimations to large regions -- such as the Great Lakes -- which preserved a basic mass balance in the calculations.

In the use of the above puff-overlap method, in some cases the puff overlapped regions of different land types (e.g., water, agricultural land, etc.). The model-estimated dry deposition velocity depends significantly on the land type. Therefore, in these cases, dry deposition estimates were made for each land type for which the puff overlapped, and the appropriate dry deposition velocity for each land type was applied to the relevant area of the puff.

Figure 7. Measured particle wet deposition washout ratios for PCDD/F

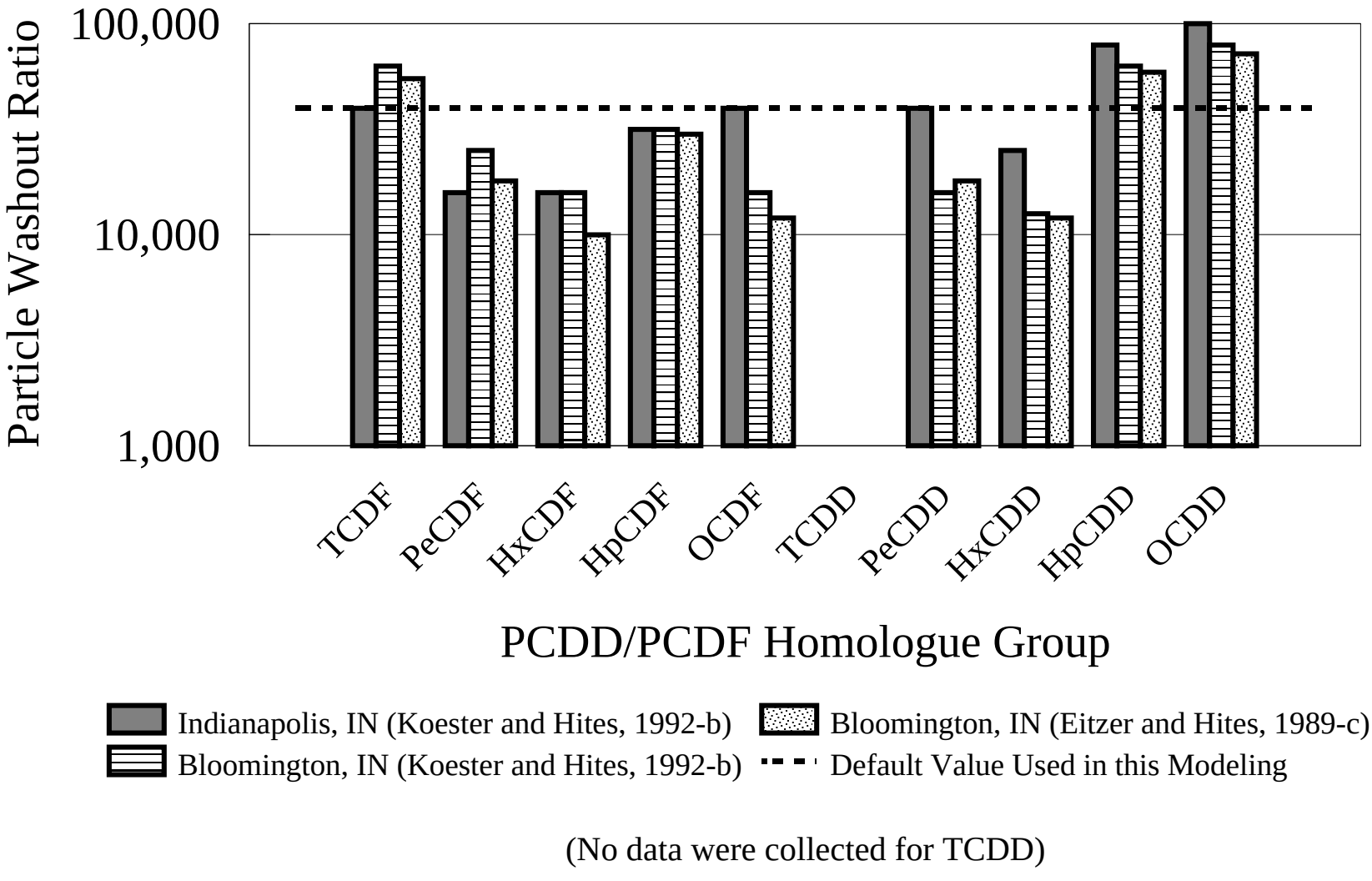

Figure 8. Influence of in-cloud particle washout ratio on simulated deposition of 2,3,7,8-TCDD to Lake Michigan arising from continuous hypothetical emissions from three selected locations.

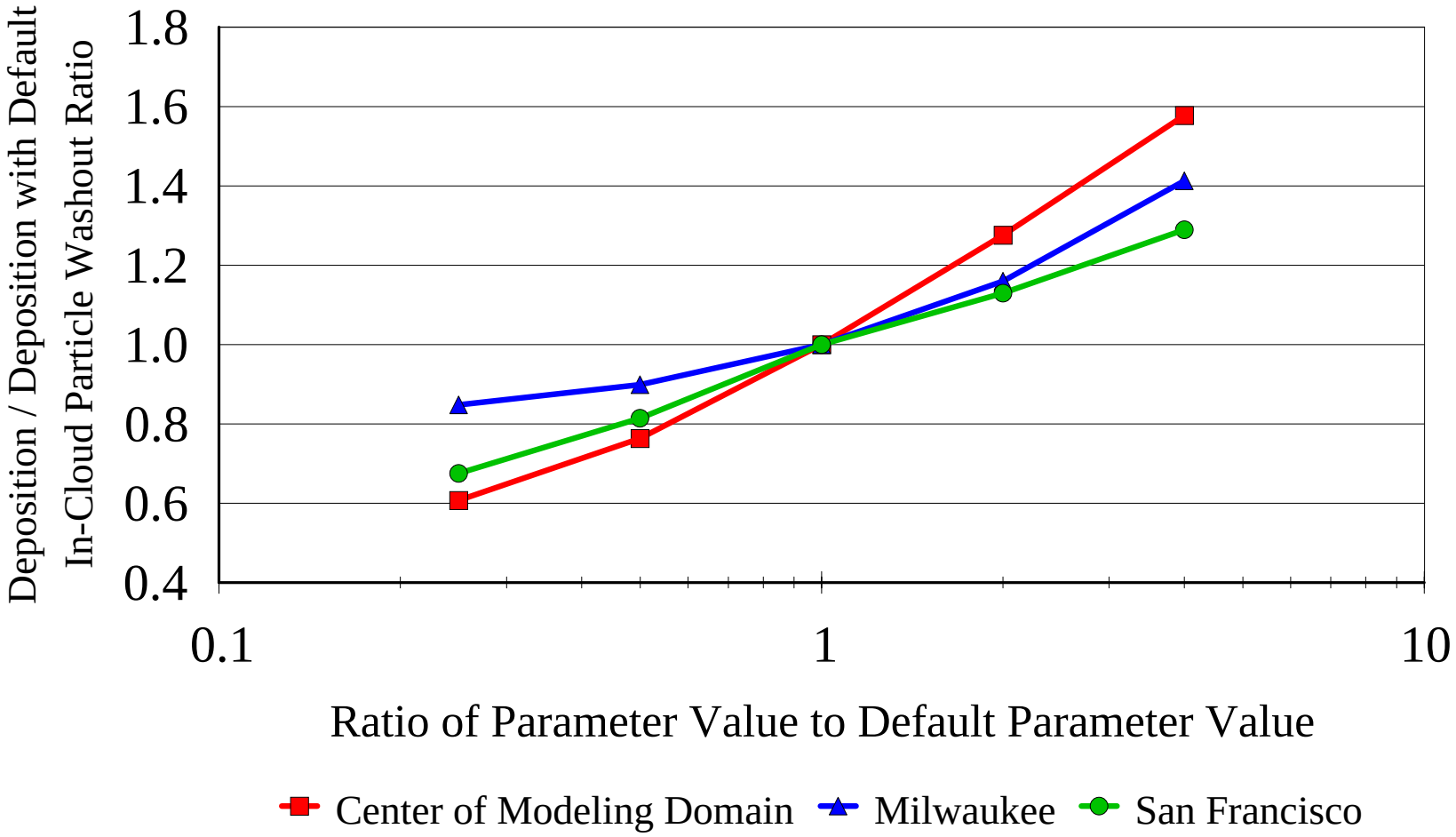

I. Model Time Step

The simulation of atmospheric transport and dispersion within the *HYSPLIT_4* model is described elsewhere (Draxler and Hess, 1997, 1998). However, here are a number of user-defined parameters (Draxler, 1999) that can be specified, and these will be discussed briefly here. First, the model time step was dynamically adjusted during the simulation, using the default *HYSPLIT* methodology. In this approach, the time step is adjusted at each model step based on the user-specified resolution of the concentration grid and the maximum horizontal wind speed any of the puffs in the simulation are encountering. The time step is selected to be small enough so that puffs will be unlikely to "skip over" any of the nodes in the concentration grid. In any event, a maximum time step of 60 minutes is allowed. In this analysis, the default variable time step method was used, with a concentration grid resolution of 1^{o} x 1^{o}. In the simulations done for this analysis, the resulting time steps were typically 15-30 minutes, with an average of approximately 20 minutes.

To evaluate the effect of variations in the model time-step, a source location on the shore of Lake Michigan was selected (Milwaukee), and a continuous emissions source of 2,3,7,8-TCDD was simulated for 1996. The shore location was selected to provide the most potentially sensitive test for the variation of this parameter. Simulations were performed with model time steps of 5, 15, 30, and 60 minutes, as well as with the HYSPLIT-default "variable time step" method, described above. Figure 9 shows the effect of model time step variation on the model estimated deposition to Lake Michigan and the other Great Lakes. It can be seen from this figure that the influence of this parameter on the results, even for Lake Michigan, is negligible. For Lake Michigan, approximately 3.4% of the emitted 2,3,7,8-TCDD is estimated to be deposited in the Lake over the simulation period, and this estimated fraction is essentially independent of the model time step used.

Figure 9. Effect of model time step on the 1996 deposition in Lake Michigan arising from a hypothetical, continuous source of 2378-TCDD at Milwaukee, Wisconsin. The variable time step method was the default, and the use of this method resulted in an average time step of approximately 20 minutes. To examine the effect of this factor, a constant time step method was used, and the model was run with time steps of 5, 15, 30, and 60 minutes.

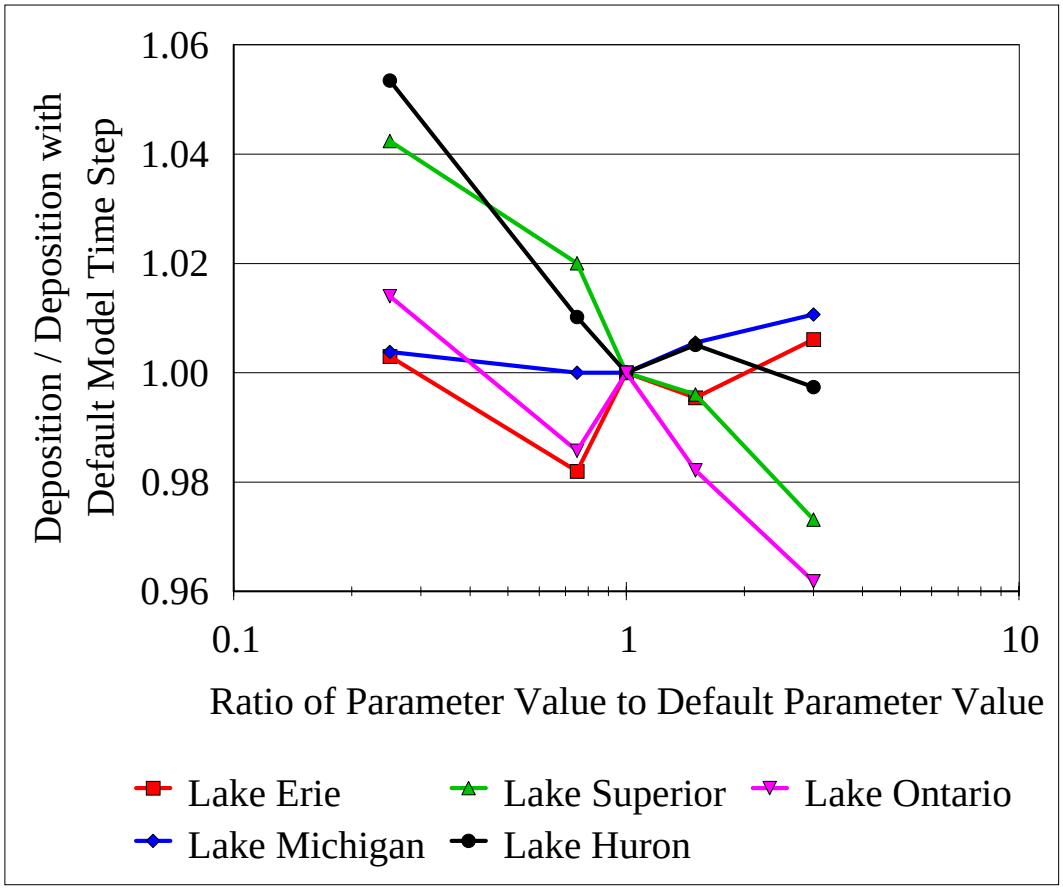

J. Maximum Number of Puffs Allowed in the Model

HYSPLIT_4 can be operated in either a puff or particle mode. In the particle mode, dispersion is simulated by emitting a cloud of particles, and allowing each of the particles to be dispersed randomly, influenced by the meteorological conditions that it encounters. In the puff mode, single puffs are emitted at a user-specified frequency and then are advected and dispersed according to meteorological phenomena encountered by each puff. While the particle mode simulation methodology may be able to provide a more realistic dispersion simulation, the computational resource requirements for its use in this application were too severe. Thus, in the analysis presented here, the *HYSPLIT_4* puff methodology was used.

In the simulation of the dispersion process in the puff mode, the vertical and horizontal dimensions of a given puff are increased with time in a manner influenced by the nature of the atmospheric turbulence encountered by the puff at each time step. If the puff becomes so big that a single meteorological grid point can no longer be used to estimate its transport and dispersion, the puff is split in the horizontally and/or vertically as needed. As a result of the continuous emissions of puffs throughout the simulation, and fact that each puff can split -- sometimes many times -- the numerical resources required to track each of the puffs can become impractically large. A number of features have been incorporated into *HYSPLIT* to ameliorate this problem. First, puffs that are in a similar location and are a similar size can be merged. Second, the user can specify a maximum number of puffs that can be simulated. When the number of puffs would go higher than this limit because of puff splitting, splitting is inhibited. Finally the user can specify that a certain percentage of the mass accounted for in the lowest-mass puffs can be discarded periodically. In the simulations performed here, this discarding process was not used, so that long-range transport would not be underestimated. In the simulations performed here, the default maximum number of puffs was chosen to be 1000.

To examine the influence of this parameter choice on the simulation results, the deposition to the Great Lakes arising from a year-long continuous source of 2378-TCDD at San Francisco, California was estimated using maximum number of puff values of 500, 1000 (the default), 2000, 5000, and 10000. The San Francisco source location – relatively distant from the Lakes – was chosen to provide a "worst case" test for the effect of this parameter, as its effect on sources close to the lakes would be expected to be smaller. The results of this test are shown in Figure 10-A. It can be seen that the choice of the maximum number of puffs has only a moderate effect on the simulated deposition. Since this was essentially a worst-case result, and the impact from sources at this distance from the lakes is relatively small, the choice of 1000 puffs maximum as default was considered reasonable. It should be noted that the computational requirements are essentially proportional to the maximum number of puffs allowed, and so, the choice of this factor can have significant consequences on the resources required to carry out the analysis.

Figure 10-A. Effect of the maximum number of puffs allowed in the simulation on the 1996 deposition to the Great Lakes arising from a hypothetical, continuous source of 2378-TCDD at San Francisco, California.The default maximum was 1000 puffs.

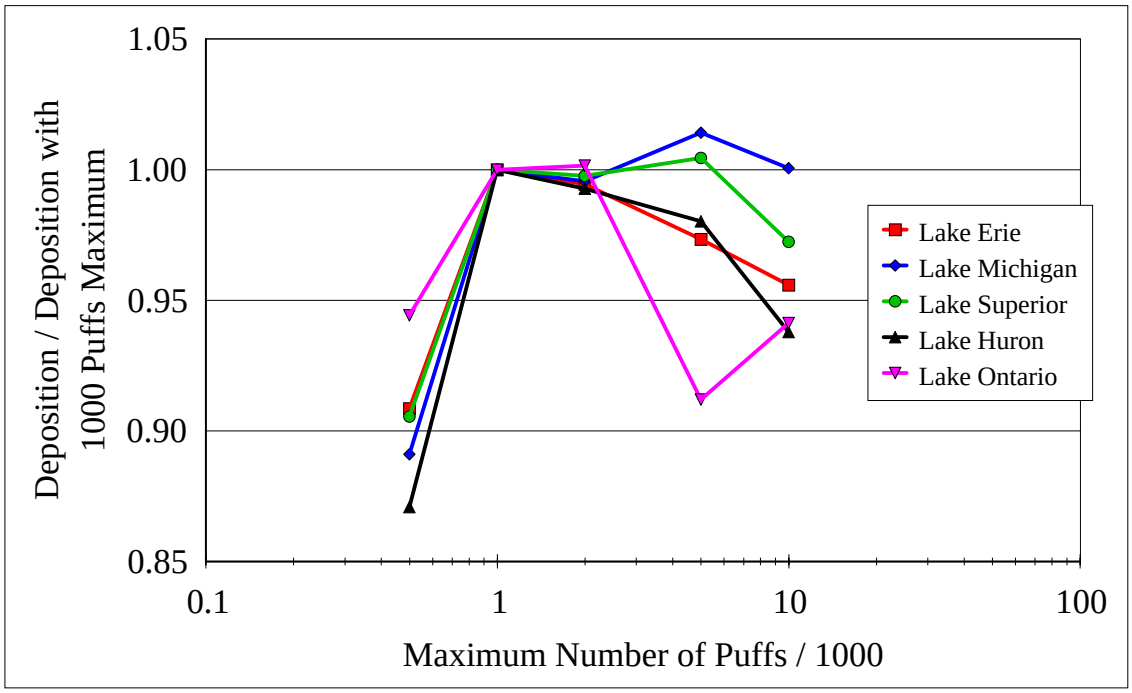

Figure 10-B. Effect of the puff emissions frequency on the 1996 deposition to the Great Lakes arising from a hypothetical, continuous source of 2378-TCDD near the center of the modeling domain. The default emissions frequency was 1 puff every 7 hours.

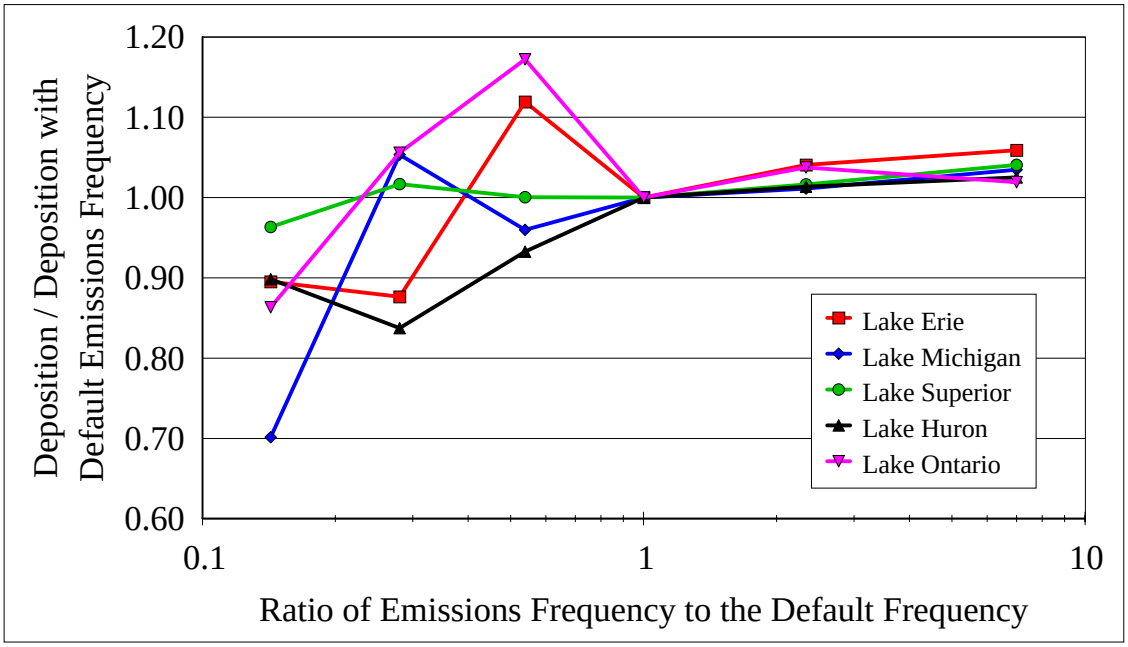

K. Puff Emissions Frequency

To simulate continuous emissions from a given source location, one puff was emitted at any given source location once every 7 hours. This emissions frequency was chosen to allow adequate simulation of the fate and transport of emitted PCDD/F without unnecessarily increasing the computational resources required in the calculation. If puffs were released more frequently, for example, then the maximum number of puffs required to "accurately" carry out the simulation would increase correspondingly. As discussed above, this would increase the computational resources required for the analysis, and thus, must be carefully considered. An odd number was chosen so that whole range of diurnal times would be sampled over the course of the year for a given source.

To examine the influence of this choice on the simulation results, the deposition to the Great Lakes arising from a year-long continuous source of 2378-TCDD at a location near the center of the modeling domain (latitude 40 ^{o}N, longitude 95 ^{o}W) was estimated using an emissions frequency of 1 puff every hour, 1 puff every 3 hours, 1 puff every 7 hours (the default), 1 puff every 13 hours, 1 puff every 25 hours, and 1 puff every 49 hours. For the simulations where the frequency was increased (once per hour, and once per 3 hours) relative to the default, the maximum number of puffs were increased proportionally. The results of this sensitivity test are shown in Figure 10-B. It can be seen that for simulations with less frequent puff emissions, the estimated deposition varies somewhat from the default value. For the lowest frequency simulated, once per 49 hours, the difference is on the order of 30%. However, for more frequent emissions than the default – once per 3 hours and once every hour – the estimated deposition does not change significantly. Thus, the choice of 1 puff every 7 hours as the default frequency was considered reasonable.

L. Source Height

The source height must be specified as an input parameter to the simulation. A single, default source height was desired, so that the simulations from any given source location would be representative of all sources at that location, no matter the source height. In estimating impacts in close proximity to a source (e.g, within a few kilometers), the source height can have a dramatic influence. However, once the plume has moved further downwind, e.g., past about 10 kilometers or so, the emitted pollutant will be relatively evenly distributed throughout the mixing layer – for all source heights that one generally find. Since only a very small fraction of the PCDD/F emissions are deposited in the near-field no matter what the source height – at most a few percent – the specification of the exact height for each source was not considered to be overly important for estimating deposition to the Great Lakes. The lakes have characteristic dimensions of a 100 kilometers or more, and thus, even for a source on the shore of a lake, the overall deposition to the lake will not be strongly affected by the source height. A default height of 50 meters was chosen for this analysis. This choice was made recognizing that much of the dioxin emitted near the lakes comes from large point sources, with relatively tall exhaust stacks.

To investigate the influence of this choice on the estimated deposition results, a source location on the shore of Lake Michigan was selected (Milwaukee), and a continuous emissions source of 2,3,7,8-TCDD was simulated for 1996. The shore location was selected to provide the most potentially sensitive test for the variation of the source height. Simulations were performed with source heights of 1, 10, 25, 50 (the default), 75, and 100 meters. Figure 11 shows the effect of these variations in source height on the model estimated deposition to Lake Michigan and the other Great Lakes. It can be seen from this figure that the influence of this parameter on the results, even for Lake Michigan, is relatively unimportant.

Figure 11. Effect of the source height on the 1996 deposition to the Great Lakes arising from a hypothetical, continuous source of 2378-TCDD at Milwaukee, Wisconsin, on the shore of Lake Michigan. The default source height was 50 meters.

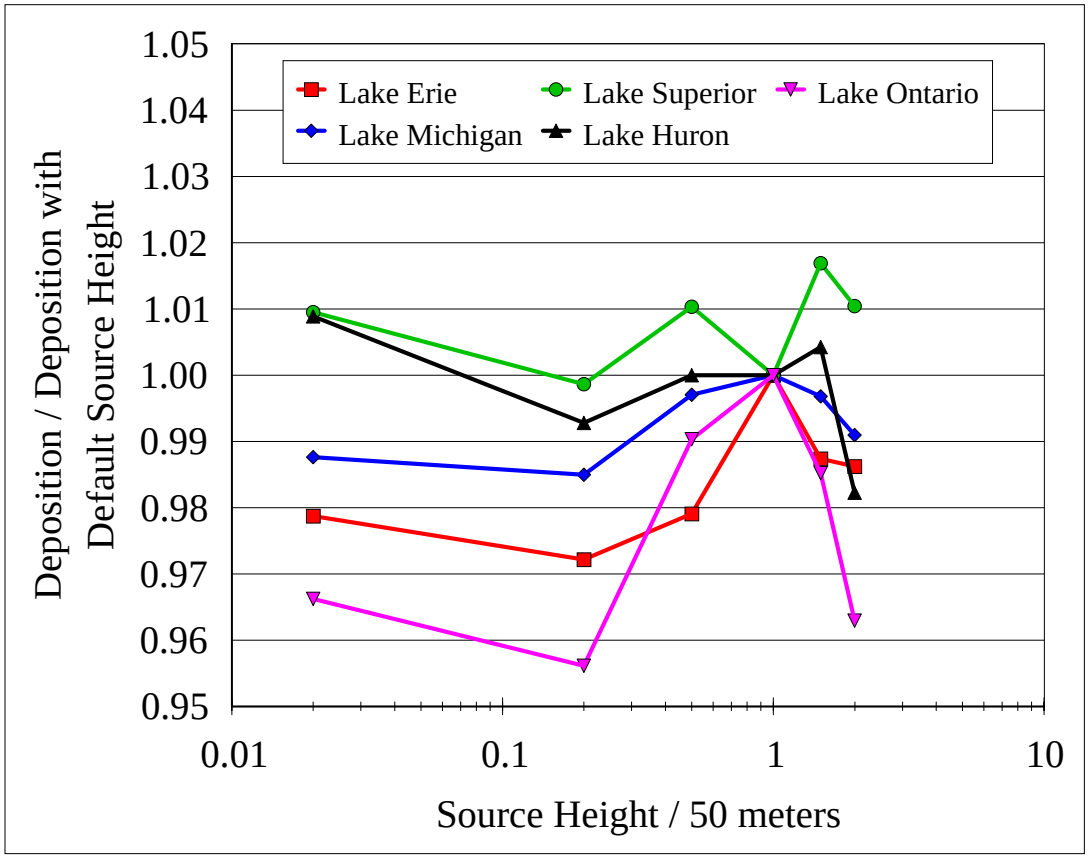

M. Summary of Sensitivity Analyses.

As discussed above, the choice of dry deposition methodology can significantly influence the model-simulated deposition to the Great Lakes. However, in this context, it should be noted that the emissions themselves probably have the largest influence on the resulting deposition. The PCDD/F deposition arising from any given source is directly proportional to the emissions from that source. Given that a typical uncertainty range for PCDD/F emissions from any given source is on the order of a factor of 3 on either side of the central estimate, the simulated deposition arising from any given source would also vary by a factor of 3 around the central estimate. This systematic variation is larger than the possible influence of any of the model parameters or methodologies evaluated here.

A summary of all of the model-associated sensitivity analyses performed here – other than the dry deposition analysis summarized in Figure 5 – is presented in Figure 12. In this figure, data for Lake Michigan only are represented, as the three hypothetical source locations chosen represent the most diverse set of relative source proximity to the lake. The degree of sensitivity exhibited in a given series is estimated from a sensitivity factor, $\epsilon = |\ln (D/D_0)/\ln (P/P_0)|$, where D_0 and D are the deposition amounts for the annual simulation with the default parameter value and with the changed parameter value, respectively, and P_0 and P are the default parameter value and the changed value. For each sensitivity series examined, the average value of ϵ is plotted, along with the range of all ϵ values in the series. In Figure 13, the following abbreviations are used for the sensitivity series: *wr* = washout ratio for in-cloud particles; *vp* = vapor-phase photolysis rate; *pc* = total particle concentration; *ef* = emissions frequency; *pn* = maximum number of puffs allowed in the simulation; *hs* = height of source; *mt* = model time step; *tcdd* = 2378-TCDD; *tcdf* = 2378-TCDF; and *c*, *s*, and *m* are used as abbreviations for hypothetical source locations at the center of the modeling domain, San Francisco, and Milwaukee.

It can be seen from this figure that the most important factors – other than the dry deposition methodology or emissions – appear to be the in-cloud particle washout ratio and the vapor-phase photolysis rate. Based on these results, these two factors, the dry deposition methodology, washout ratio, vapor-phase photolysis rate, and the emissions rates were chosen for a more comprehensive sensitivity analysis, for multiple sources, presented below.

Figure 12. Summary of sensitivity analyses for factors other than the dry deposition methdology or emissions.

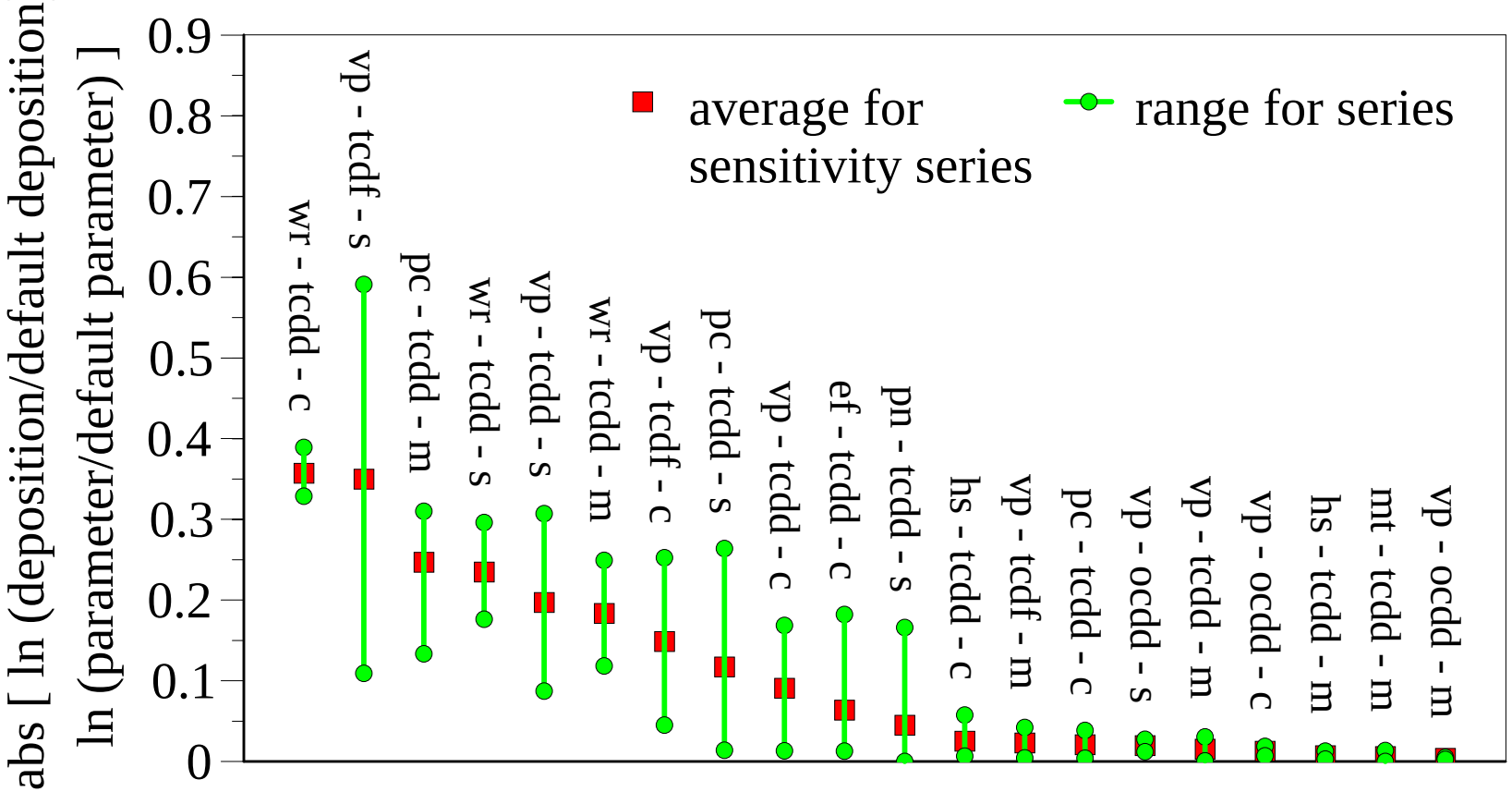

wr = washout ratio for in-cloud particles; vp = vapor-phase photolysis rate; pc = total particle concentration; ef = emissions frequency; pn = maximumnumber of puffs allowed in the simulation; hs = height of source; mt = model time step; tcdd = 2378-TCDD; ; tcdf = 2378-TCDF; c, s, and m are used as abbreviations for hypothetical source locations at the center of the modeling domain, San Francisco, and Milwaukee.

N. Deposition and Flux at Different Distances from the Source

In the main body of this paper, the deposition and flux at different distances from a mid-domain source were presented for 2378-TCDD (Figure 5). Corresponding results for simulation of 2378-TCDF, 23478-PeCDF, and OCDD are presented in Figures 13, 14, and 15, respectively. While the balance between wet and dry deposition varies somewhat among the congeners, the overall pattern of deposition and flux at different distance ranges from the source is generally similar.

O. Computational Resource Requirements.

All of the model runs described here were run on personal computers. The typical time for a single 1-year simulation was on the order of 5 hours, for an 800 MHz machine, and in practice, the time required for any simulation has been found to be inversely proportional to the clock-speed, e.g., an 800 MHz machine will be four times as fast as a 200 MHz machine.

Figure 13. Deposition amount and flux of 23478-PeCDF in successive, concentric, annular 200-km-radius-increment regions away from a continuous 1996 year-long source at the center of the modeling domain. The deposition amount has been divided by the total amount emitted in the simulation to give the fraction of the emissions deposited in any given concentric region. The deposition flux for each region has been normalized to correspond to an emissions rate of 1 gram/year.

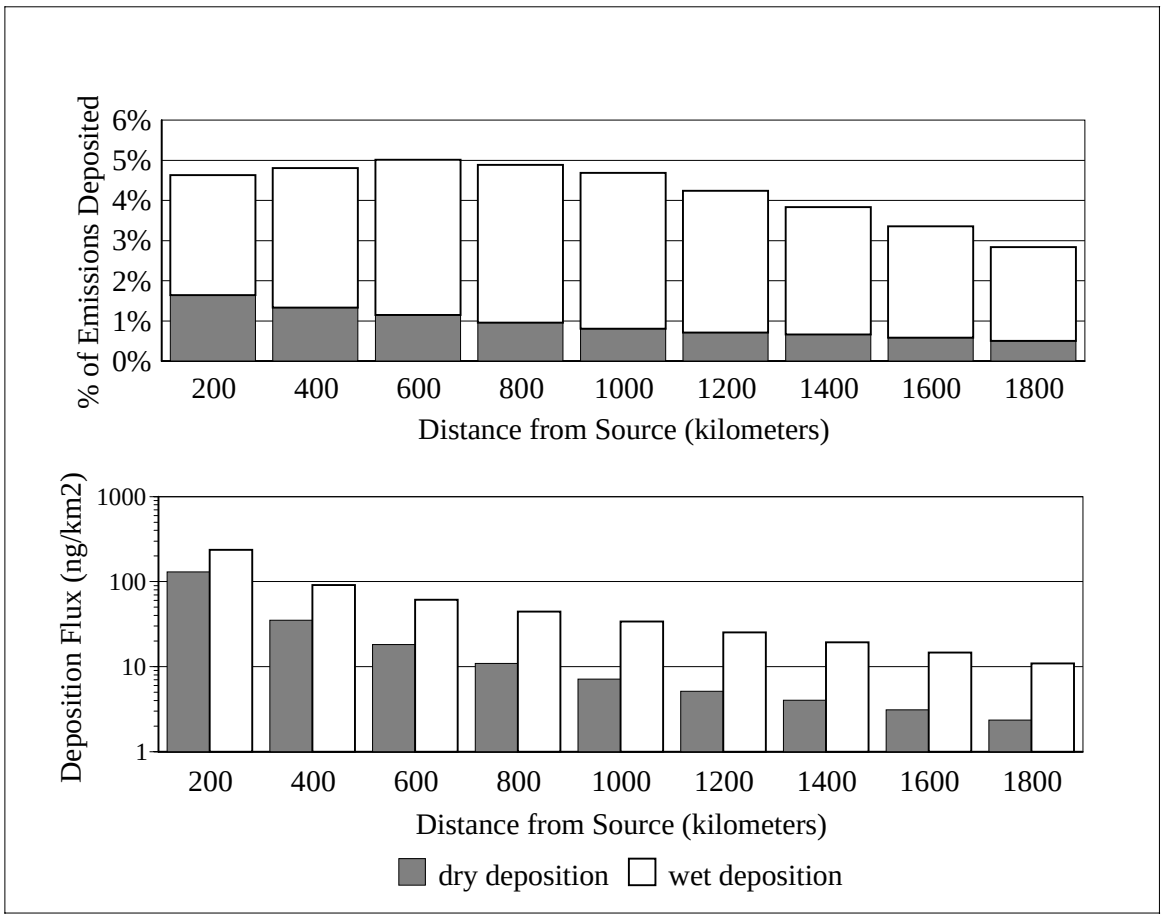

Figure 14. Deposition amount and flux of 2378-TCDF in successive, concentric, annular 200-km-radius-increment regions away from a continuous 1996 year-long source at the center of the modeling domain. The deposition amount has been divided by the total amount emitted in the simulation to give the fraction of the emissions deposited in any given concentric region. The deposition flux for each region has been normalized to correspond to an emissions rate of 1 gram/year.

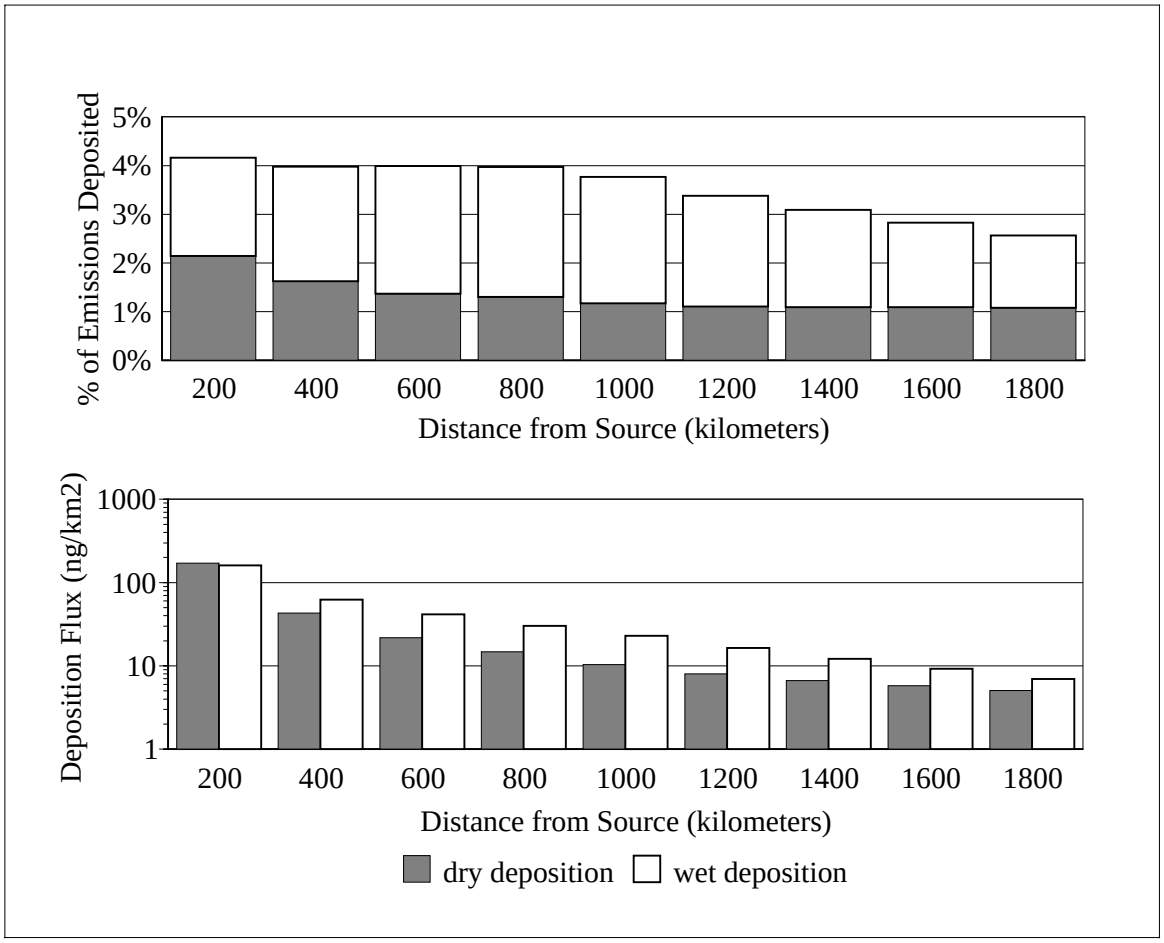

Figure 15. Deposition amount and flux of OCDD in successive, concentric, annular 200-km-radius-increment regions away from a continuous 1996 year-long source at the center of the modeling domain. The deposition amount has been divided by the total amount emitted in the simulation to give the fraction of the emissions deposited in any given concentric region. The deposition flux for each region has been normalized to correspond to an emissions rate of 1 gram/year.

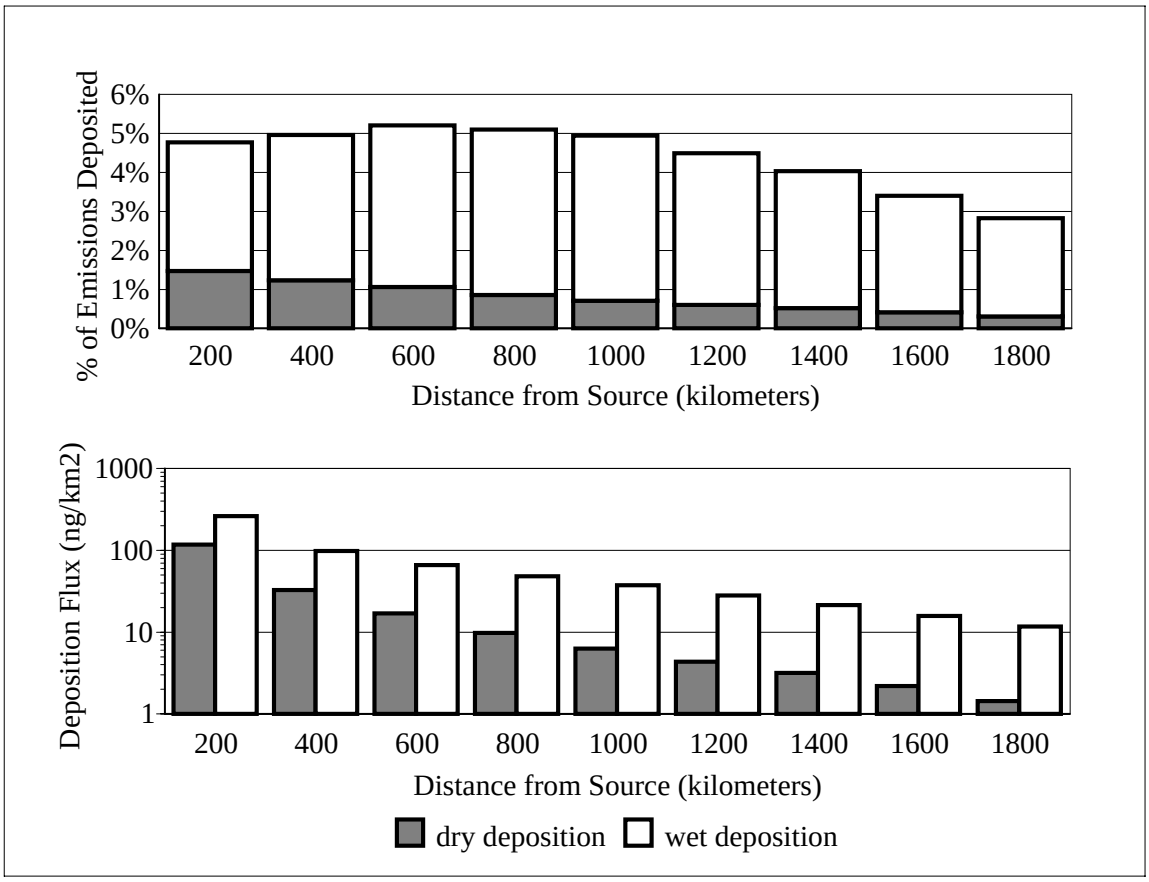

3. Interpolations Methods for Estimating Source-Receptor Relationships for Many Congeners Emitted from Many Sources

As briefly described in the main body of this paper, explicit HYSPLIT modeling of emissions from a given location were only performed for a *limited* number of source locations, to reduce the computational requirements necessary for analysis. In cases where emissions from a given source were not explicitly simulated, a weighted-average spatial interpolation method was used to estimate the source's impact on any given receptor.

For the Great Lakes deposition estimates presented here, the analysis was based on 84 standard source locations. For the purposes of conducting sensitivity analyses, in some cases only 28 such locations were used. A map showing the overall modeling domain (as defined by the meteorological dataset used (*1*) and the locations of the 84 standard locations (with the 28 point subset marked) is shown in Figure 3 of the main paper. The first 28 locations are essentially those used in an earlier analysis of dioxin transport to the Great Lakes (Cohen *et al.*, 1995) Locations 29-84 were added in this analysis in an attempt to provide additional accuracy in the estimation procedure. It can be seen that there is a much higher density of locations in the Great Lakes region. In the remainder of the modeling domain, there is a higher density of locations in the eastern half of the domain, as emissions are generally higher (see Figure 2 in the main body of the paper). However, additional locations were included even where there is little emissions, for the purposes of being able to make at least crude estimates for all sources in the modeling domain.

In addition, as discussed below in Section 4, additional standard source locations were used in regions within approximately 100 km of any model evaluation (i.e., ambient sampling) location.

For source locations other than the locations explicitly simulated by the model, the following spatial interpolation procedure was used. The spatial interpolation is based on a weighted average of the nearest explicitly modeled locations (the weighting is done by distance and angular orientation). First, for a given arbitrary source location, the n closest standard source locations were identified. For each of these n locations, a distance mismatch factor x_n was defined for each of these n closest standard source locations as d_n/d_{max}, where d_n is the distance from the n^{th} standard location and the arbitrary source location, and d_{max} is the maximum such distance for the n closest standard source locations. Then, an angular orientation mismatch factor α_n was defined for each of the n closest standard locations as $|(\theta_n - \theta_s)|/\pi$, where θ_n and θ_s were the angular orientation of the n^{th} closest standard location and the arbitrary source location, respectively, relative to the centroid of the receptor of interest. Both x_n and α_n are positive numbers with a maximum value of 1. A weighting factor z_n was then defined as:

$$z_n = (x_n^a + \alpha_n^b)^{-1} / \sum_{i=1,n} (x_i^a + \alpha_i^b)^{-1} \quad (7)$$

The transfer coefficient of the arbitrary source location to the receptor of interest (E) was then estimated from those of the n standard source locations from the following:

$$\ln E = \sum_{i=1,n} z_i \ln (E_i) \quad (8)$$

where E_i is the transfer coefficient of the i^{th} closest standard source location. If one or more of the E_i are zero, an arithmetic weighted average was used, i.e.,

$$E = \sum_{i=1,n} z_i E_i \quad (9)$$

This latter situation generally only occurs for sources in regions with very low transfer coefficients and thus with relatively low contributions to the Lakes.

A comparison of the interpolation results obtained using various values of the parameters n, a, and b in equation *7* above is presented in Section 5 below.

To create the transfer coefficient maps shown in Figure 9 of the main body of the paper, the average congener emissions profile for the entire U.S./Canadian dioxin emissions inventory was used. This profile is shown below in Figure 16 below.

Figure 16. Average congener emissions profile for the entire U.S./Canadian dioxin emissions inventory
(used for making transfer coefficient example maps in Figure 9 of the paper)

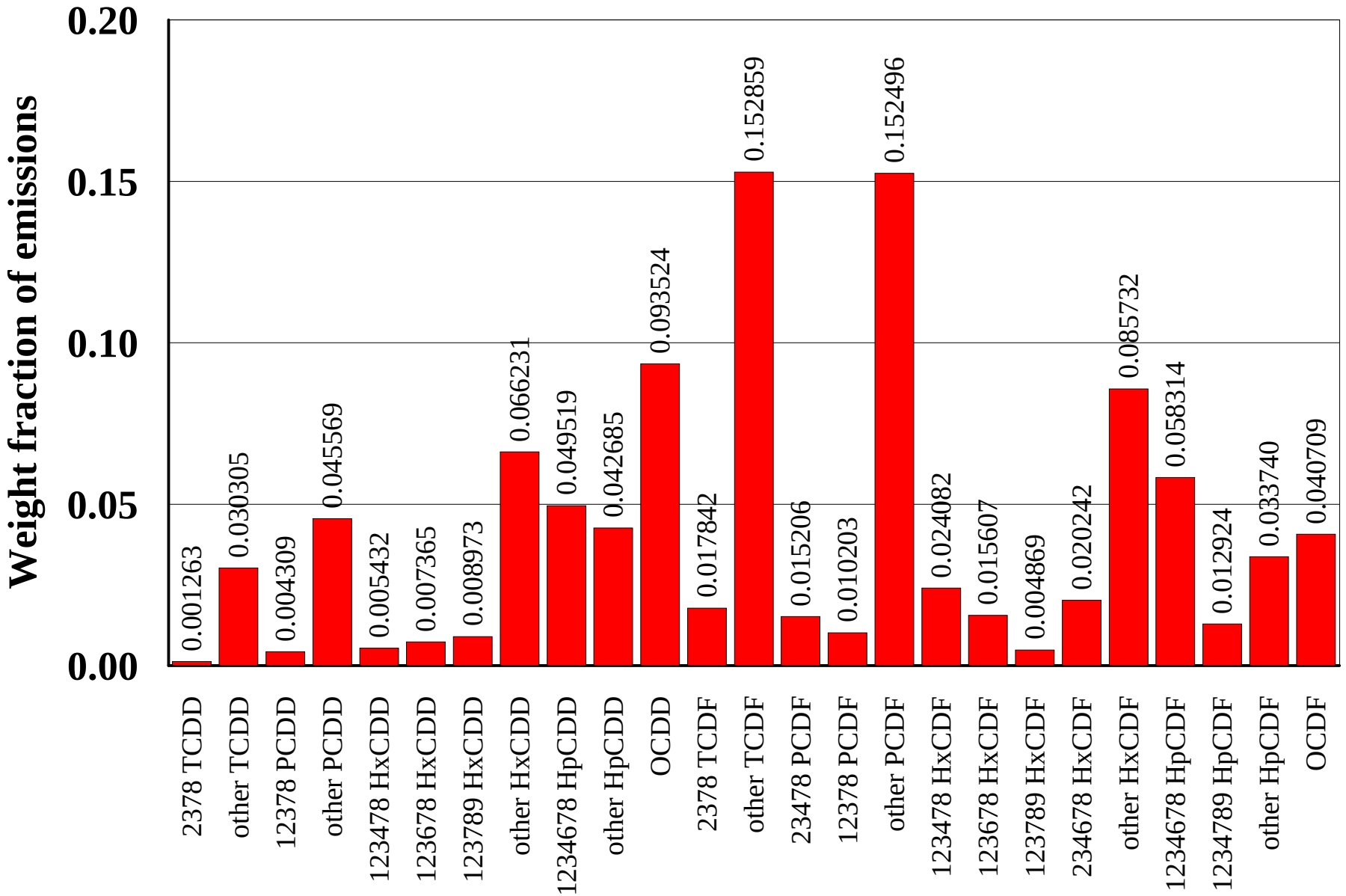

4. Model Evaluation

To generate the model-predicted concentrations, explicit simulations were performed for a number (~25) source locations in addition to the 84 standard source locations discussed above. These additional simulations were performed only for the period relevant to a given ambient sample, and so, were not particularly computationally intensive. Shorter time steps were utilized during these simulations to ensure that puffs would not leap-frog over the measurement location. In addition, puffs were emitted every hour, rather than every 7 hours in the general simulation, in an attempt to increase the accuracy of the simulation. The additional locations used were generally different for each sample, and were chosen to (a) provide additional geographical resolution for the interpolation procedures close to the sampling location and (b) explicitly simulate transport from locations of the largest contributing sources to the predicted ambient concentration corresponding to the sample. These types of additional simulations would not add significantly to the accuracy of the Great Lakes deposition estimates given the large size of the receptors in that case. The additional simulations were performed to rule out interpolation errors as a cause of any major discrepancies between the model predictions and the observed concentrations.

In using the TEQ approach, this analysis has focused on the potential toxicity of the deposition. The HpCDD/F and OCDD/F homologue groups are expected to contribute little to the toxicity of the deposition, as the toxic equivalency factors (relative to 2378 TCDD) are 0.01 for 2378-substituted HpCDD/F and 0.0001 for OCDD/F (Van den Berg et al., 1998). Figures 17-21 show the relative contributions of the 2378-substituted PCDD/F congeners to the total estimated TEQ deposition to each of the Great Lakes. The PeCDD/F congeners are the biggest model-estimated contributors – contributing about 50% of the total TEQ, with hexachlorinated dibenzo-p-dioxins and dibenzofurans (HxCDD/F) and TCDD/F congeners also contributing significantly. The HpCDD and OCDD congeners contribute very little to the total TEQ deposition. Thus, while it will be important to improve the model to account for the atmospheric formation of HpCDD and OCDD, the effect on the overall results here of their unrealistic simulation is not likely to be significant.

In the main body of the paper, the difficulties of comparing the modeling results with short-term measurements are noted. Thus, a series of short-term measurements in Canada (Dann, 1998) were not used for primary model evaluation. For completeness, however, the comparison between the predicted and measured values are shown in Figure 22.

Figures 23-32 show comparisons for each homologue group of the model predictions with ambient measurements for the 5 month-long samples used in the primary model evaluation exercise discussed above.

Figure 17. Relative contribution of the seventeen 2,3,7,8-substituted PCDD/F congeners to the overall model-predicted deposition to Lake Superior.

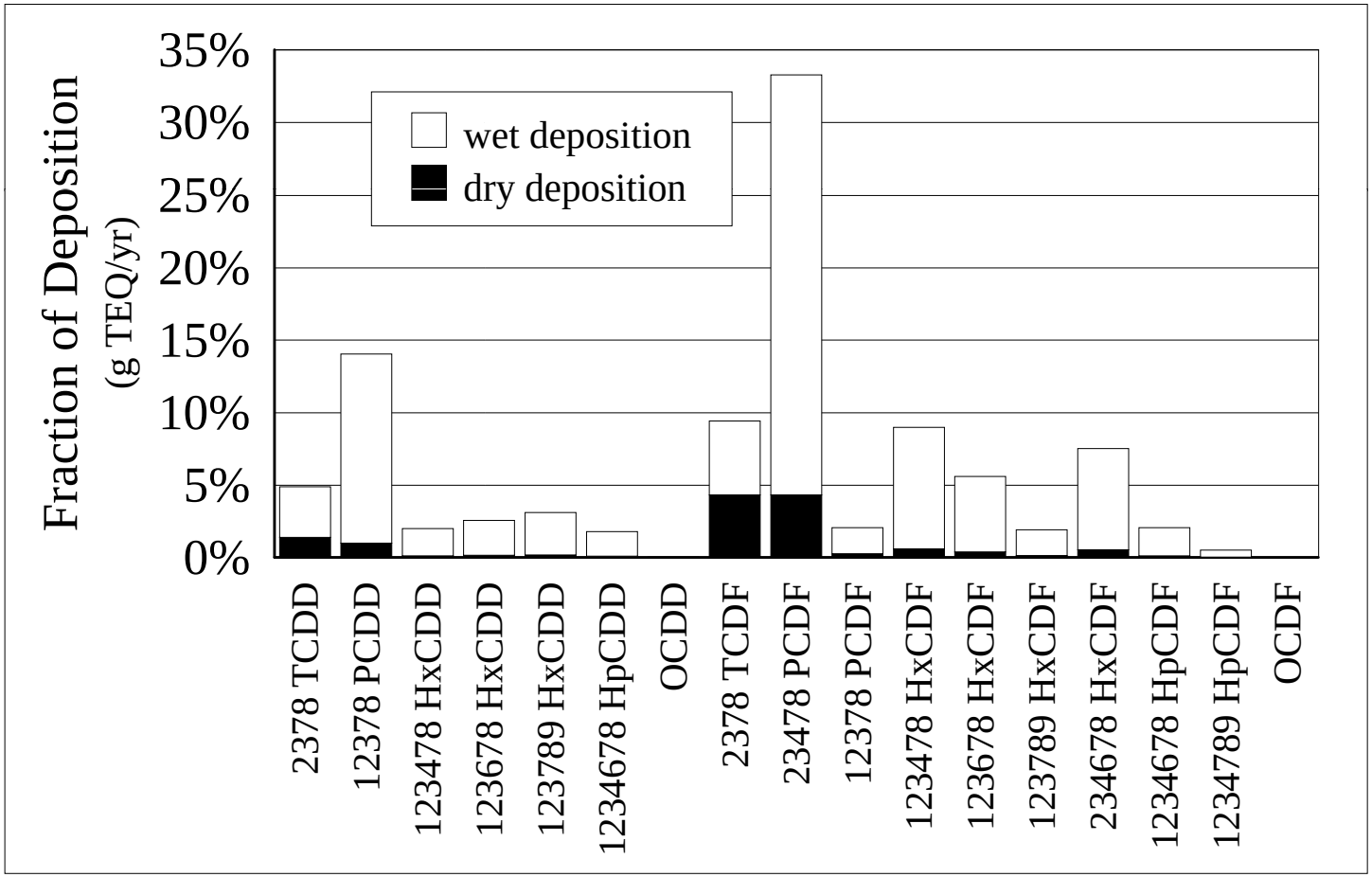

Figure 18. Relative contribution of the seventeen 2,3,7,8-substituted PCDD/F congeners to the overall model-predicted deposition to Lake Michigan.

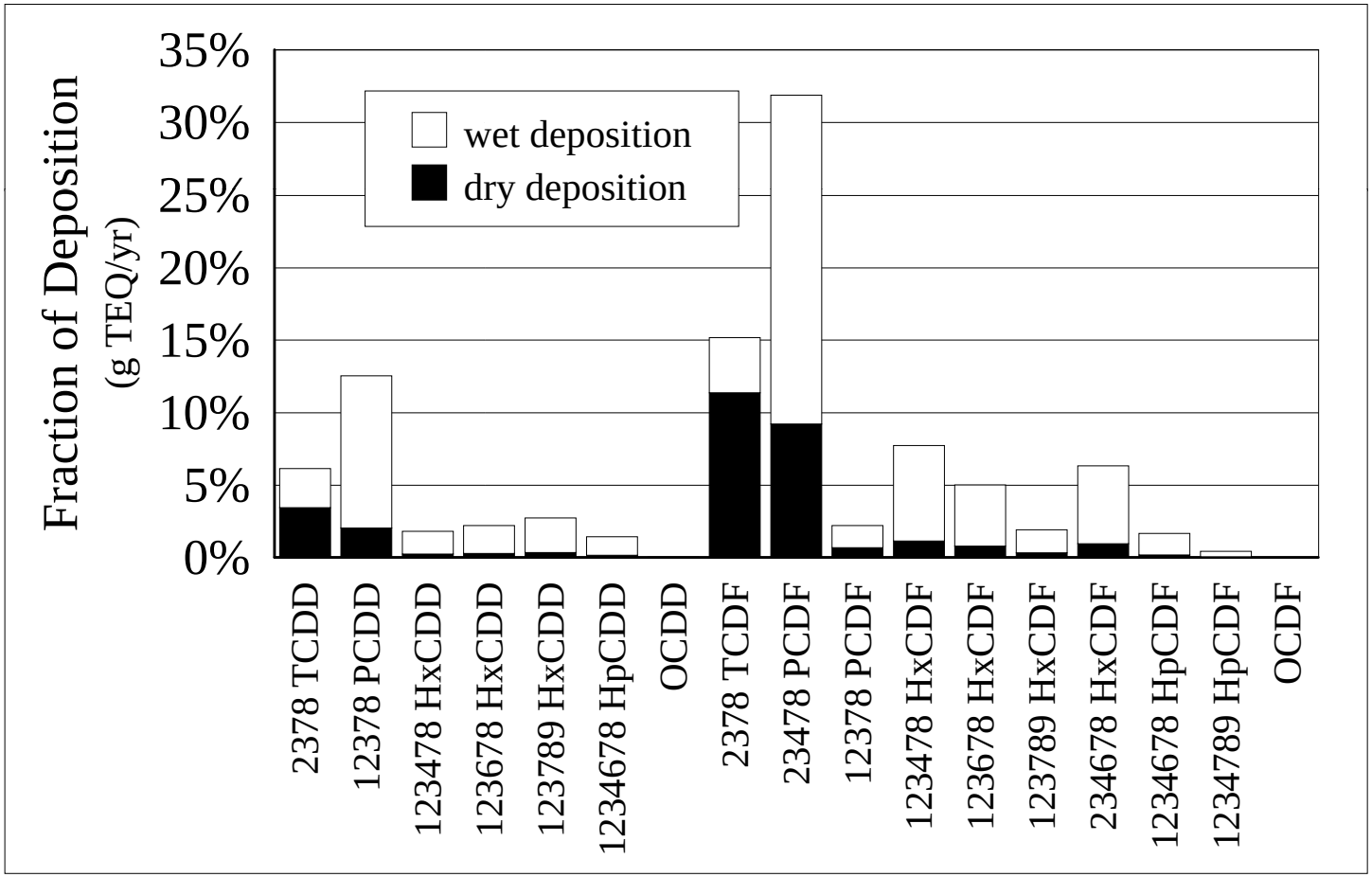

Figure 19. Relative contribution of the seventeen 2,3,7,8-substituted PCDD/F congeners to the overall model-predicted deposition to Lake Huron.

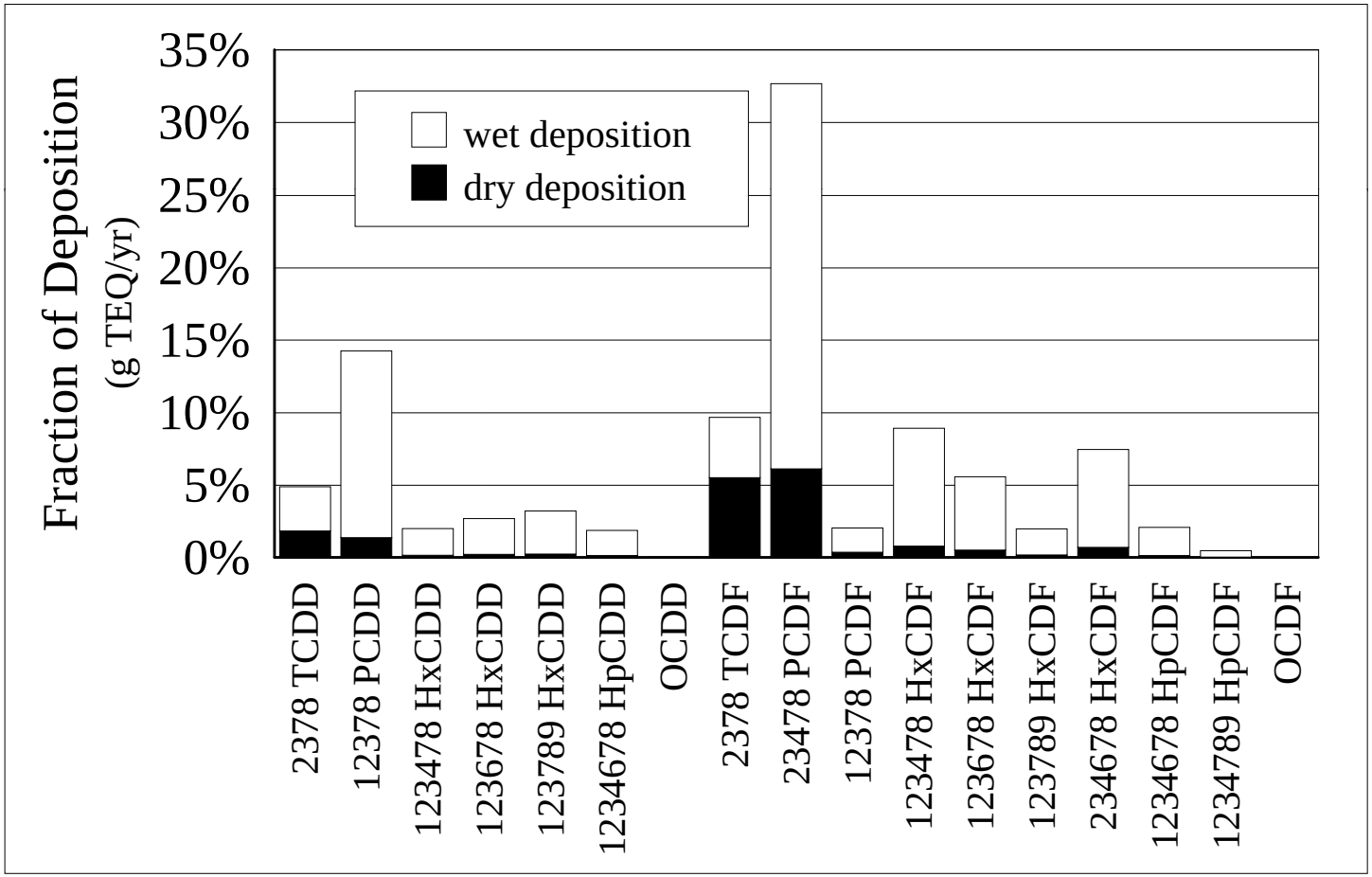

Figure 20. Relative contribution of the seventeen 2,3,7,8-substituted PCDD/F congeners to the overall model-predicted deposition to Lake Erie.

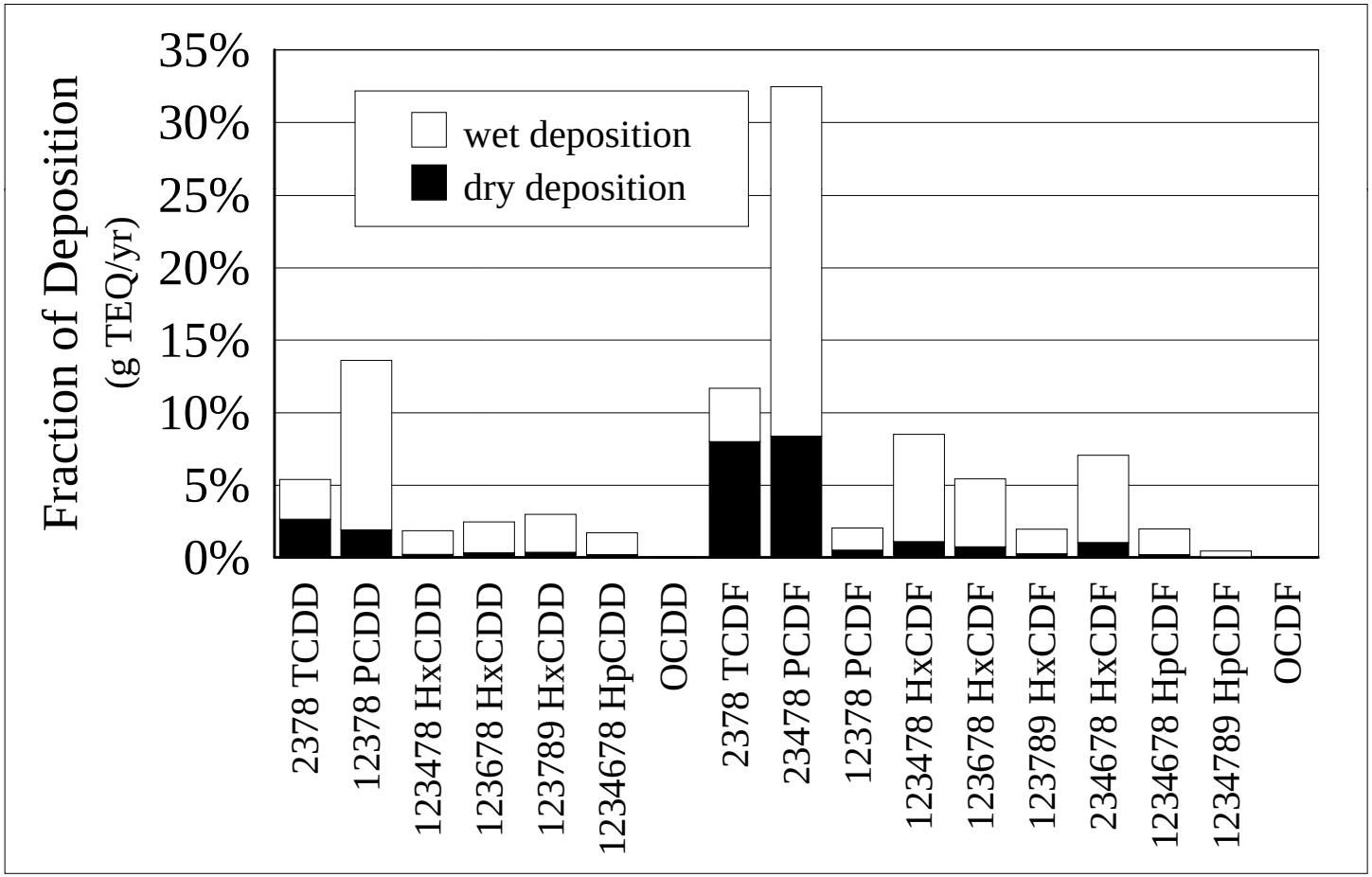

Figure 21. Relative contribution of the seventeen 2,3,7,8-substituted PCDD/F congeners to the overall model-predicted deposition to Lake Ontario.

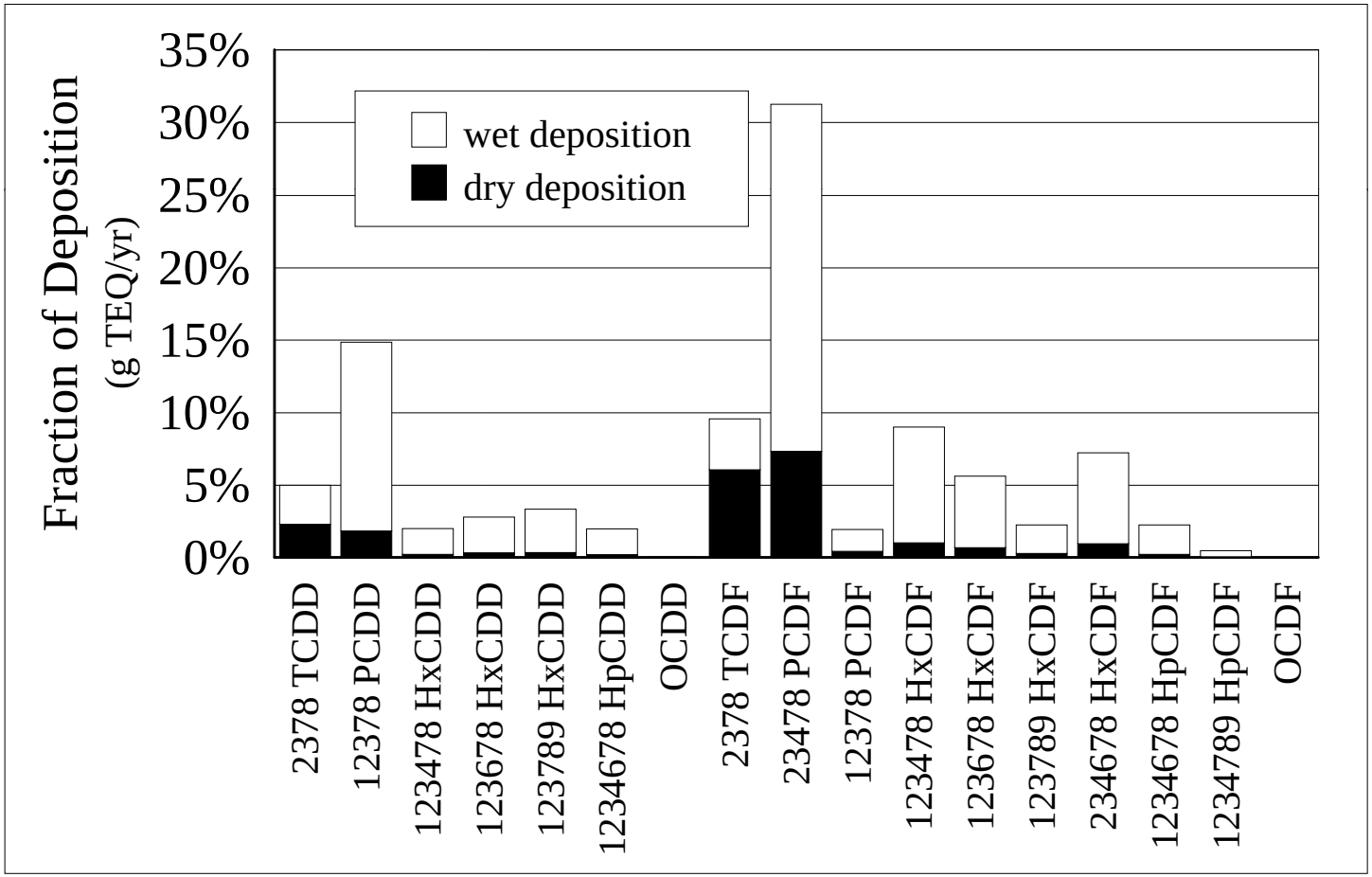

Figure 22. Comparison of model predictions with 2-day ambient measurements of total PCDD/F (TEQ) at rural and semi-rural locations in Canada.

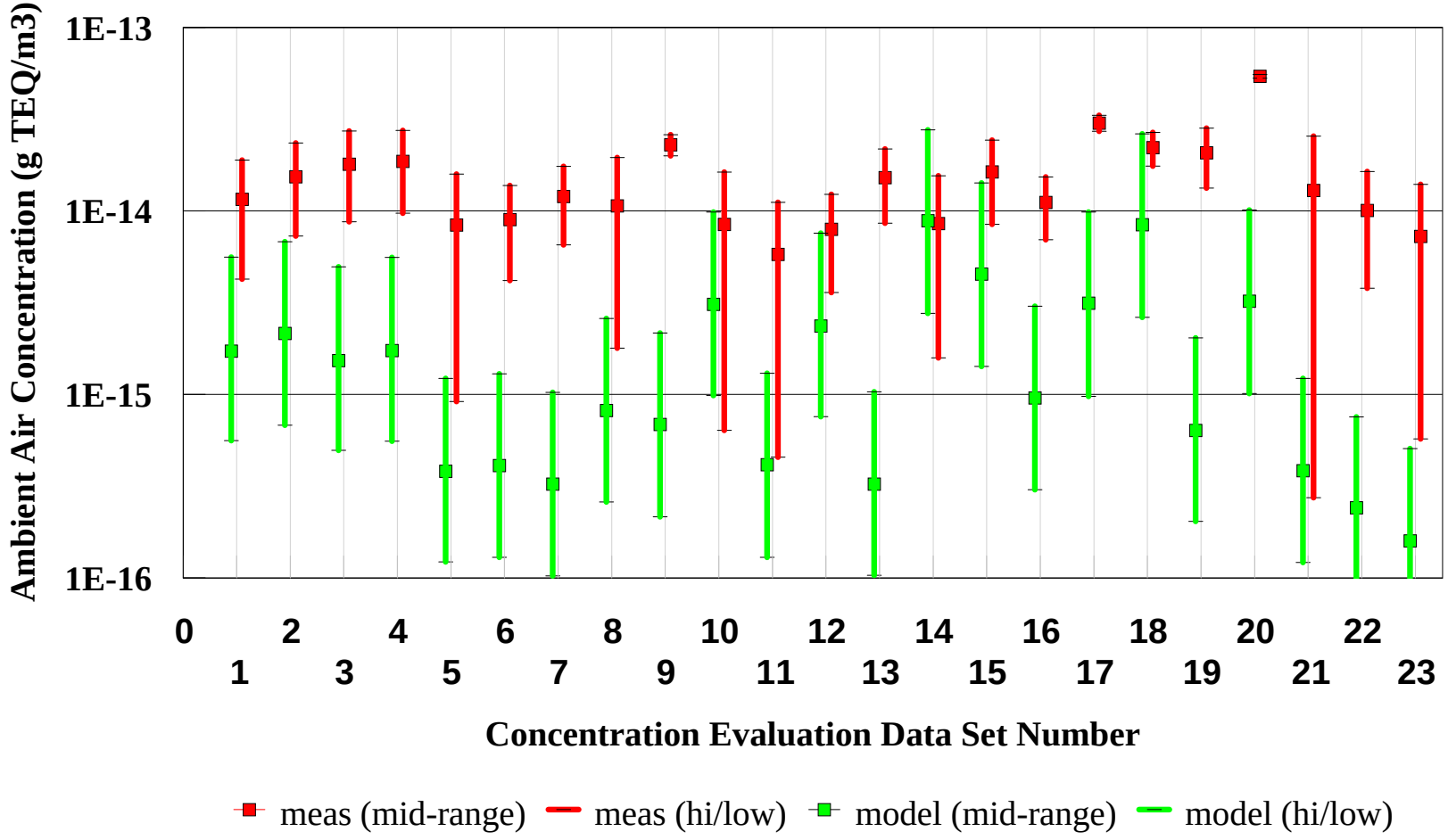

2-day samples: Kejimkujik NS (1-5); St. Andrews NB (6-14); Pt. Petre (15-18); Simcoe ON (19-20); Gray SK (21-23)

Figure 23. Comparison of Model Predictions with Ambient Measurements at Month-Long Sample Sites
TCDD

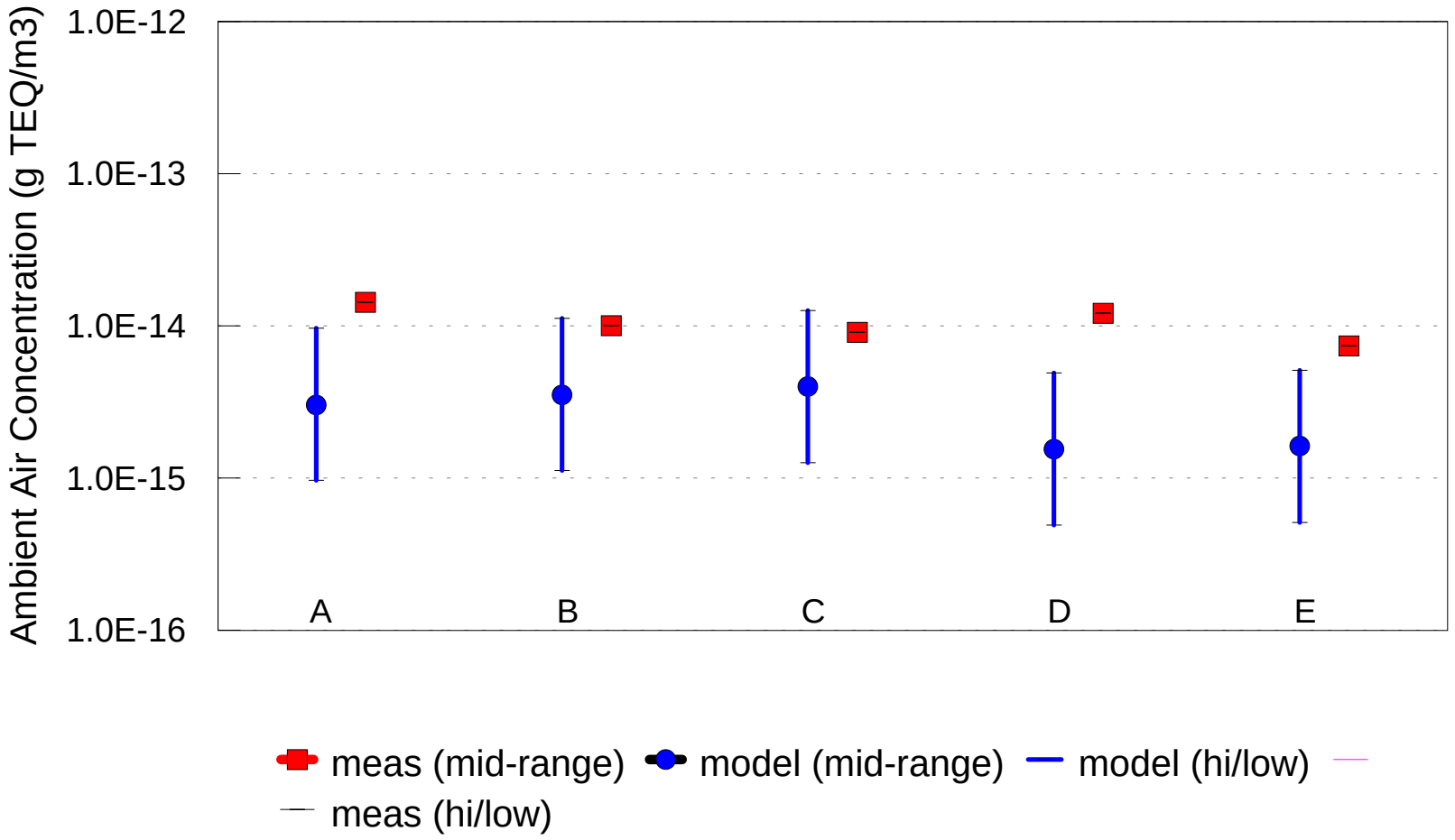

1-month samples: Mohawk Mtn CT (A-C); Northern VT (D); Southern VT (E)

Figure 24. Comparison of Model Predictions with Ambient Measurements at Month-Long Sample Sites
PeCDD

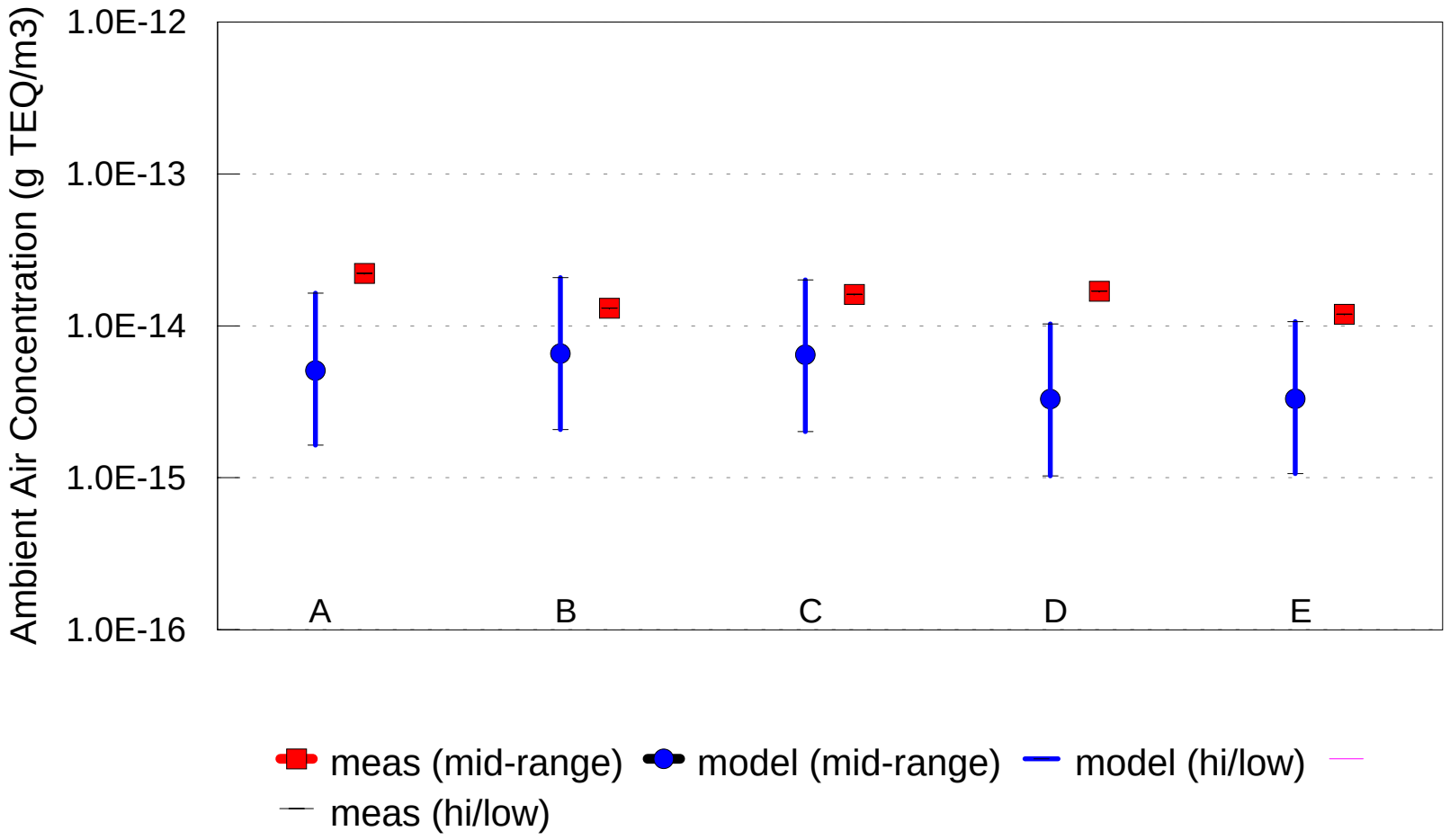

1-month samples: Mohawk Mtn CT (A-C); Northern VT (D); Southern VT (E)

Figure 25. Comparison of Model Predictions with Ambient Measurements at Month-Long Sample Sites
HxCDD

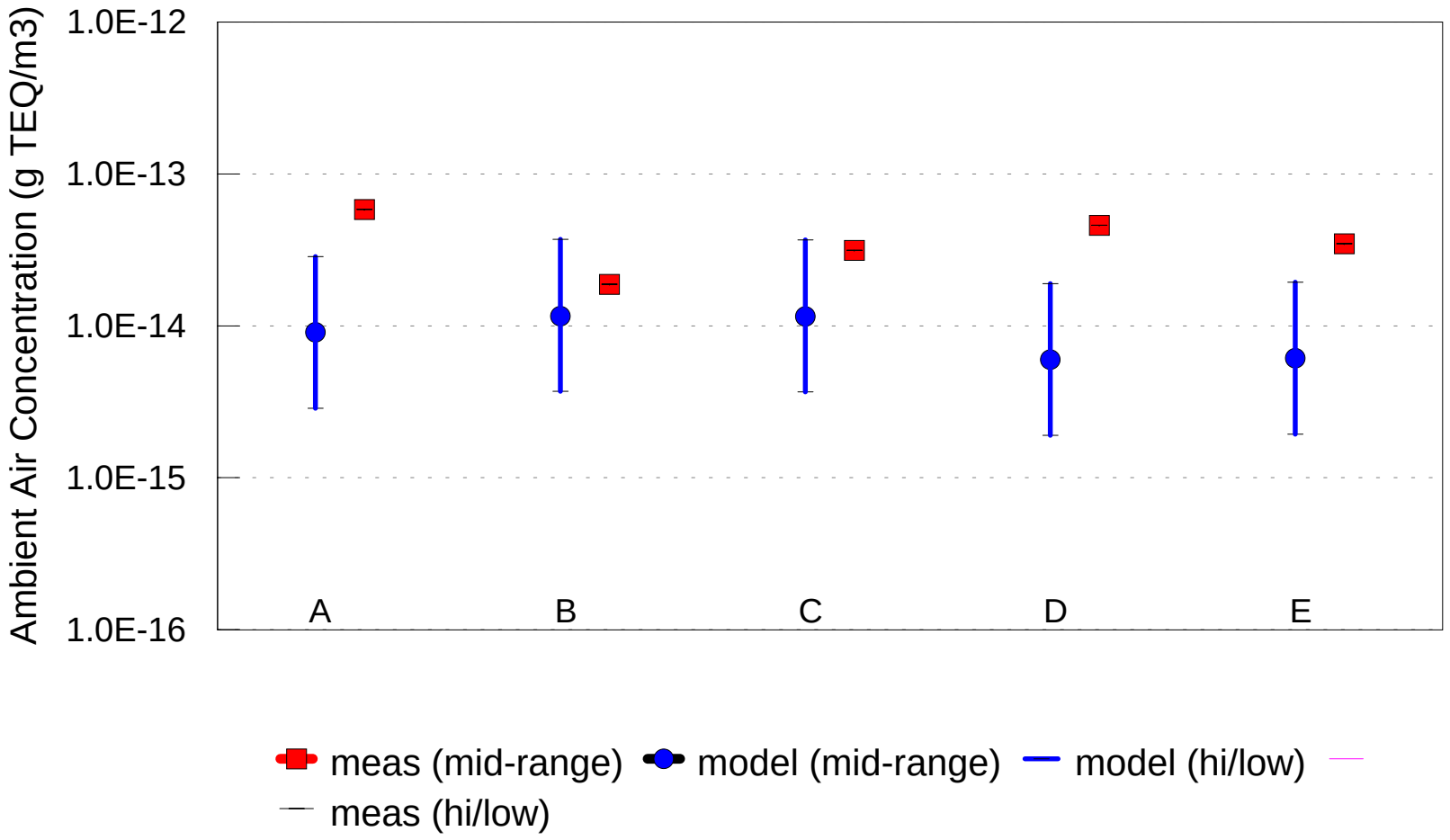

Figure 26. Comparison of Model Predictions with Ambient Measurements at Month-Long Sample Sites
HpCDD

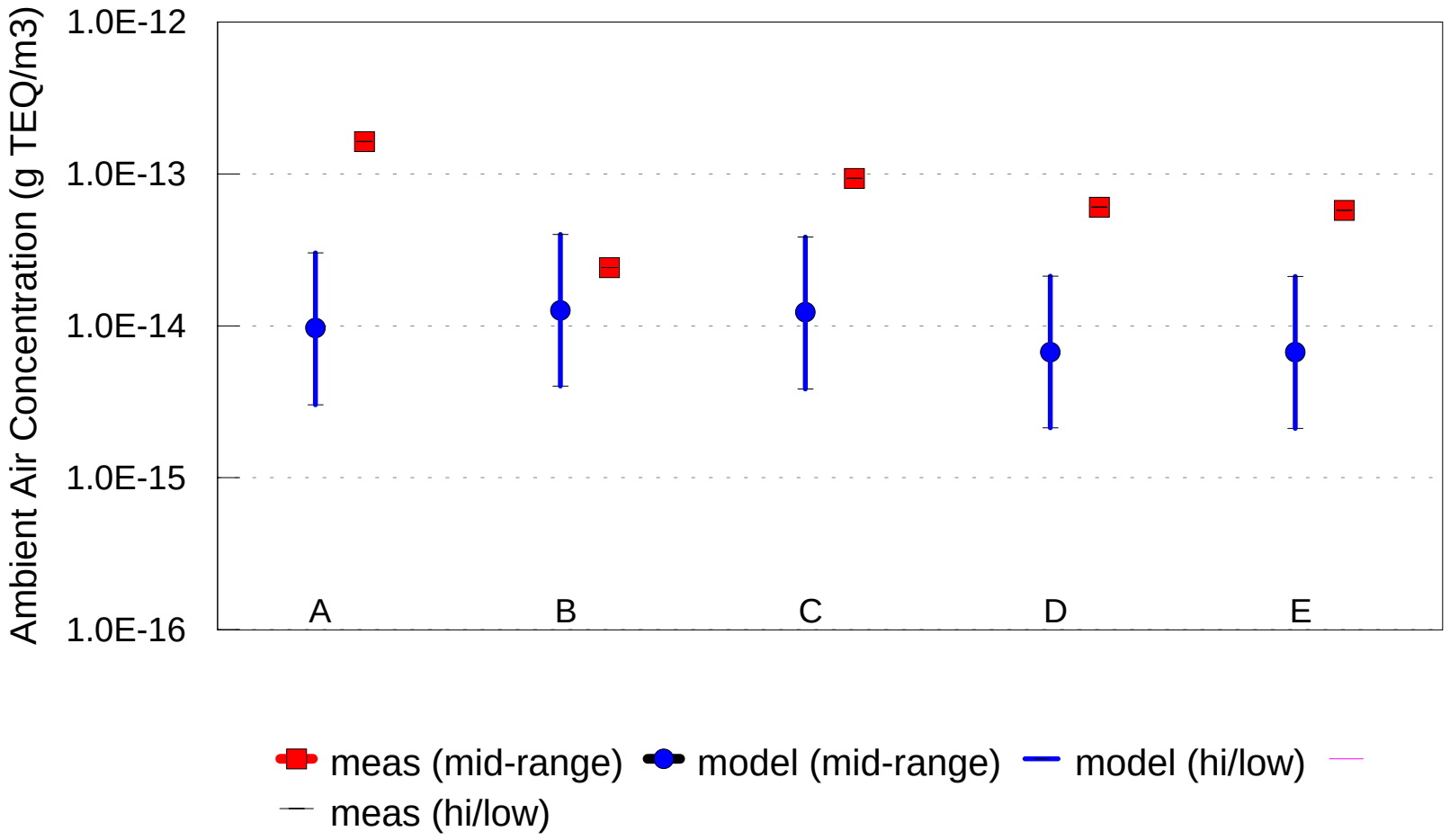

1-month samples: Mohawk Mtn CT (A-C); Northern VT (D); Southern VT (E)

Figure 27. Comparison of Model Predictions with Ambient Measurements at Month-Long Sample Sites
OCDD

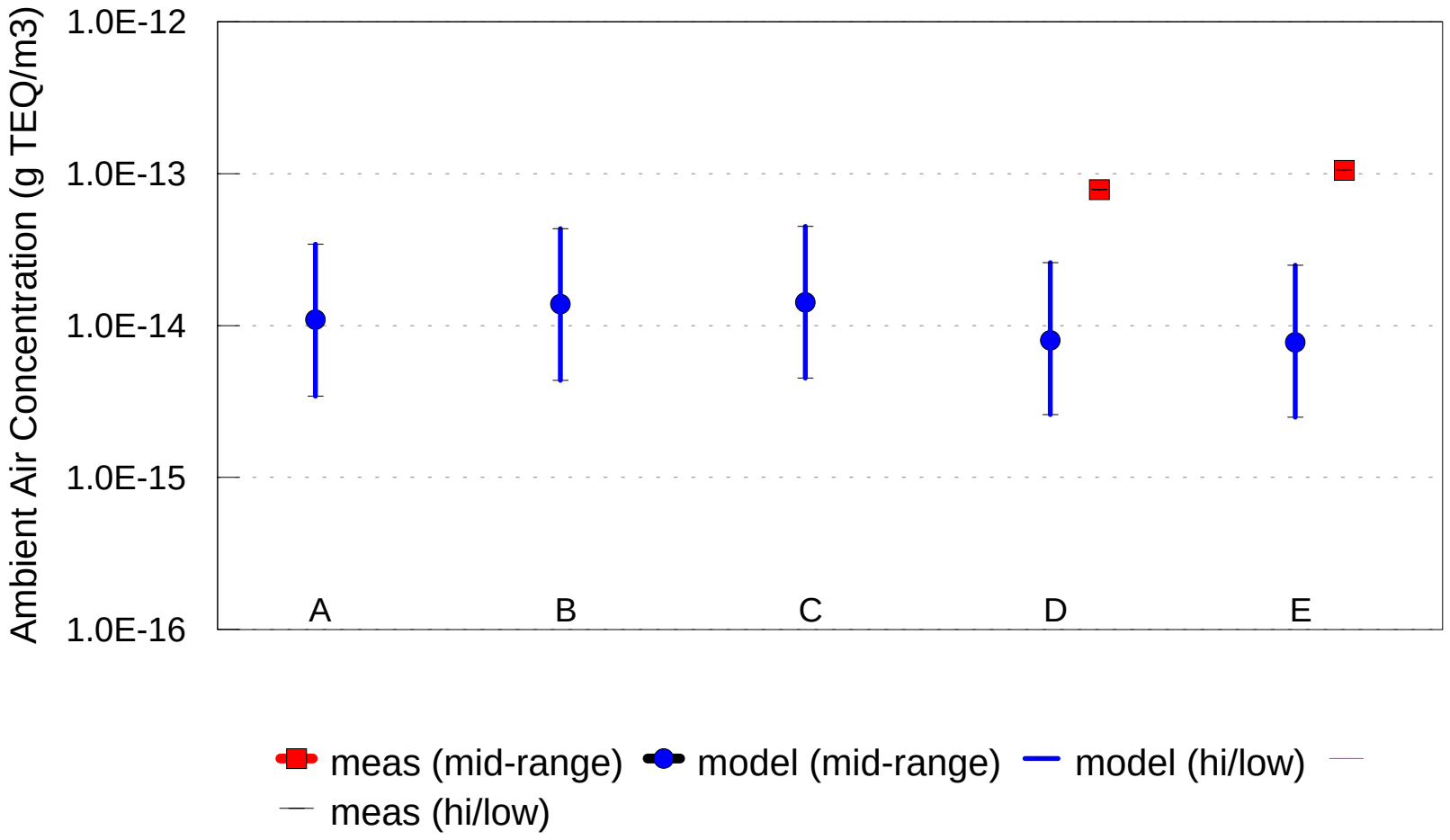

1-month samples: Mohawk Mtn CT (A-C); Northern VT (D); Southern VT (E)

Figure 28. Comparison of Model Predictions with Ambient Measurements at Month-Long Sample Sites
TCDF

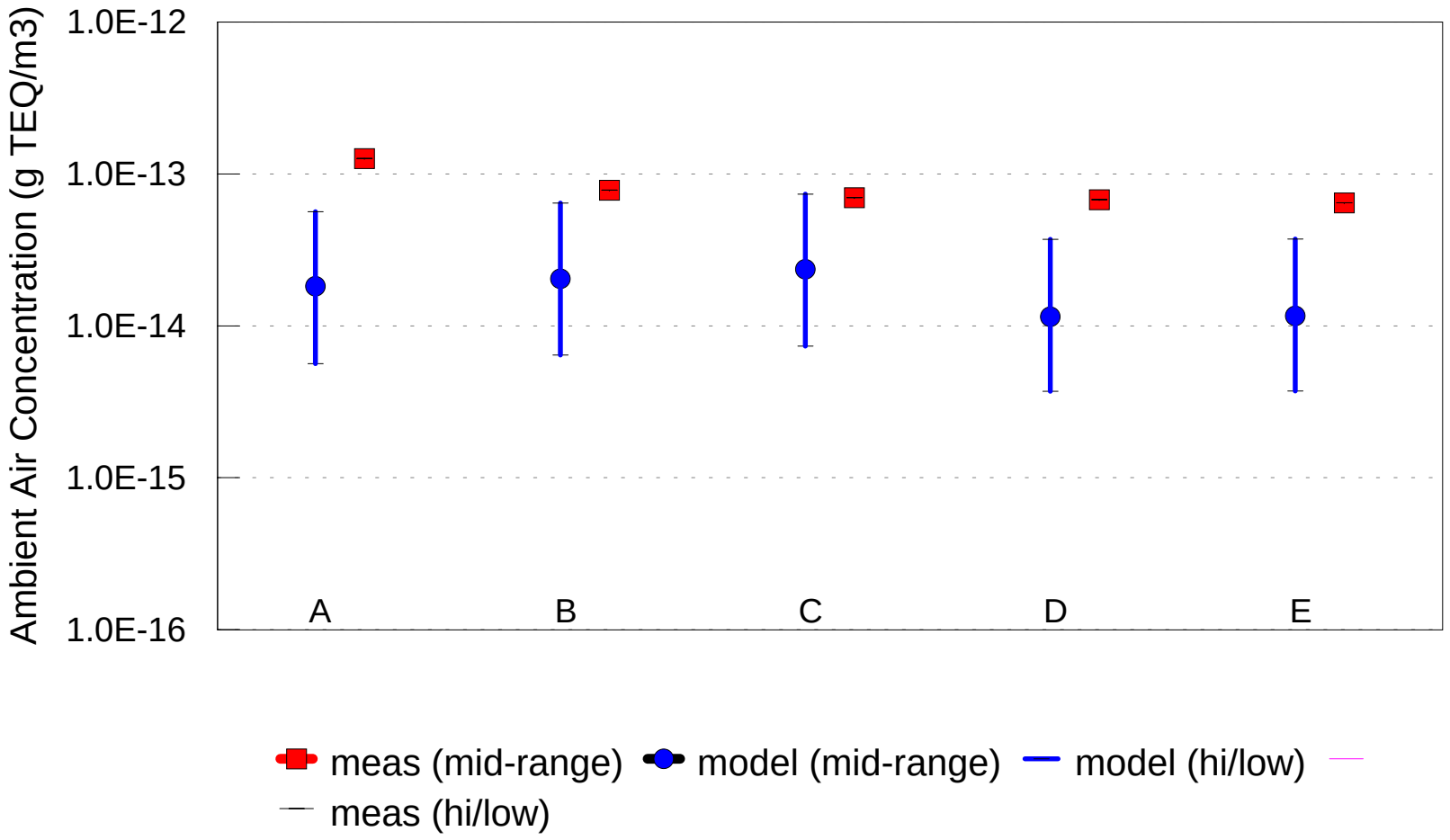

1-month samples: Mohawk Mtn CT (A-C); Northern VT (D); Southern VT (E)

Figure 29. Comparison of Model Predictions with Ambient Measurements at Month-Long Sample Sites
PeCDF

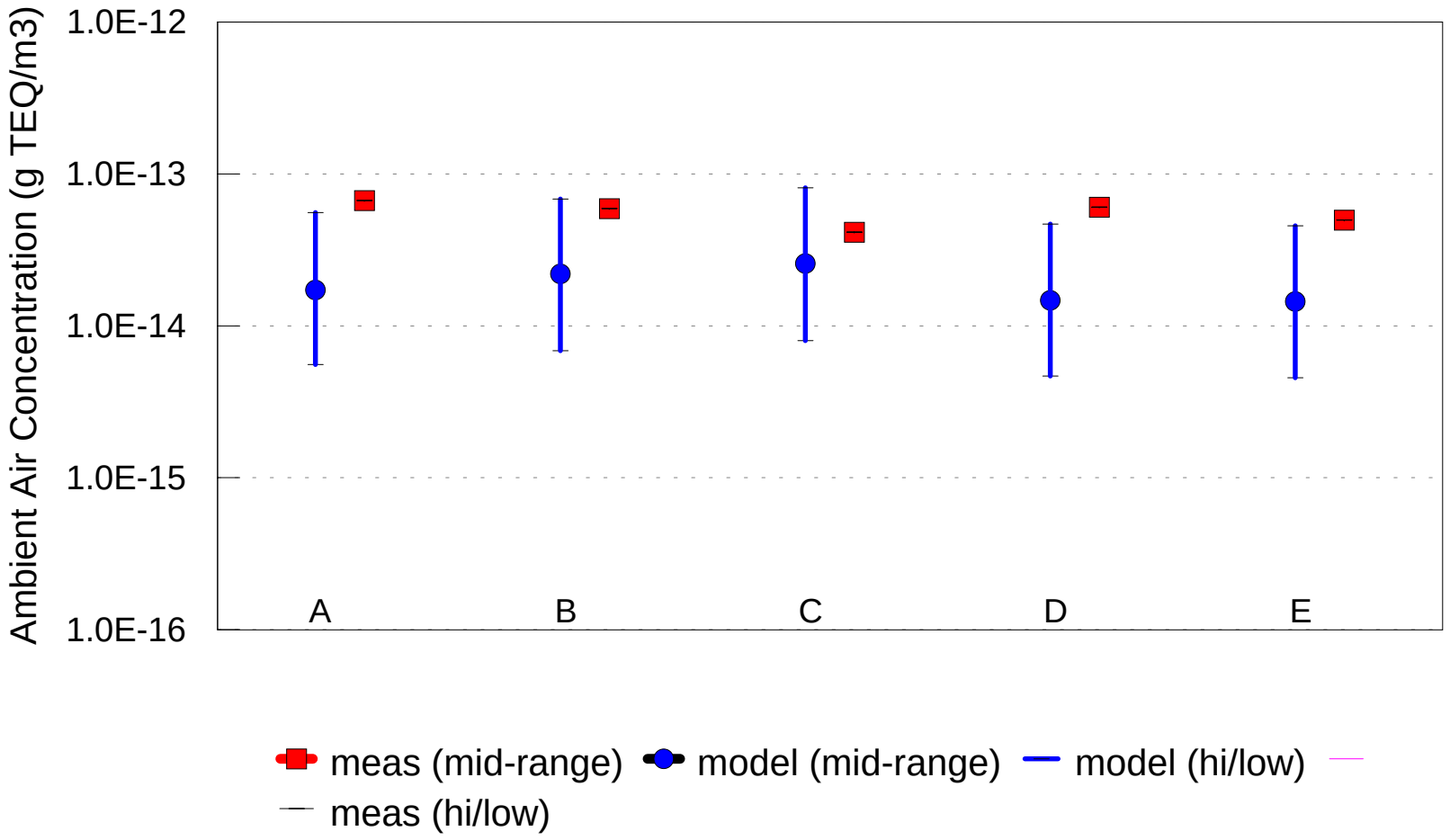

1-month samples: Mohawk Mtn CT (A-C); Northern VT (D); Southern VT (E)

Figure 30. Comparison of Model Predictions with Ambient Measurements at Month-Long Sample Sites
HxCDF

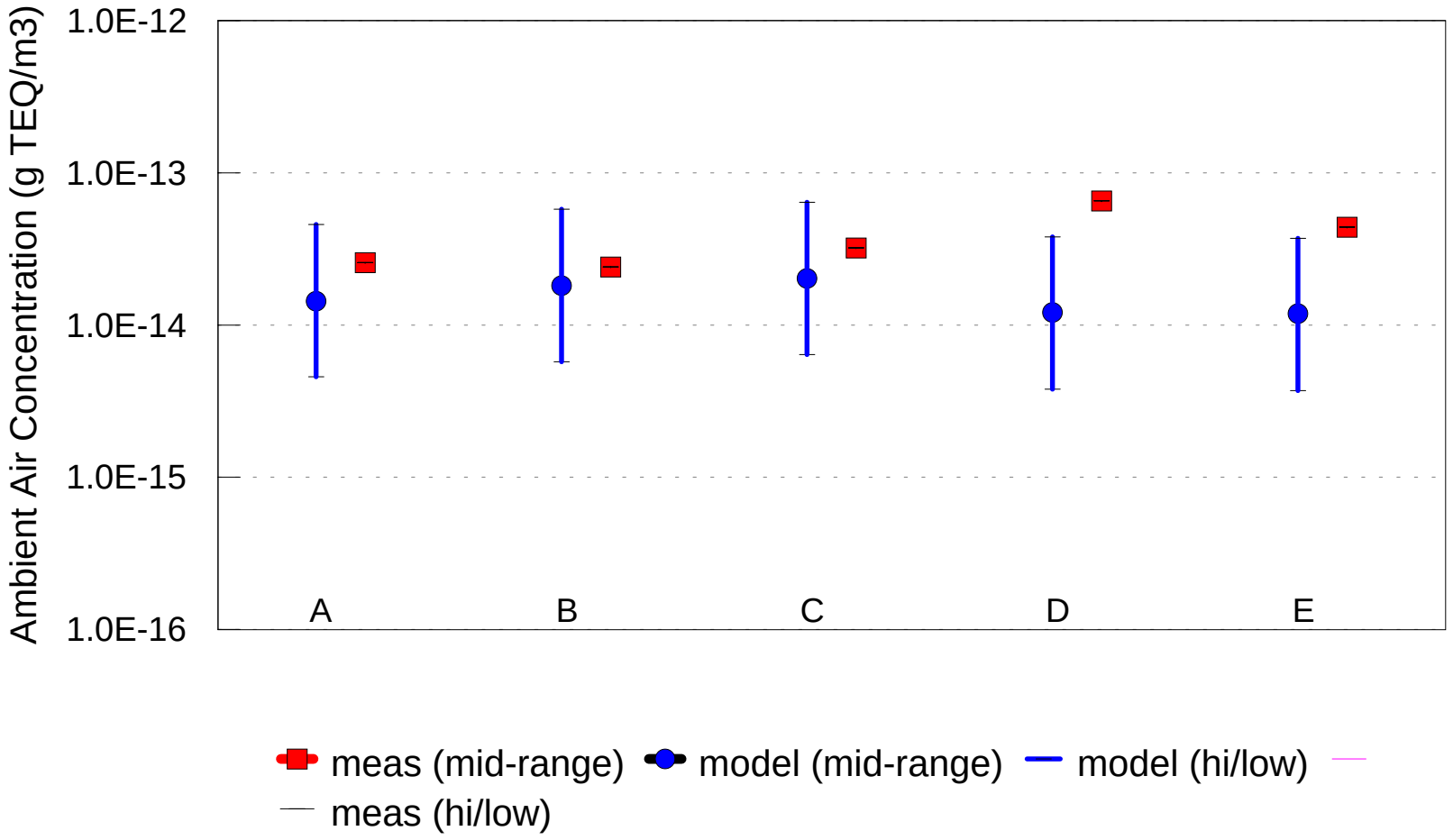

1-month samples: Mohawk Mtn CT (A-C); Northern VT (D); Southern VT (E)

Figure 31. Comparison of Model Predictions with Ambient Measurements at Month-Long Sample Sites
HpCDF

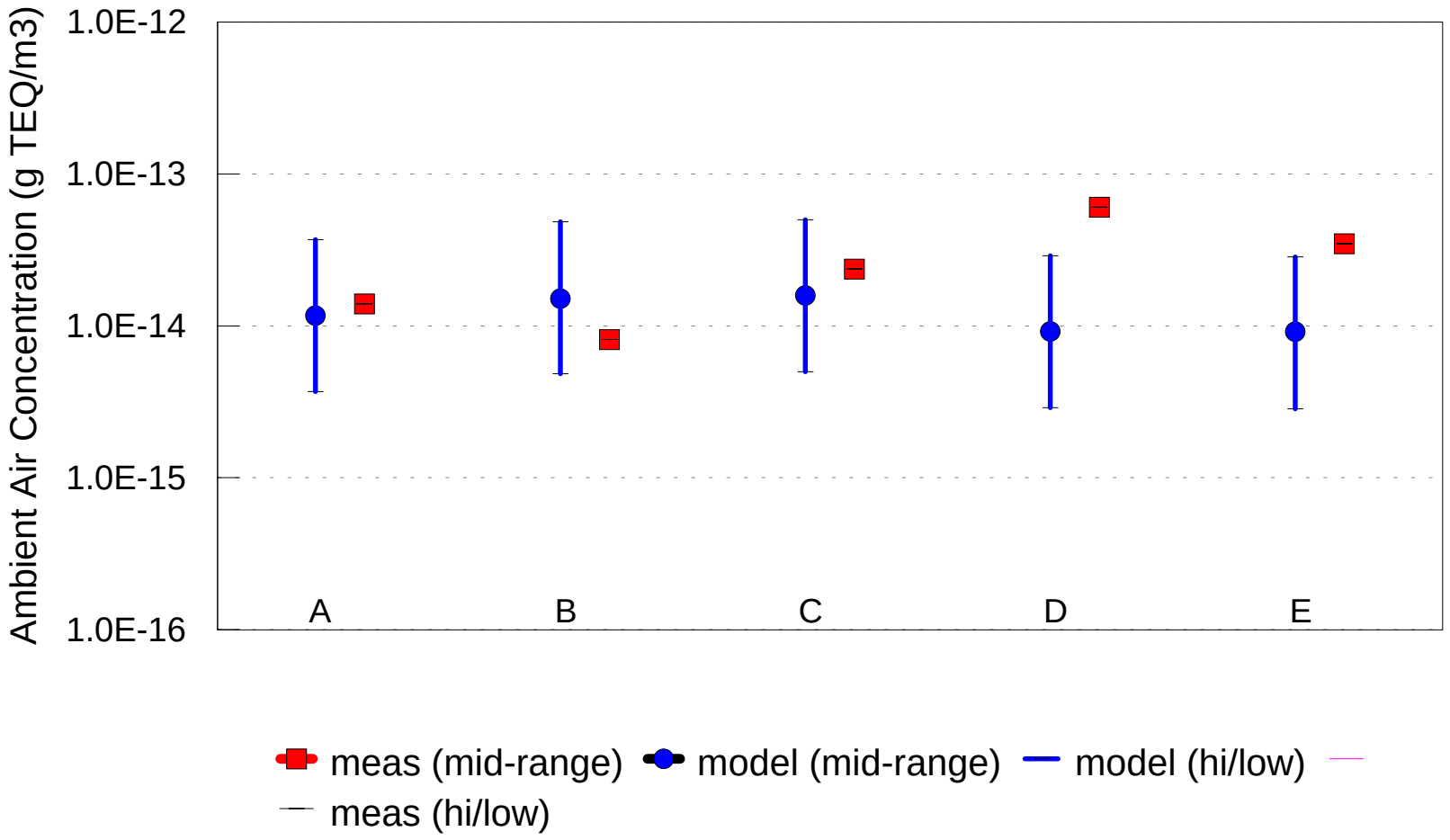

1-month samples: Mohawk Mtn CT (A-C); Northern VT (D); Southern VT (E)

Figure 32. Comparison of Model Predictions with Ambient Measurements at Month-Long Sample Sites
OCDF

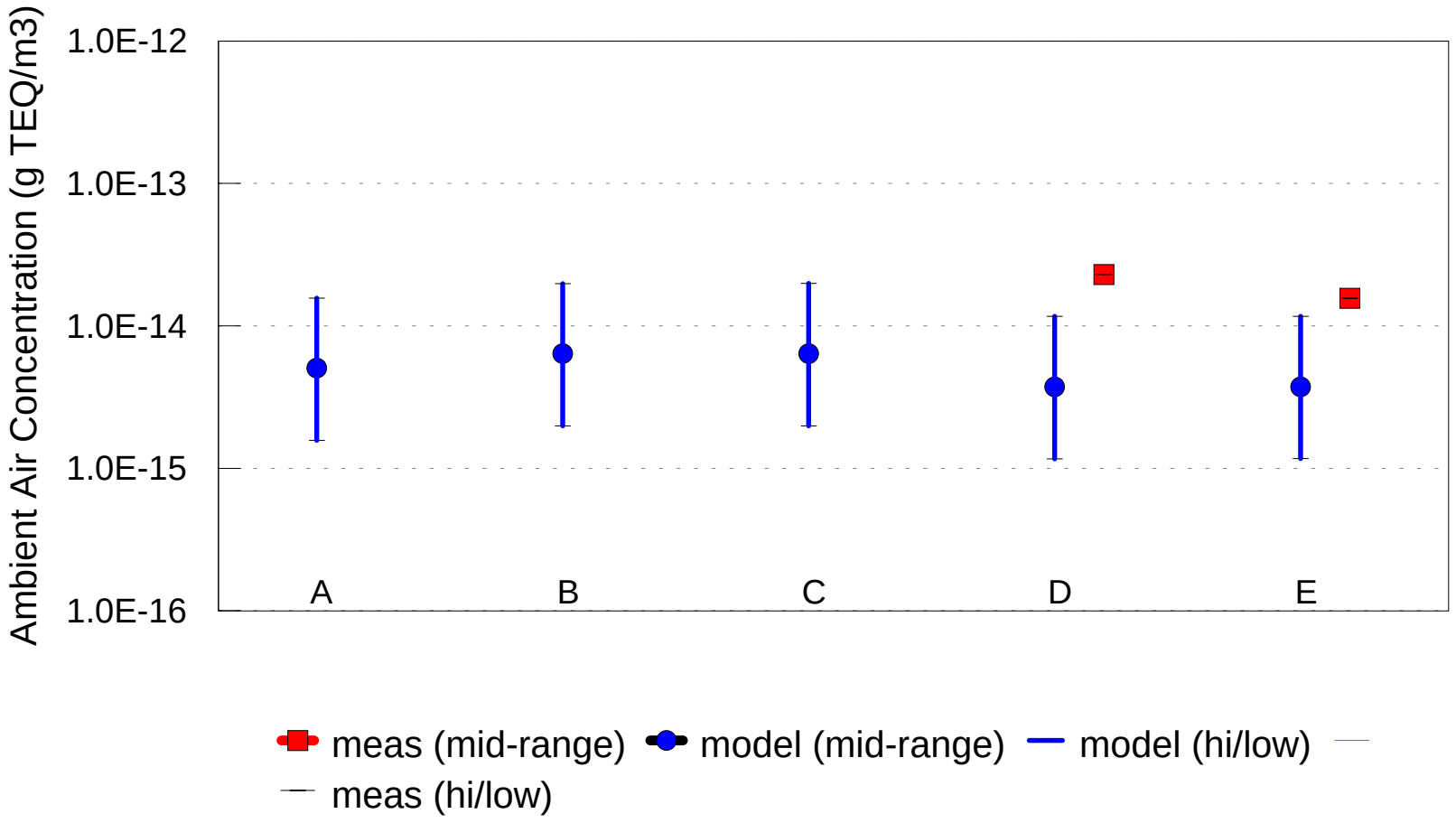

1-month samples: Mohawk Mtn CT (A-C); Northern VT (D); Southern VT (E)
(Note: no data were available for OCDF at the three CT sites)

5. Sensitivity Analyses of Spatial Interpolation Methodology

As a screening analysis, the interpolation procedure was directly evaluated by comparing its predictions against a series of explicitly simulated source locations. Eleven such "spatial interpolation test locations" were selected, as shown in Figure 3 of the main body of this paper. Twelve different schemes were used, corresponding to values of *n*,*a*, and *b* of the following: *n* = 2,3,4, and 5; *a* = *b* = 1,2, and 3 [see Section 3 (equation 7) above for the meaning of these variables]. The results of these tests are summarized in Figure 33. It can be seen that the overall accuracy of the interpolation is not particularly sensitive to the values of *n*, *a*, and *b* chosen, but, that for the evaluation above, the best-performing values were *n*,*a*,*b* = 4,2,2 and 4,1,1, respectively. We used the" 422" scheme as the default method in this analysis. It should be noted that the test locations were not chosen for their overall importance as source regions contributing PCDD/F to the Great Lakes, but, for their ability to provide a general sense of the level of errors one might expect in the interpolation procedure.

To provide a more comprehensive measure of the potential errors introduced in the spatial interpolation procedure, the total deposition of dioxin to each of the Great Lakes was estimated using different parameter values for the spatial interpolation methodology. The entire emissions inventory was used, i.e., a full analysis was conducted. A summary of results for these different analyses is presented below in Table 4 and Figure 34, for the same set of twelve interpolation schemes. It can be seen that the variation in total deposition arising from the use of different interpolation procedures with 84 standard source locations is at most on the order of 5%, and in most cases is much less than this.

Figure 33. Errors associated with different interpolation schemes in predicting explicitly simulated transfer coefficients to the Great Lakes

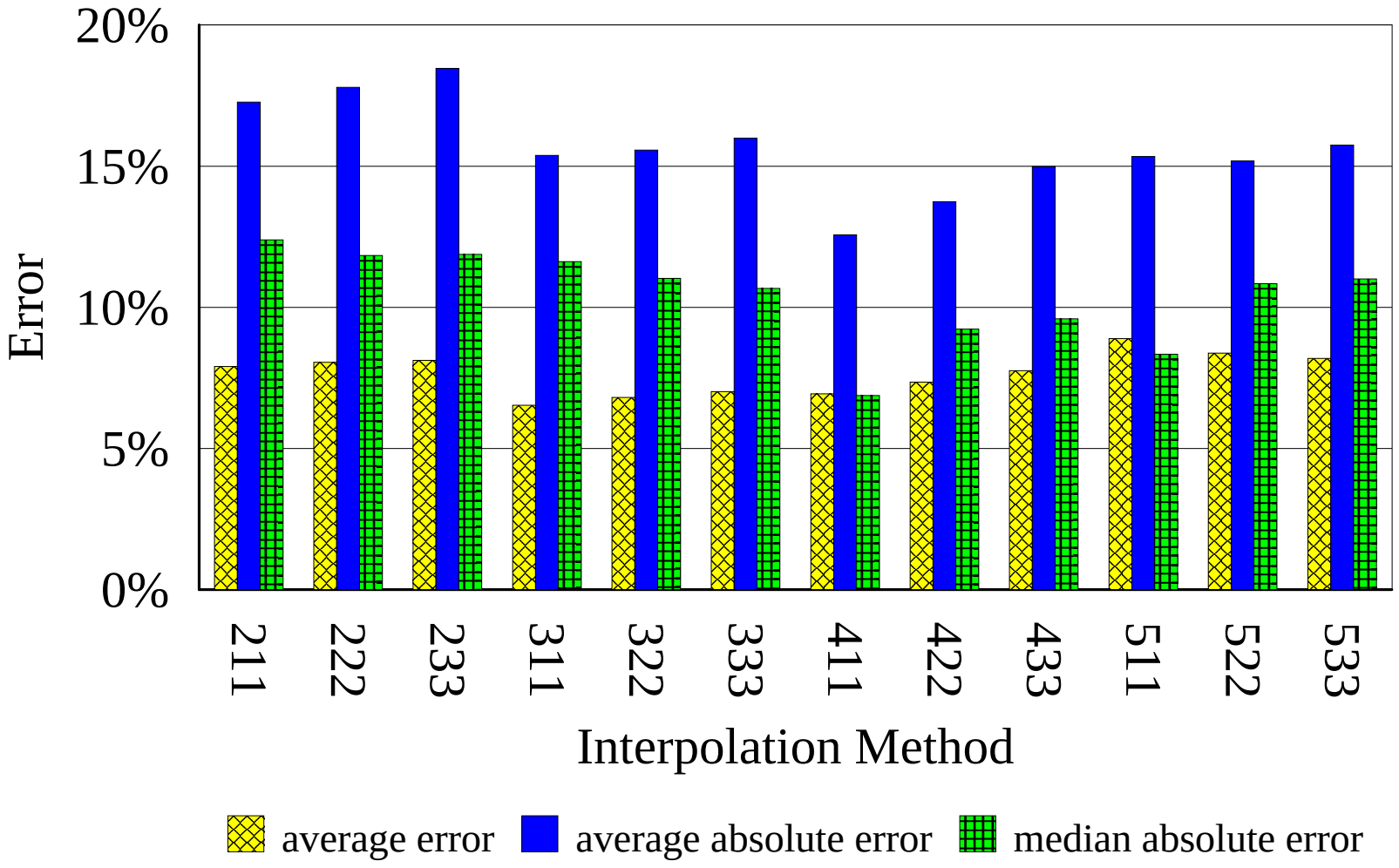

Figure 34. Influence of different spatial interpolation methodologies on the total estimated 1996 dioxin deposition to the Great Lakes (g TEQ/year).

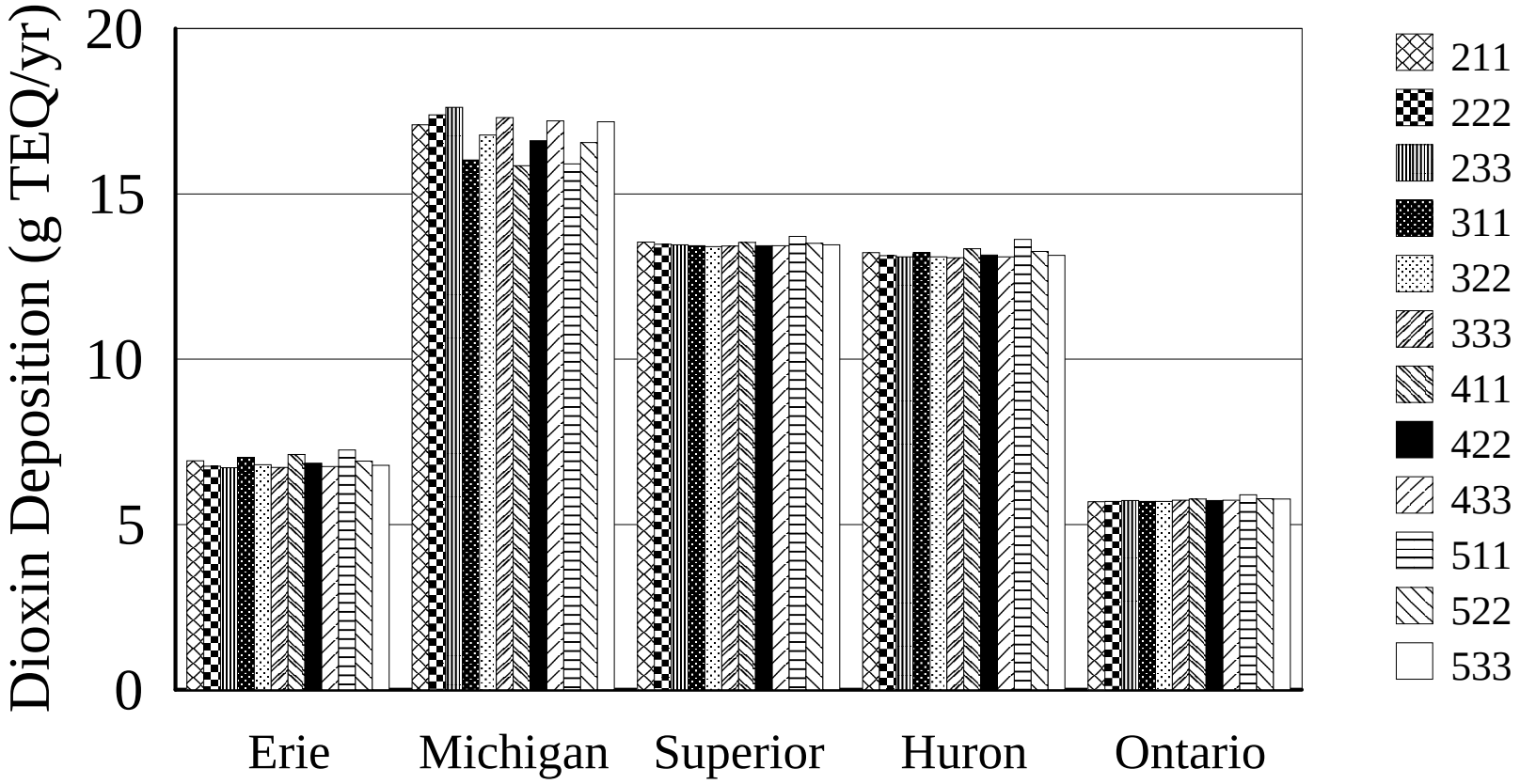

In these simulations, the default fate parameters & algorithms were used (e.g., dry deposition method "A")
"211" represents the spatial interpolation method where the 2 closest points are selected,
and the exponent on the distance and angular weighting factors are 1 and 1, etc

Table 4. Summary of Interpolation Method Sensitivity Calculations						
Lake	Model-Estimated 1996 Atmospheric Deposition of Dioxin to the Great Lakes (grams TEQ/year)					
	base case: 84 standard source locations, interpolation scheme = *422*	84 standard source locations, interpolation scheme = *411*	12 interpolation sensitivity calculations (84 standard source locations)		abbreviated calculation (28 standard source locations)	
			avg. for all methods (*211, 222,* ...)	standard deviation for all methods	interpolation scheme = *422*	interpolation scheme = *411*
Erie	6.85	7.12	6.89	0.16	6.50	6.64
Michigan	16.61	15.86	16.80	0.58	16.99	15.65
Superior	13.44	13.53	13.49	0.08	12.43	12.56
Huron	13.15	13.34	13.21	0.15	12.95	13.24
Ontario	5.73	5.78	5.75	0.06	5.92	5.98

6. The Effect of Variations in PCDD/F Atmospheric Fate Estimation Methodologies on the Total Predicted Deposition to the Great Lakes

To investigate the impact of particularly uncertain aspects of the fate and transport modeling, a series of abbreviated analyses were performed, using the same emissions inventory.

In these analyses, only 28 standard source locations were used (1/3 the number in the "full" calculation discussed above). The calculations were abbreviated to allow a number (6) of additional fate variations to be analyzed without unnecessarily increasing computational requirements. Table 4 above shows the results of this abbreviated calculation for the "422" interpolation scheme (the default scheme) and the "411" scheme. It can be seen that the overall predicted deposition to the Lakes with either abbreviated 28-location calculations is comparable (within ~10%, and generally much closer) to the estimates of the full 84-location calculation. Thus, the abbreviated calculations should be sufficient to provide information on the sensitivity of the overall calculation to changes in the modeling methodology.

As discussed above in Section 2, important factors contributing uncertainty in the fate and transport simulation are: (a) the choice of dry deposition algorithm; (b) the in-cloud particle washout ratio; and (c) the vapor-phase photolysis rate. In this previous section, a number of different dry deposition methodologies were described and evaluated (denoted as *A*, *A′*, *B*, *C*, *D*, and *E*), and all of these but one are evaluated here. One methodology (*A′*) was not evaluated in this analysis as it was found to represent only a very slight variation from the default.

In addition to investigating the overall effect of different dry deposition estimation methodologies, the influence of variations in two other fate mechanisms was evaluated. In one variation, the particle in-cloud washout ratio was increased by a factor of 4, from 4×10^4 to 1.6×10^5 (grams pollutant per liter of air/grams of pollutant per liter of precipitation), representing what is believed to be the order of magnitude in the uncertainty in this parameter. In a second variation, the photolysis rate of vapor-phase PCDD/F was decreased to essentially zero from the base-case photolysis rate (the base-case rate was characterized by a minimum half-life of 2 days). The justifications for the base-case values and the uncertainties in these parameters are discussed above in Section 2.

While it is believed that the base-case parameterizations yielded the most accurate simulation, it is acknowledged that there is significant uncertainty in the characterization of PCDD/F atmospheric fate processes. The purpose of comparing these five different dry deposition approaches and variations in the wet deposition and photolysis rates is to provide a measure of the influence of these uncertainties on the overall modeling results.

Figure 35 shows the 1996 model-predicted PCDD/F deposition to each of the Great Lakes with the various methodological variations described above. For comparison, the results for the "base case", with dry deposition method *A* and 84 standard source locations, are included. Predicted deposition for the various simulations are generally within a factor of 3 of the base-case results, and in most cases, the differences are somewhat less than this.

Figure 15 *in the main body of this paper* shows the relative contributions from sources within different distance ranges from Lake Superior for the same eight simulation methodologies, including the base-case results. It can be seen that the same general pattern exists for all the variations. While not shown here, the same consistency was found for the other Great Lakes.

Figure 36 shows the effect of the same methodological variations on the relative contribution of different source sectors to Lake Huron (as an example). In this figure, source types were aggregated into three different general categories – waste incineration, metallurgical operations, and fuel combustion. More detailed results for sub-classifications of these different general categories are presented in the main body of this paper (Figure 13) and in Section 7 below. This figure illustrates that the relative contributions of different source categories are essentially the same for all the simulation methodologies used. While not presented here, the same consistency was found for the other Great Lakes, and, for more detailed breakdowns of source categories.

Figure 35. Effect of Fate Simulation Variations on the Total Predicted Deposition of PCDD/F to the Great Lakes

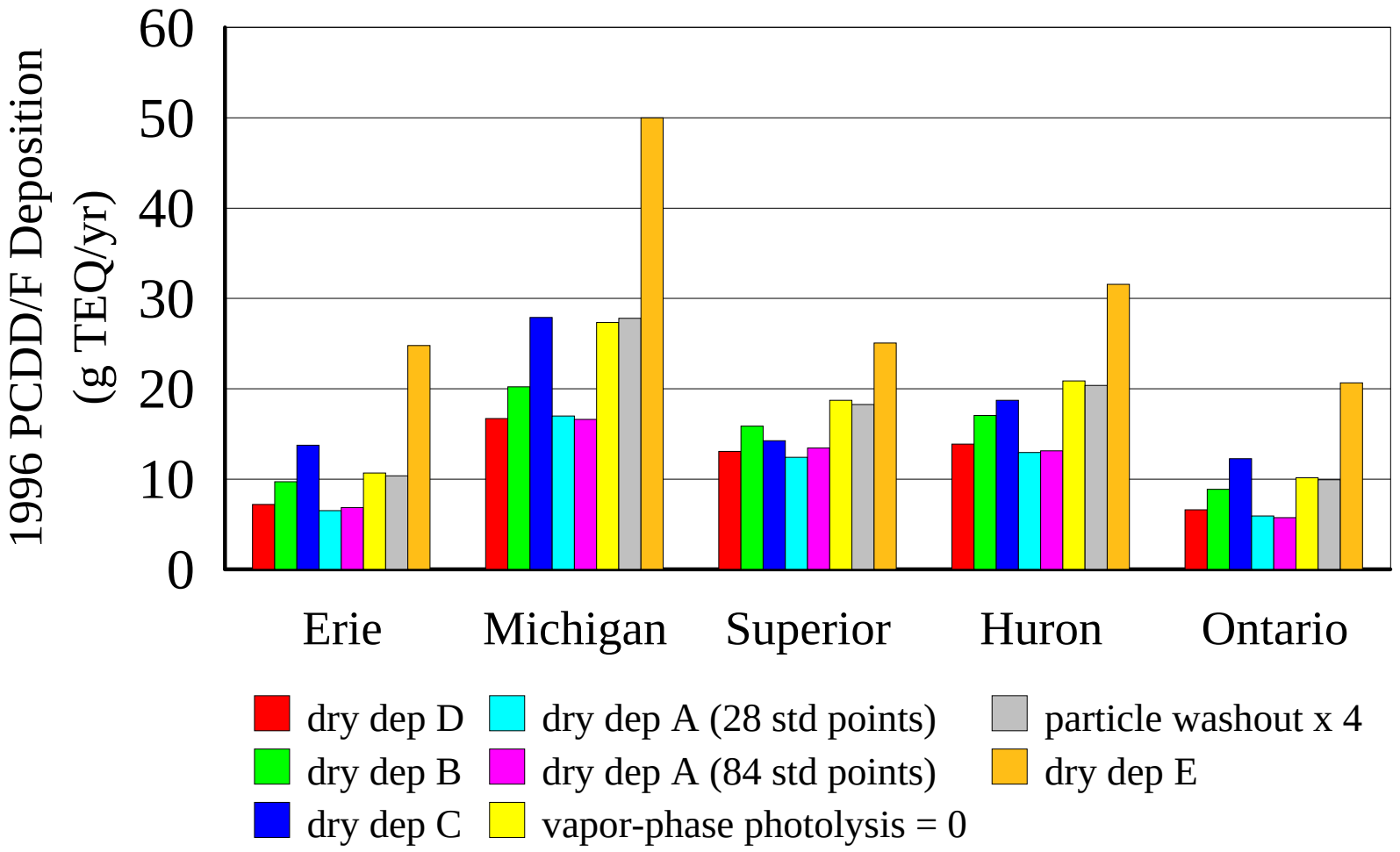

Figure 36. Effect of Fate Simulation Variations on the Relative PCDD/F Contributions of Different Source Sectors to Lake Huron

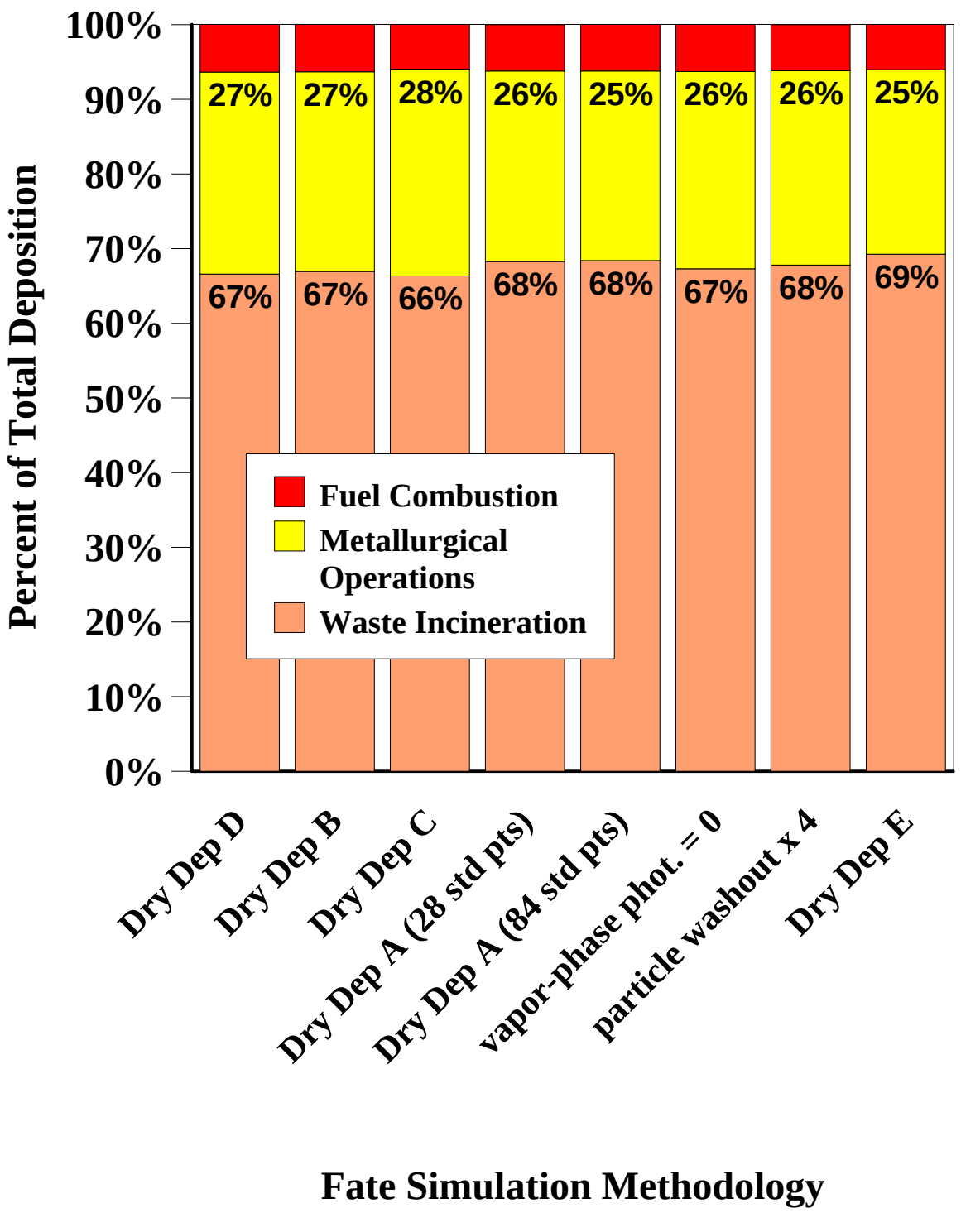

7. Deposition to the Great Lakes for 1996

Figure 12 in the main body of this paper shows the estimated contributions to the 1996 atmospheric to Lake Superior. Figures 37-40 below present comparable figures for the other Great Lakes.

Figure 14 in the main body of this paper shows the emissions and deposition arising from within different distance ranges of Lakes Superior and Michigan. Figures 41-43 show the analogous data for the other Great Lakes. In order to see the differences between the Lakes more clearly, Figure 44 shows these data for each of the Great Lakes (together on the same page).

Figure 45 shows the emissions and atmospheric deposition contributions from within and outside the overall Great Lakes watershed. This figure shows that less than 50% of the dioxin deposition to each of the Great Lakes (or to the Lakes as a whole) arises from the entire Great Lakes watershed. For any given lake, an even smaller fraction would be contributed from sources within that individual lake's watershed. These results indicate that transport from both inside and outside the Great Lakes Basin contributes significantly to the atmospheric deposition of dioxin to the Great Lakes.

Figure 13 in the main body of this paper shows the fraction of estimated 1996 PCDD/F atmospheric deposition contributions to Lake Superior from U.S. and Canadian sources arising from different source categories. Figures 46-49 below show analogous data for the other Great Lakes.

Figure 50 summarizes the per-capita contribution of generalized source categories to the annual dioxin deposition flux (grams TEQ deposited per square kilometer of lake) to each lake. In order to summarize these results succinctly, the various source categories in the inventories were aggregated into three general categories: incineration, metallurgical processes, and fuel combustion. The estimated impacts (grams TEQ deposited to a given lake per year from each category) were divided by the area of the lake to get a flux (grams TEQ per km^2 per year). This normalization by lake area was done so that the deposition contributions to the lakes could be compared on an equal basis. That is, all things being equal, there will be more atmospheric deposition (e.g., grams per year) to a large lake than a small lake (since the surface area for deposition is larger), but, a large and small lake will have the same atmospheric deposition flux (e.g., grams per year per square kilometer of lake). This flux amount was then divided by the population of the source country to obtain a per-capita value for the contribution. On average, using 1995-1996 emissions inventory data, various types of incinerators were the major source category of dioxin deposition to the entire Great Lakes basin.

Finally, Figures 51-55 show the model-estimated total 1996 deposition for different PCDD/F homologue groups to each of the Great Lakes. Dry deposition appears to be generally less important than wet deposition for most congeners, but this is somewhat influenced by the choice of dry deposition methodology. In preparing these figures, the default dry deposition methodology was used. However, dry deposition to the Lakes is larger in some other deposition estimation schemes (e.g., method *E*, as described in Section 2 above).

Figure 37. Mid-Range Estimate of the Contributions to 1996 Atmospheric Deposition of Dioxin to Lake Michigan (µg TEQ/km²-yr)

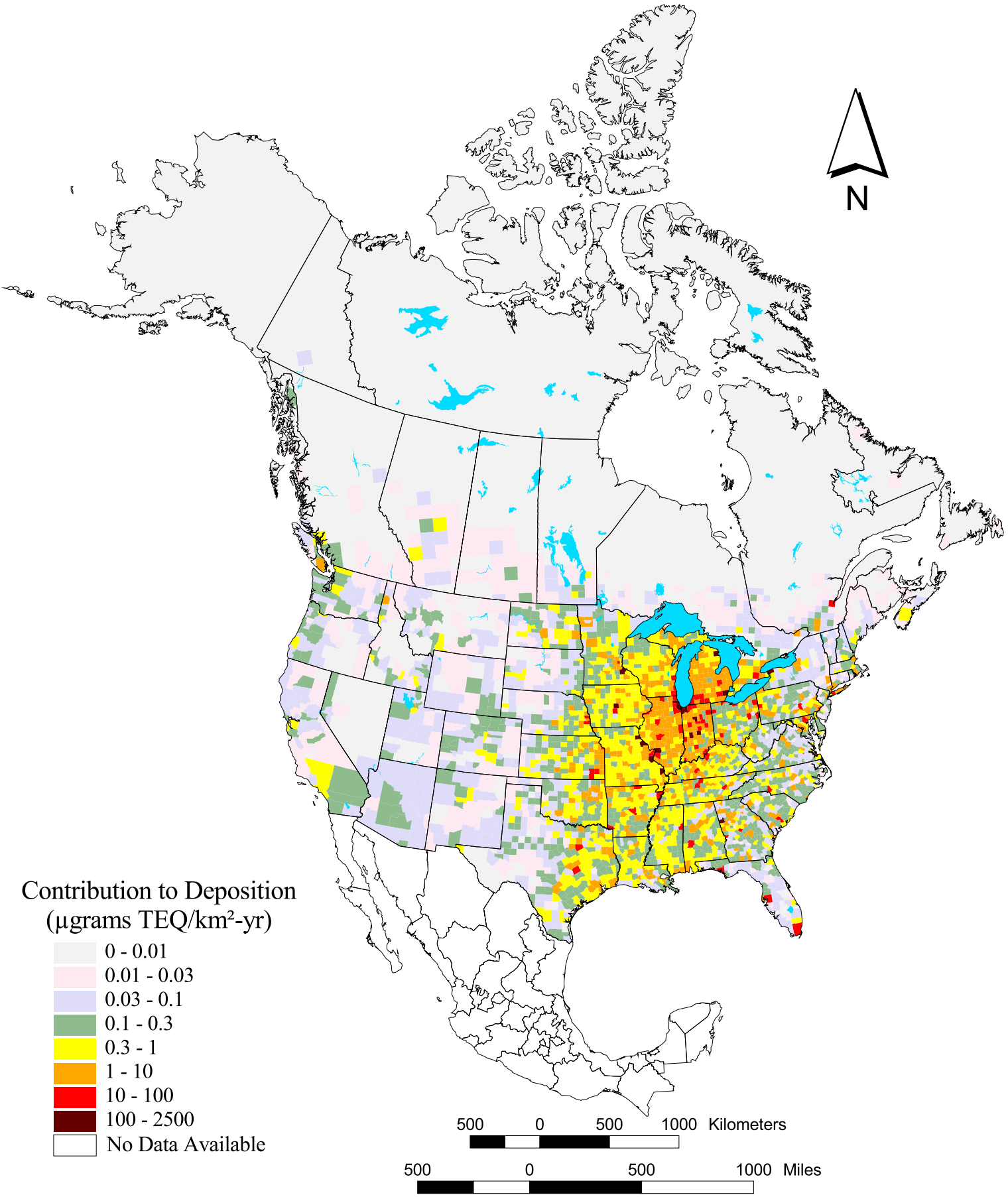

Figure 38. Mid-Range Estimate of the Contributions to 1996 Atmospheric Deposition of Dioxin to Lake Huron (µgTEQ/km²-yr)

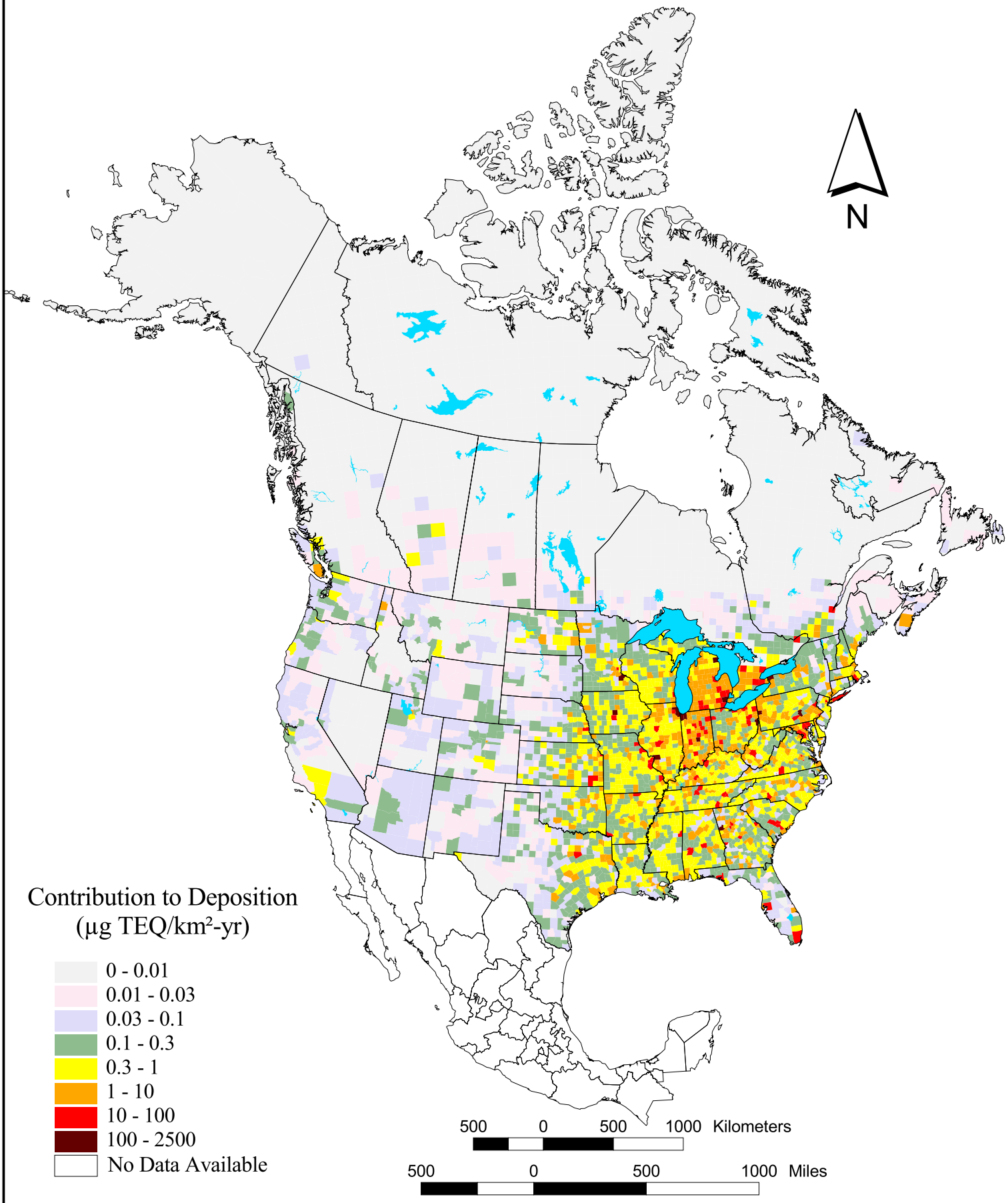

Figure 39. Mid-Range Estimate of the Contributions to 1996 Atmospheric Deposition of Dioxin to Lake Erie (µg TEQ/km²-yr)

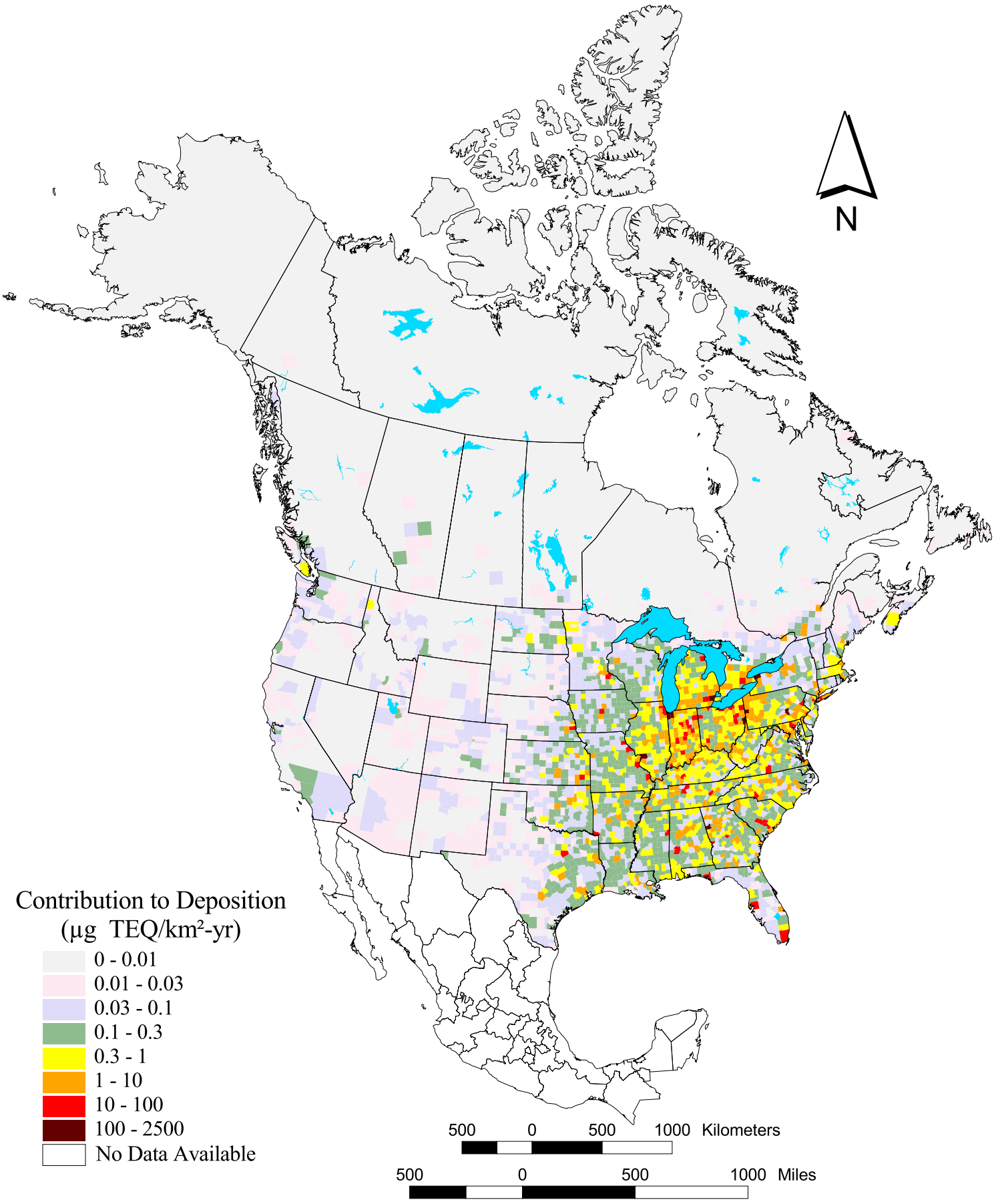

Figure 40. Mid-Range Estimate of the Contributions to 1996 Atmospheric Deposition of Dioxin to Lake Ontario (µg TEQ/km²-yr)

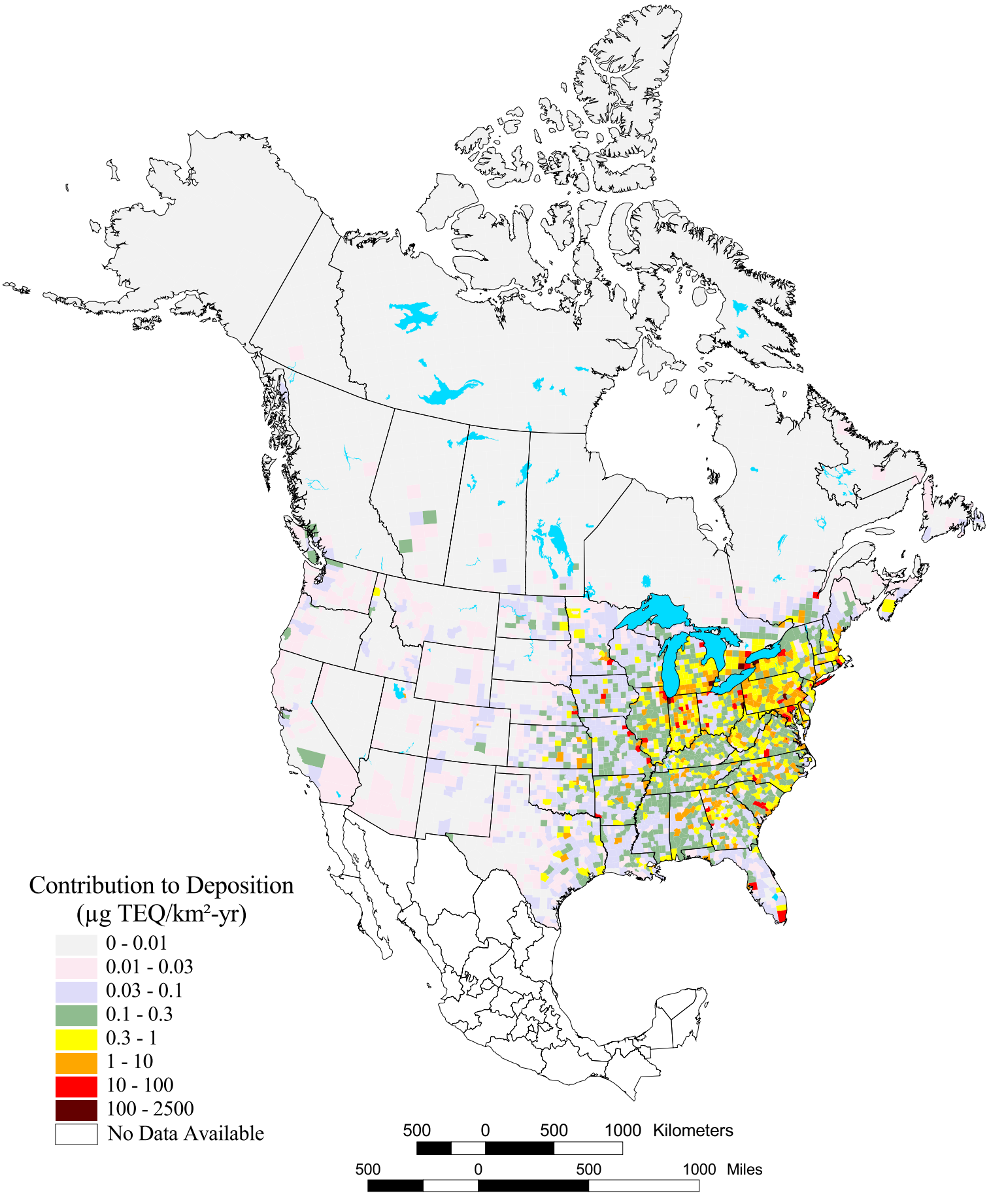

Figure 41. Percent of Total Emissions or Total Deposition of Dioxin (1996) Arising from Within Different Distance Ranges from Lake Huron

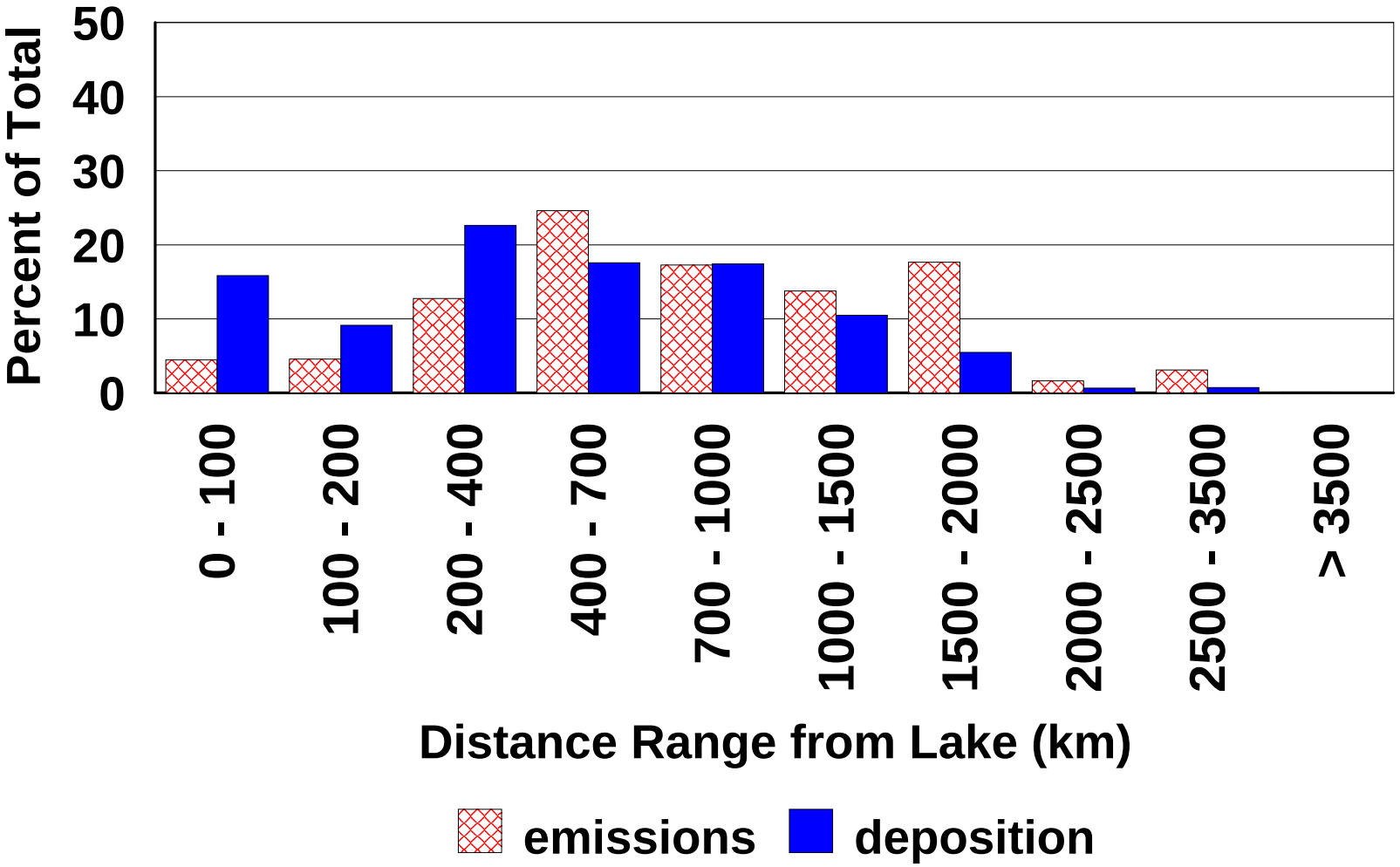

Figure 42. Percent of Total Emissions or Total Deposition of Dioxin (1996) Arising from Within Different Distance Ranges from Lake Erie

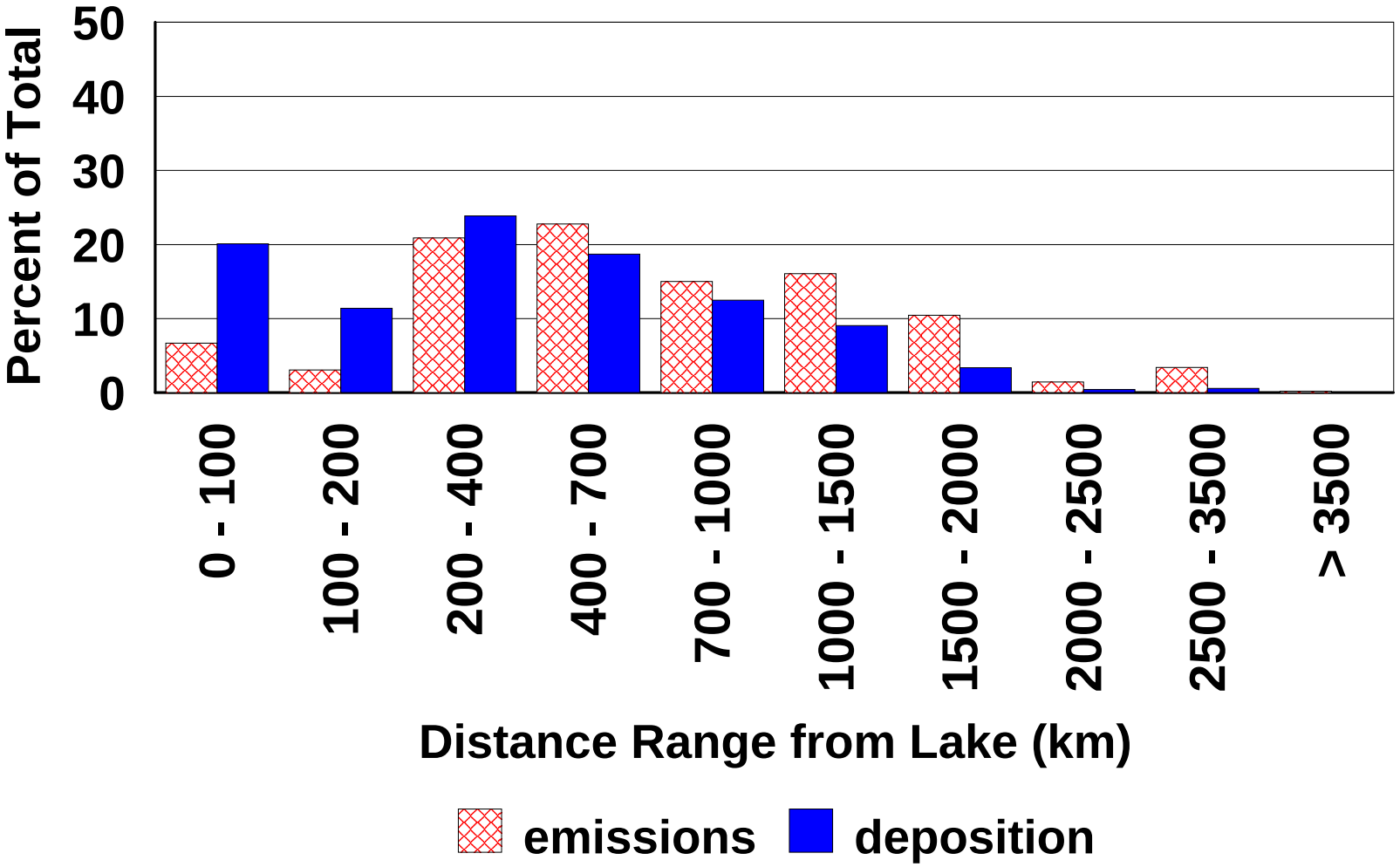

Figure 43. Percent of Total Emissions or Total Deposition of Dioxin (1996) Arising from Within Different Distance Ranges from Lake Ontario

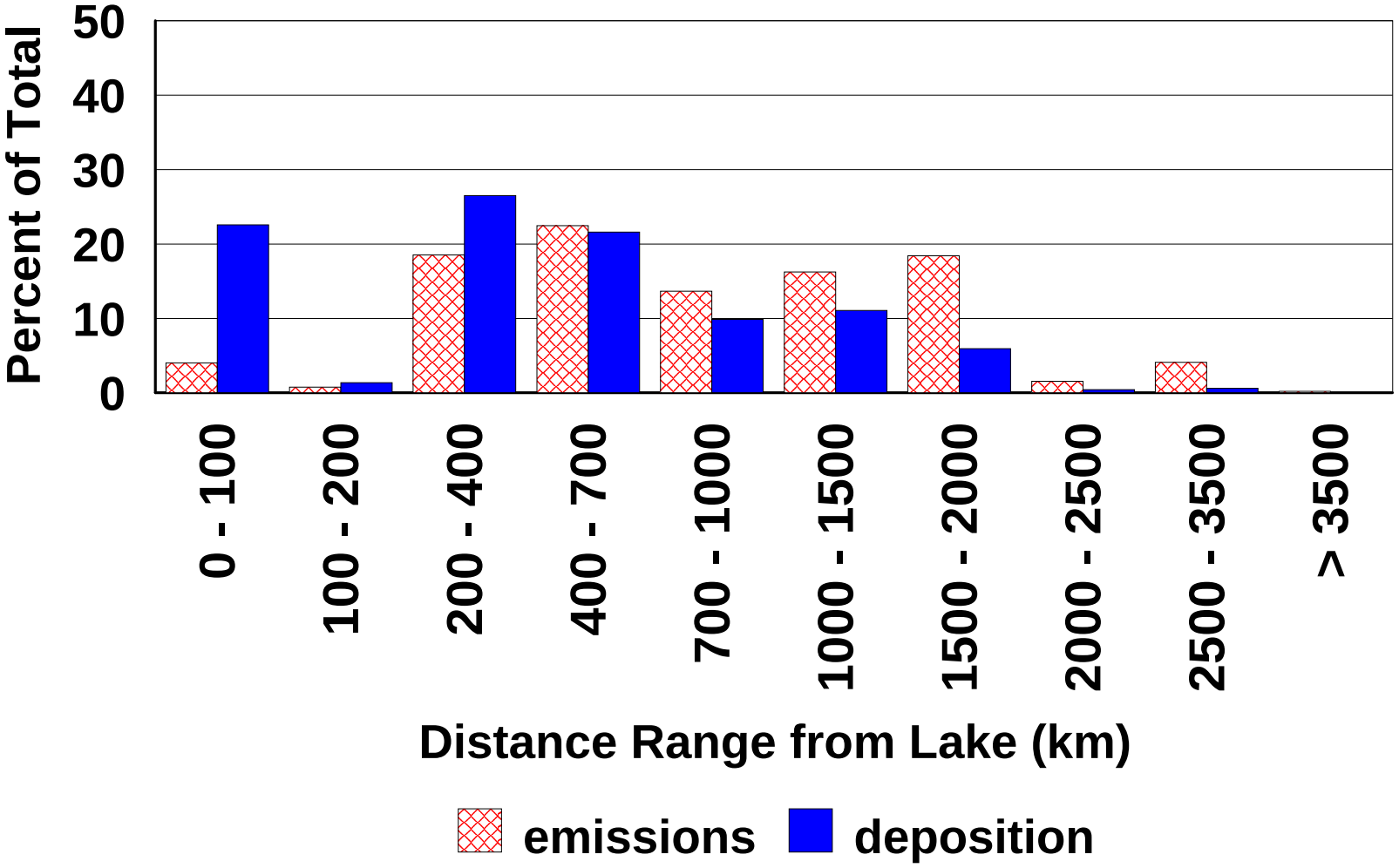

Figure 44. Percent of Total Emissions or Total Deposition of Dioxin (1996) Arising from Within Different Distance Ranges From Each of the Great Lakes

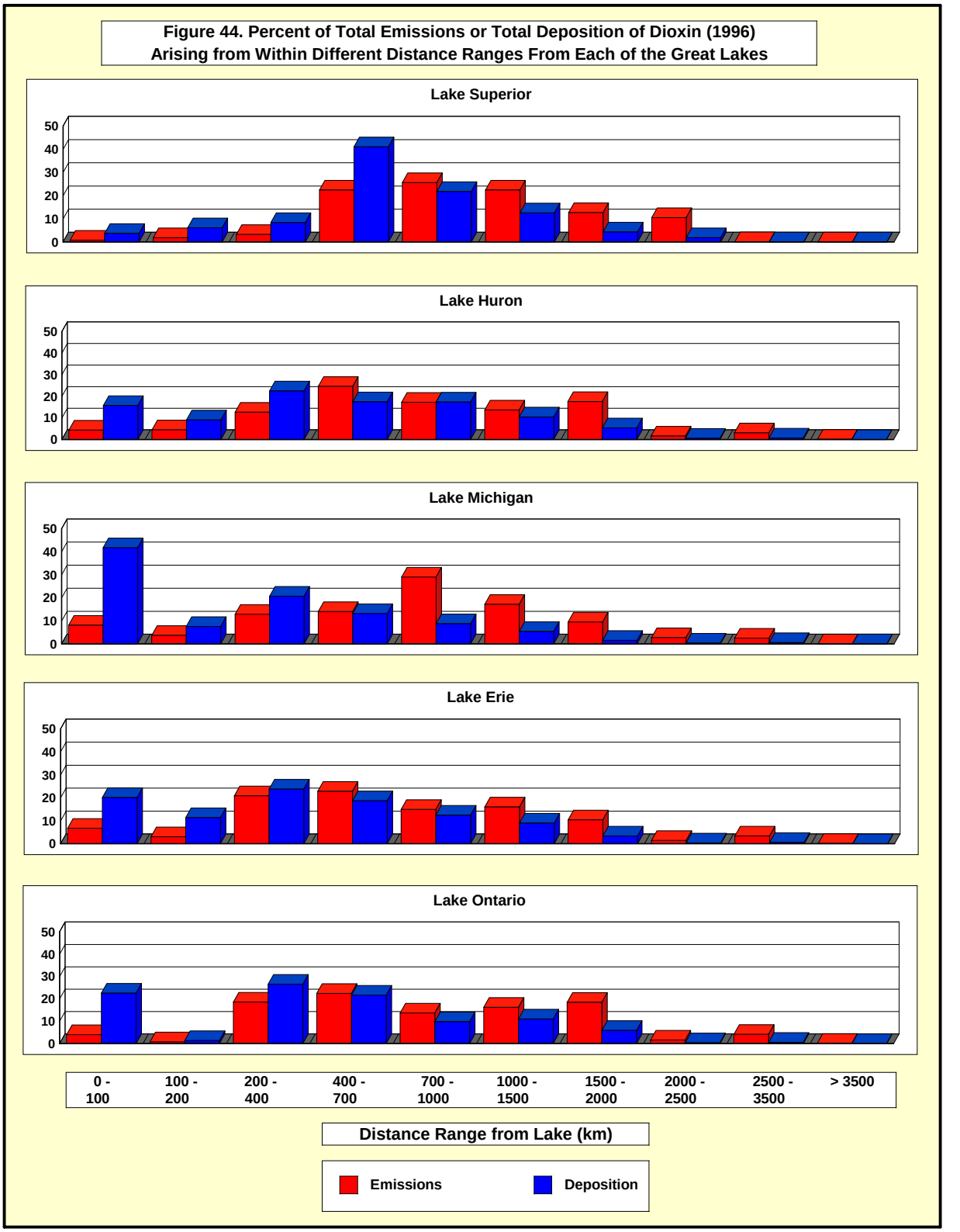

Figure 45. Air Emissions and Atmospheric Deposition Contributions to the Great Lakes from Within and Outside the Overall Great Lakes Watershed (from air emissions sources in the United States and Canada, 1996)

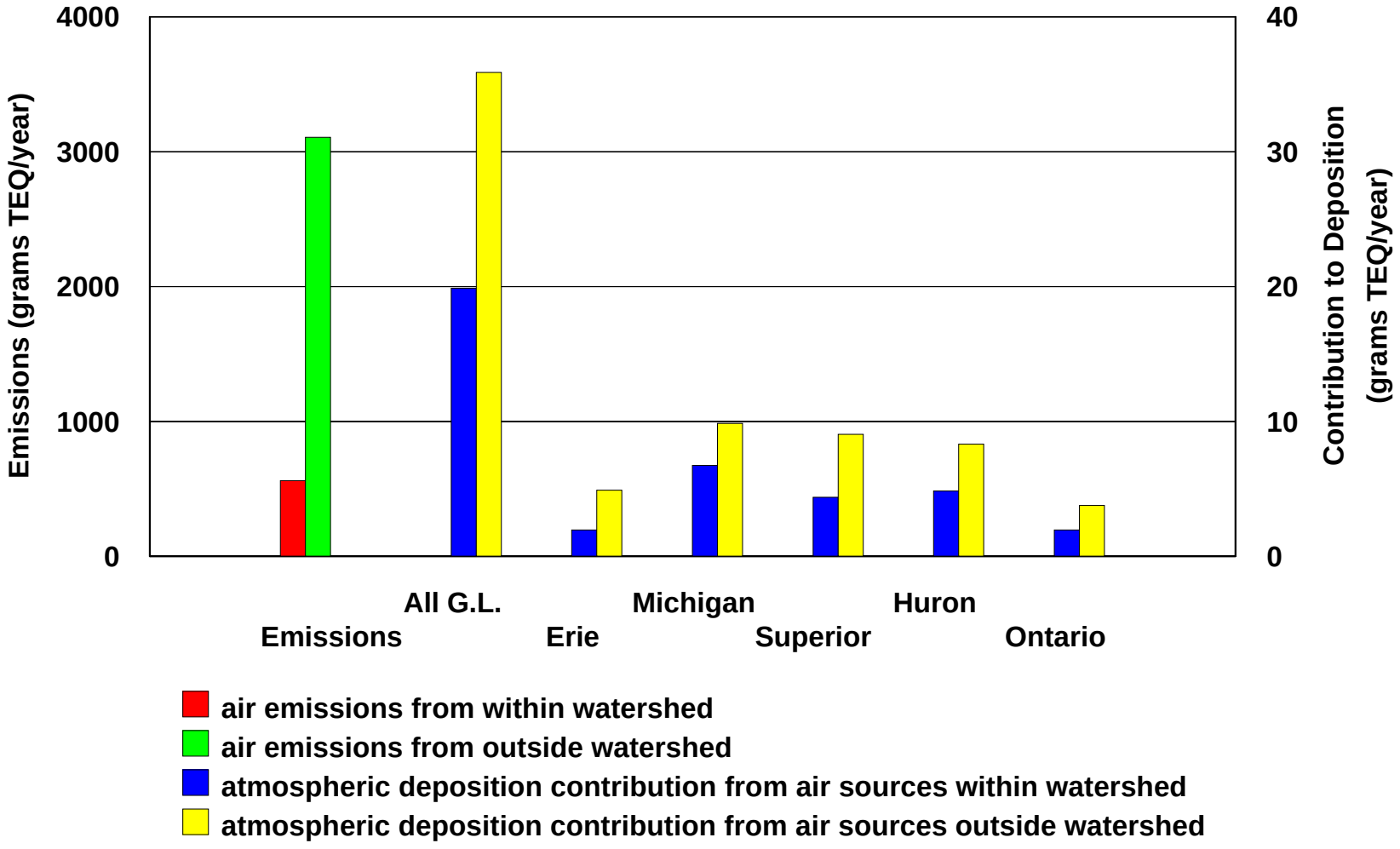

Figure 46. Fraction of estimated 1996 PCDD/F atmospheric deposition contributions to Lake Michigan from U.S. and Canadian sources arising from different source categories

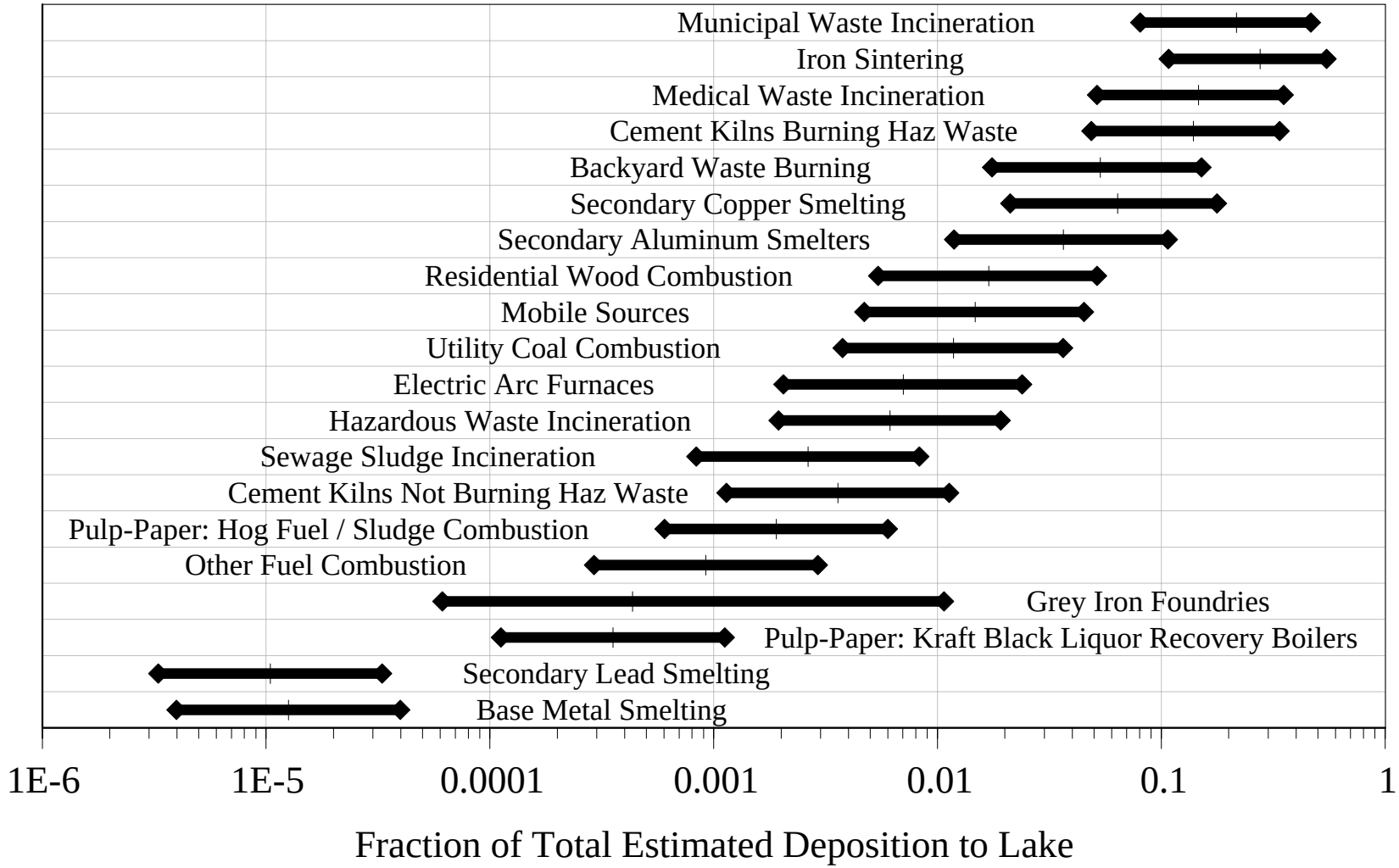

Figure 47. Fraction of estimated 1996 PCDD/F atmospheric deposition contributions to Lake Huron from U.S. and Canadian sources arising from different source categories

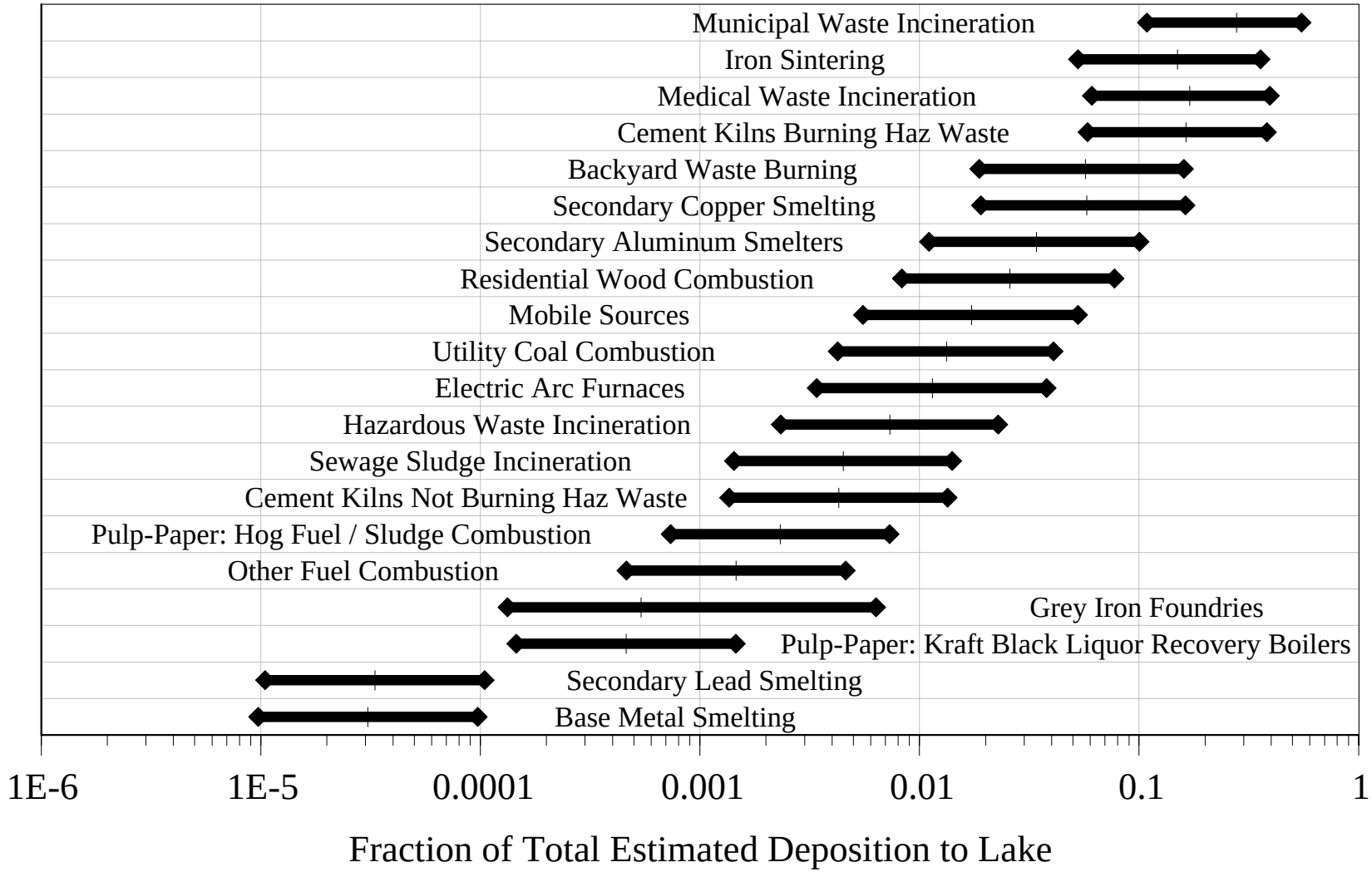

Figure 48. Fraction of estimated 1996 PCDD/F atmospheric deposition contributions to Lake Erie from U.S. and Canadian sources arising from different source categories.

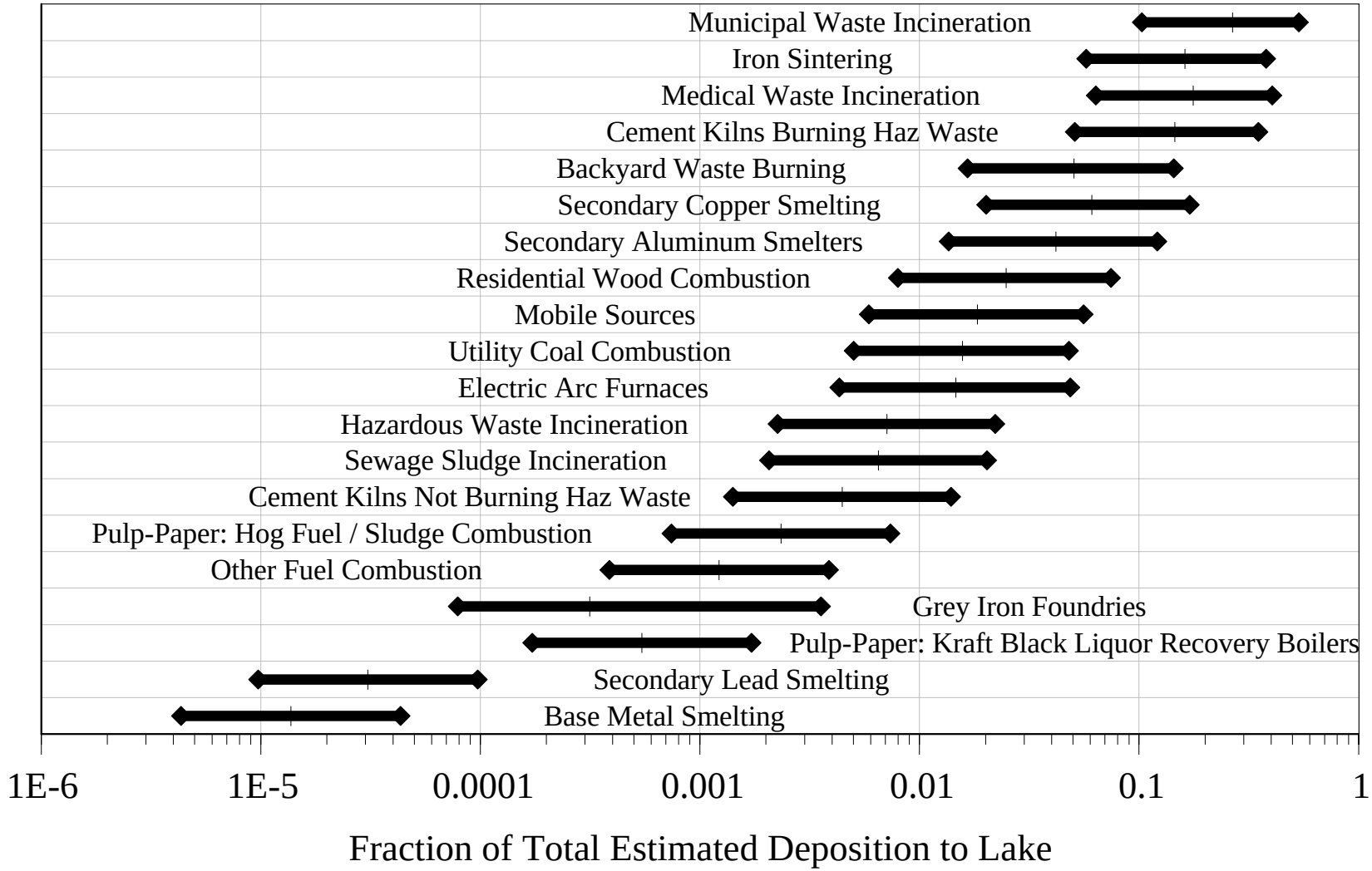

Figure 49. Fraction of estimated 1996 PCDD/F atmospheric deposition contributions to Lake Ontario from U.S. and Canadian sources arising from different source categories

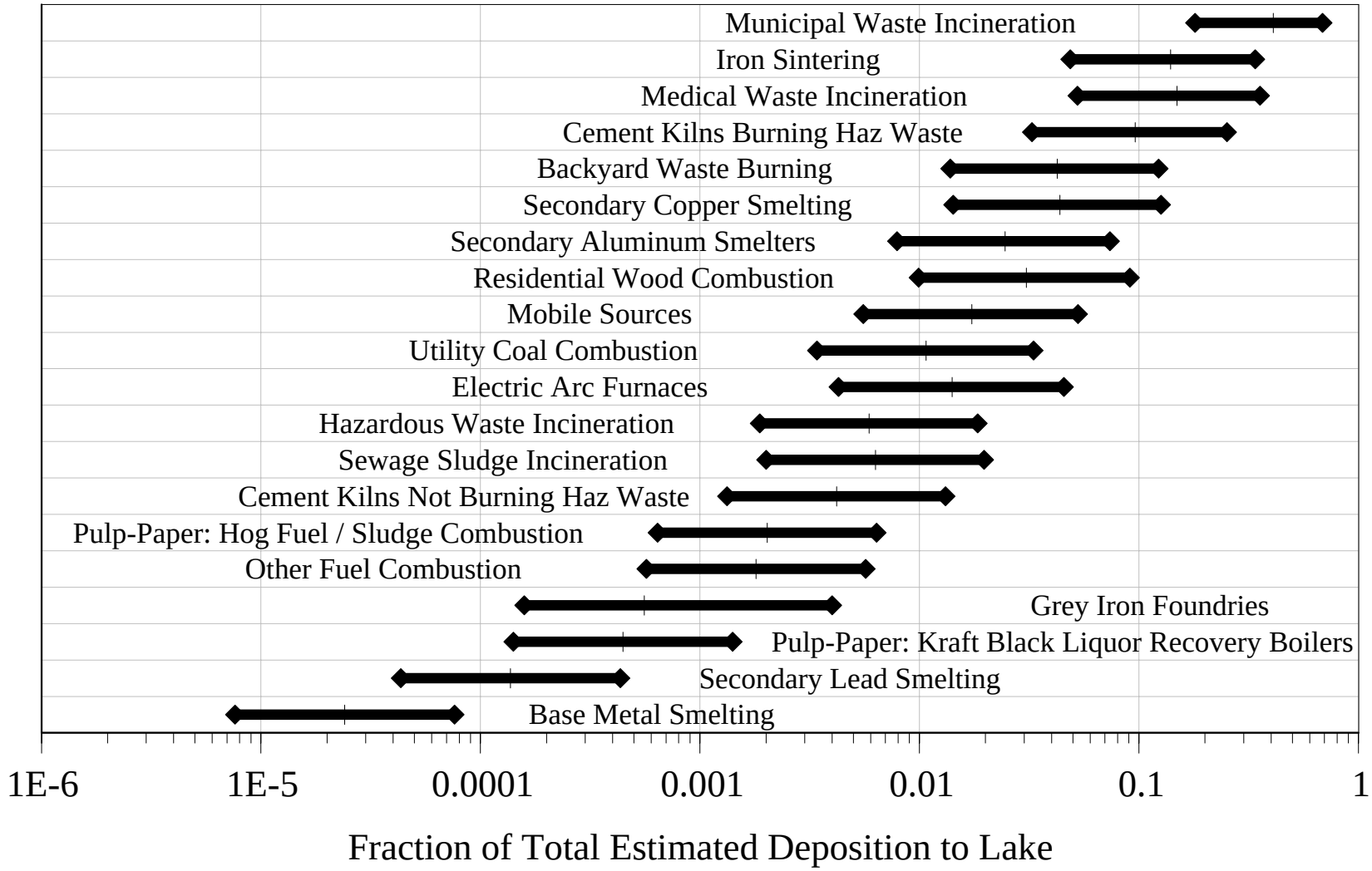

Figure 50. Contribution of Different Source Sectors to Atmospheric Deposition of Dioxin (pg TEQ deposition / km2) / (person - year)

(Each country's annual deposition flux contribution amount normalized by their total population)

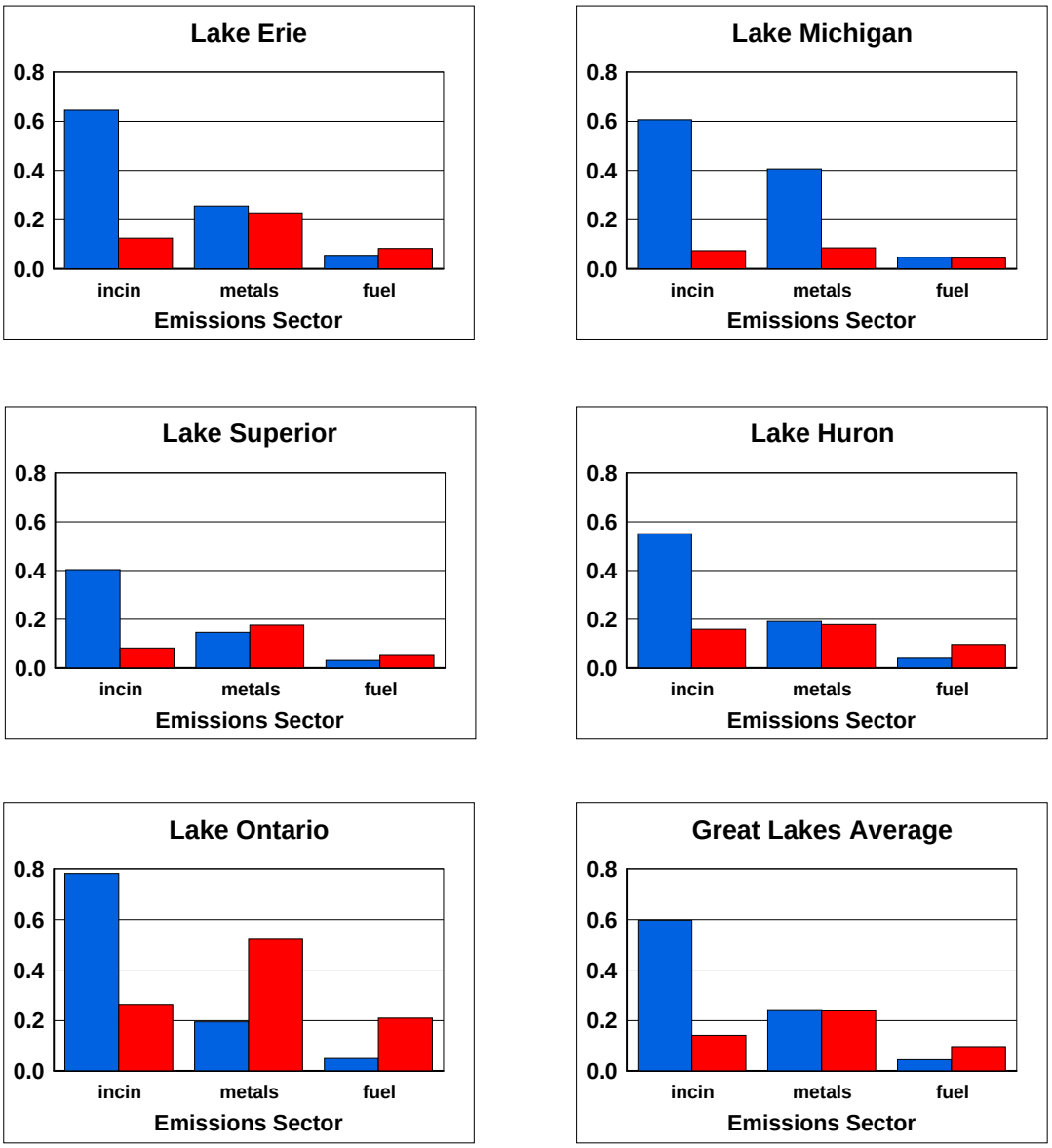

"incin" = waste incineration; "metals" = metallurgical processing; "fuel" = fuel combustion

Figure 51. Model-estimated total 1996 deposition for different PCDD/F homologue groups to Lake Superior

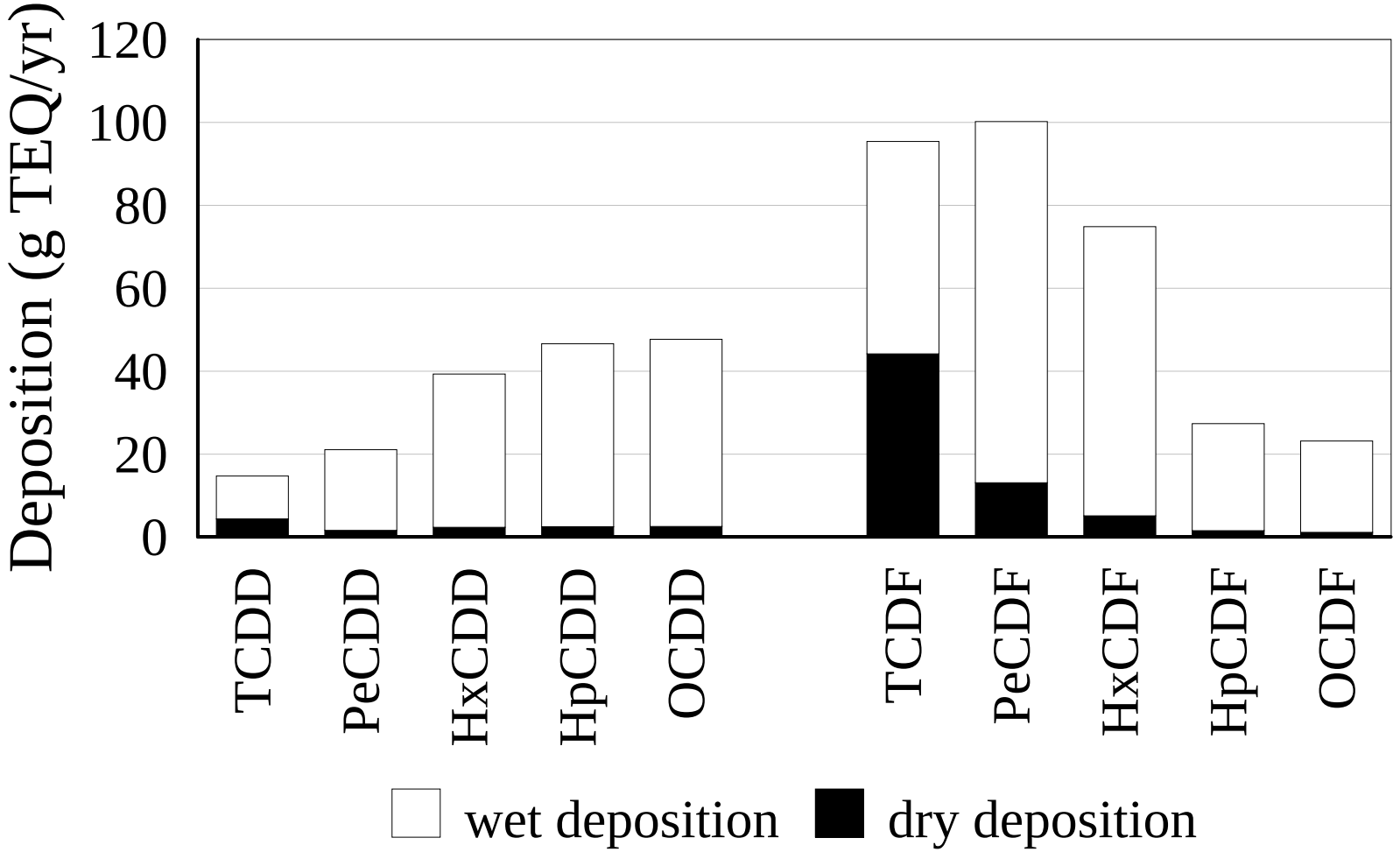

Figure 52. Model-estimated total 1996 deposition for different PCDD/F homologue groups to Lake Michigan

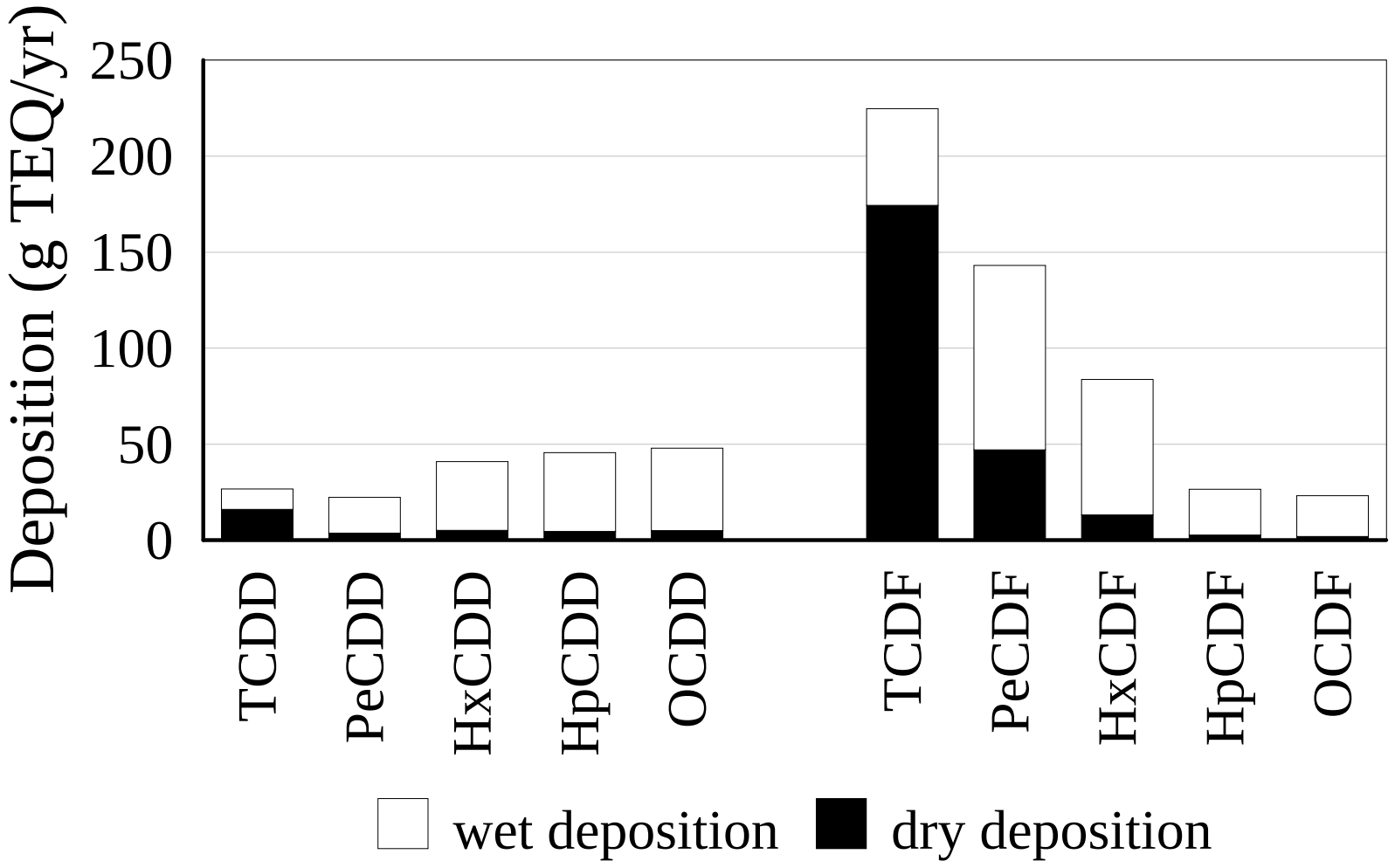

Figure 53. Model-estimated total 1996 deposition for different PCDD/F homologue groups to Lake Huron

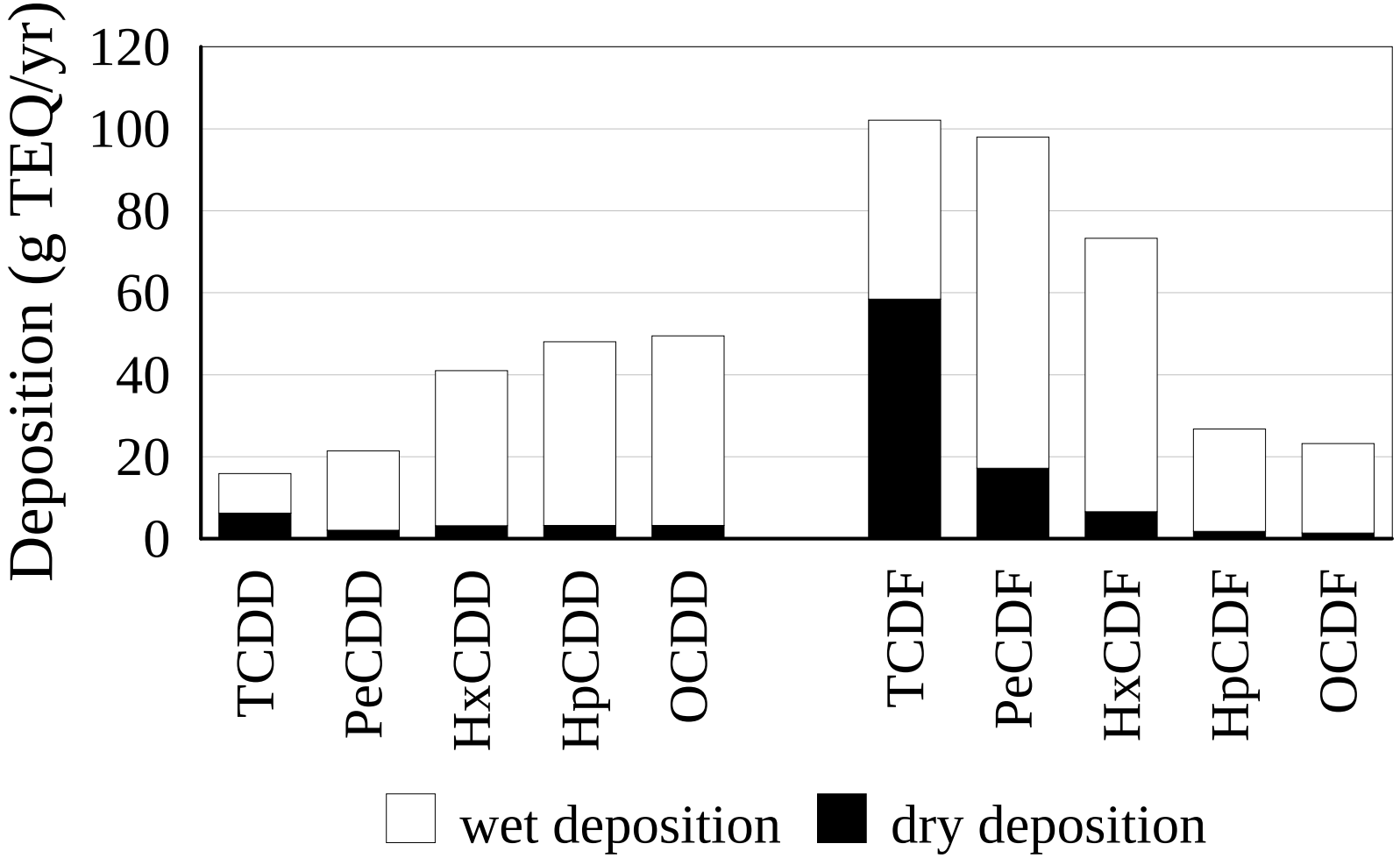

Figure 54. Model-estimated total 1996 deposition for different PCDD/F homologue groups to Lake Erie

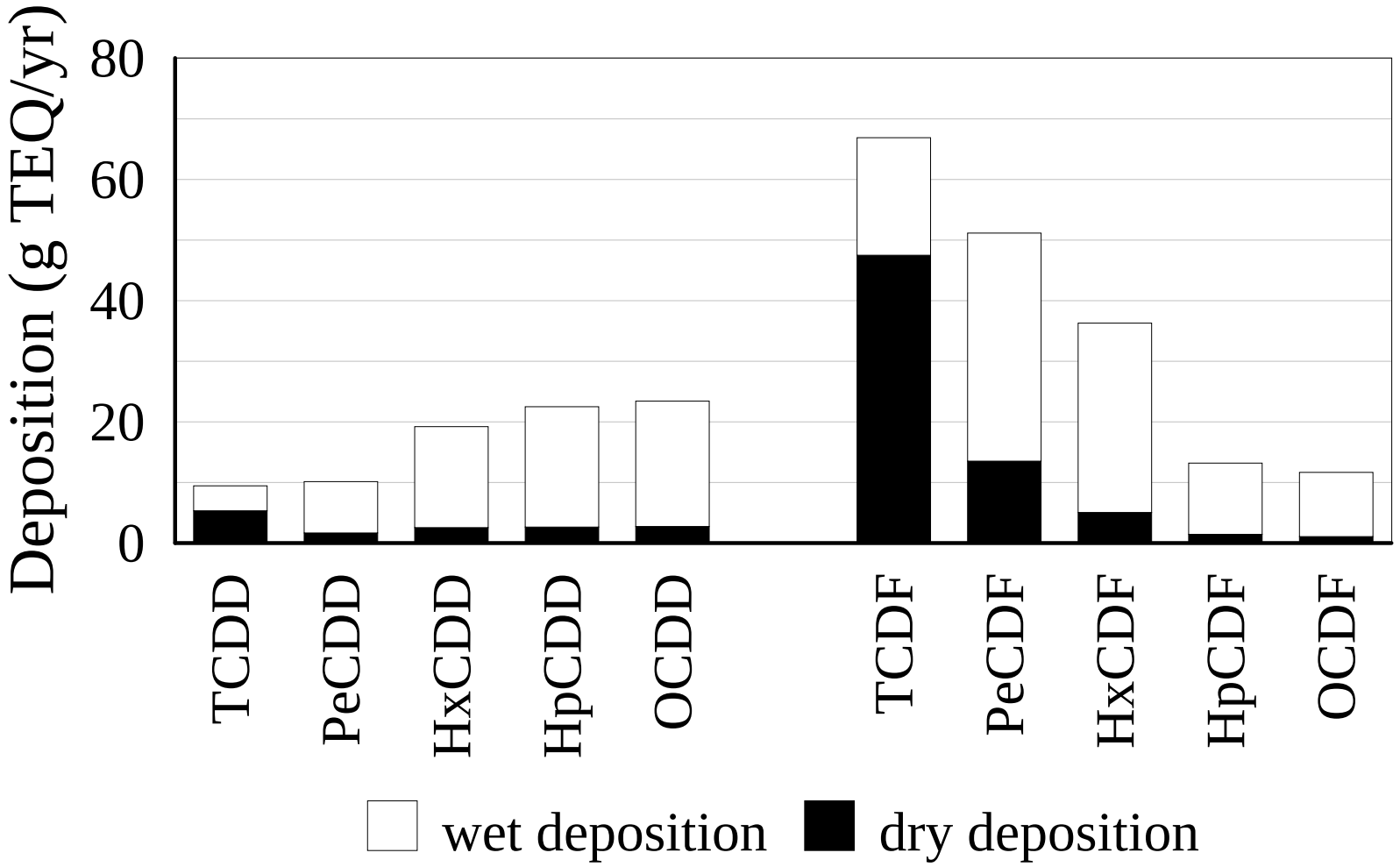

Figure 55. Model-estimated total 1996 deposition for different PCDD/F homologue groups to Lake Ontario

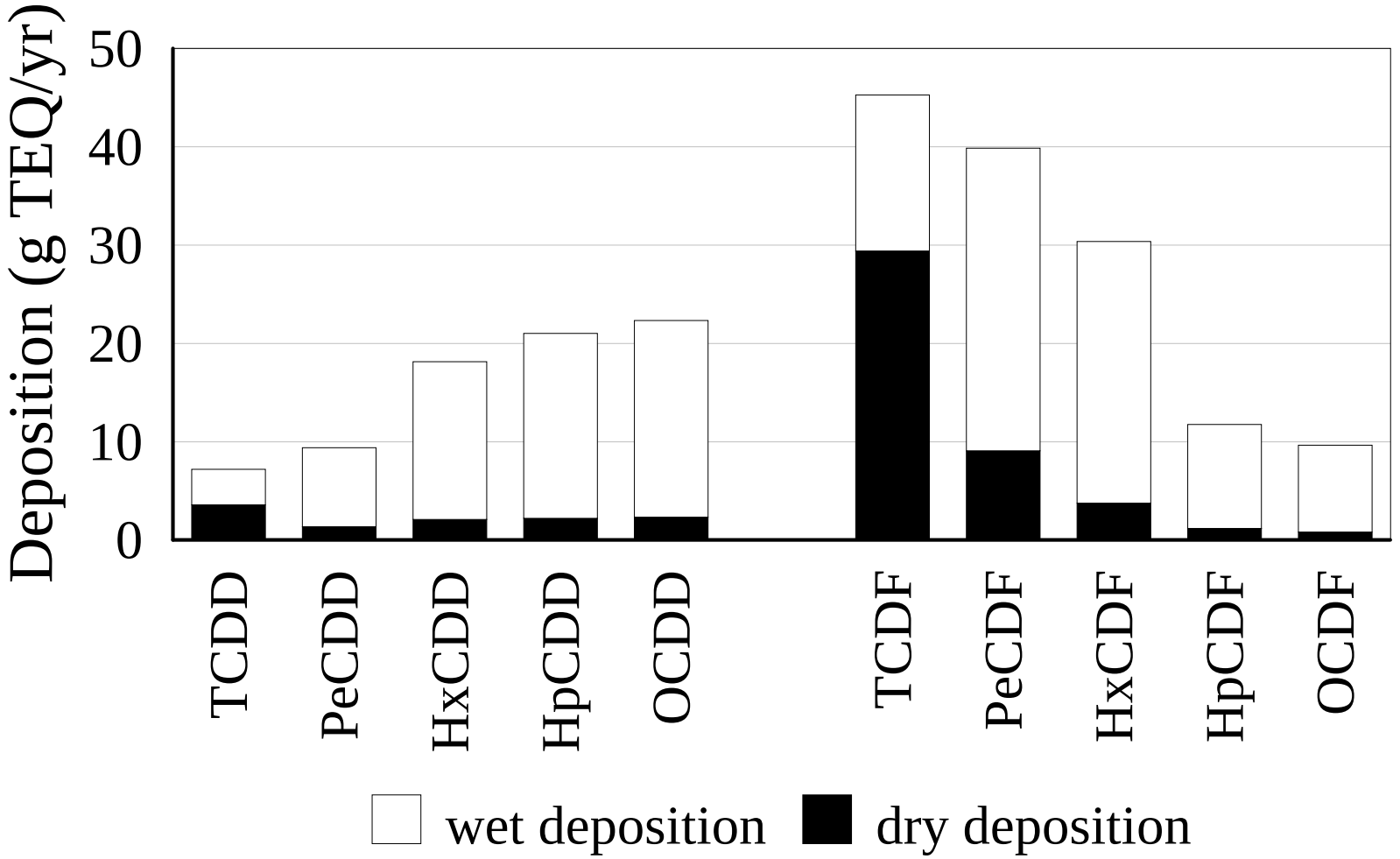

8. Literature Cited in Supplementary Information

Achman, D.R.; Hornbuckle, K.C.; Eisenreich, S.J. *Environ. Sci. Technol.* **1993**, *27*, 75.

Atkinson, R.; Aschmann, S.M.; Arey, J.; Zielinska, B. *Atmos. Environ.* **1989**, *23*, 2679.

Atkinson, R. *Sci. Total Environ.* **1991**, *104*, 17.

Bidleman, T.F. *Environ. Sci. Technol*. **1988**, *22*, 361.

Chang, J.S. In *Acidic Deposition: State of Science and Technology. Volume 1: Emissions, Atmospheric Processes, and Deposition*, Irving, P.M., Ed., U.S. Govt. Printing Office: Washington D.C., 1990, Report 4.

Choudry, G.G.; Webster, G.R.B. *J. Agric. Food Chem.* **1989**, *37*, 254

Cleverly, D.; Monetti, M.; Phillips, L.; Cramer, P.; Heit, M.; McCarthy, S.; O Rourke, K.; Stanley, J.; Winters, D. *Organohalogen Compd.* **1996**, *28*, 77.

Cohen, M.; Commoner, B.; Eisl, H; Bartlett, P.; Dickar, A.; Hill, C.; Quigley, J; Rosenthal, J. *Quantitative Estimation of the Entry of Dioxins, Furans, and Hexachlorobenzene into the Great Lakes from Airborne and Waterborne Sources.* Center for the Biology of Natural Systems, Queens College, Flushing, NY, 1995.

Cohen, M.; Commoner, B.; Eisl, H; Bartlett, P.; Dickar, A.; Hill, C.; Quigley, J; Rosenthal, J. *Organohalogen Compd.* **1997**, 33, 214.

Cohen, M.; Commoner, B; Bartlett, P.W.; Cooney, P.; Eisl, H. *Exposure to Endocrine Disruptors from Long Range Air Transport of Pesticides*. Center for the Biology of Natural Systems, Queens College, Flushing, NY, 1997.

Commoner, B.; Richardson, J.; Cohen, M.; Flack, S.; Bartlett, P.W.; Cooney, P.; Couchot, K.; Eisl, H.; Hill, C. *Dioxin Sources, Air Transport, and Contamination in Dairy Feed Crops and Milk.* Center for the Biology of Natural Systems, Queens College, Flushing, NY, 1998.

Crosby, D.G.; Moilanen, K.W.; Wong, A.S. *Environ. Health Perspect.* **1973**, *Sept*., 259.

Dann, T. Personal communication; and *Ambient Air Measurements of Polycyclic Aromatic Hydrocarbons (PAH), Polychlorinated Dibenzo-p-Dioxins (PCDD) and Polychlorinated Dibenzofurans in Canada (1987-1997).* 1998. Report AAQD 97-3. Environmental Technology Center, Environment Canada, Gloucester, ON.

Draxler, R.R.; G.D. Hess. *Description of the HYSPLIT_4 Modeling System*. NOAA Technical Memorandum # ERL ARL-224. NOAA Air Resources Laboratory, Silver Spring, MD, 1997.

Draxler, R.R.; Hess G.D. *Australian Meteorological Magazine* **1998**, *47*, 295.

Draxler, R.R. *HYSPLIT_4 User s Guide*. NOAA Technical Memorandum # ERL ARL-230. NOAA Air Resources Laboratory, Silver Spring, MD, 1999.

Dulin, D.; Drossman, H.; Mill, T. *Environ. Sci. Technol.* **1986**, *20*, 72.

Dung, M.H.; O Keefe, P.W. *Environ. Sci. Technol.* **1994**, *28*, 549.

Eitzer, B.D.; Hites, R.A. *Chemosphere* **1989** (b), *18*, 593.

Eitzer, B.D.; Hites, R.A. *Environ. Sci. Technol.* **1989** (a), *23*, 1389.

Eitzer, B.D.; Hites, R.A. *Environ. Sci. Technol.* **1989**(c), *23*, 1396.

Georgi, F. *J. Geophys. Res.* **1986**, *91 (D9)*, 9794.

Hicks, B. In *Aerosols: Research, Risk Assessment and Control Strategies, Proceedings of the Second U.S.-Dutch International Symposium, Williamsburg Virginia, May 19-25, 1985*, Lee, S.D. *et al.*, Eds., Lewis Publishers: Chelsea, Michigan, 1986, 973-982.

Hicks, B.B.; Baldocchi, D.D.; Meyers, T.P.; Hosker, R.P.; Matt, D.R. *Water, Air, Soil Pollut.* **1987**, *36*, 311.

Hites, R.A. *Environ. Sci. Technol*. **1998**, *32*, 2804.

Hornbuckle, K.C.; Jeremiason, J.D.; Sweet, C.W.; Eisenreich, S.J. *Environ. Sci. Technol.* **1994**, *28*, 1491.

Junge, C.E. In *Fate of Pollutants in the Air and Water Environments*, Suffet, I.H., Ed., John Wiley & Sons: New York, 1977, 7-22.

Koester, C.; Hites, R. *Environ. Sci. Technol.* **1992 (a)**, *26*, 502.

Koester, C.; Hites, R. *Environ. Sci. Technol.* **1992 (b)**, *26*, 1375.

Kwok, E.S.C.; Atkinson, R.; Arey, J. *Environ. Sci. Technol.* **1995**, *29*, 1591.

Kwok, E.S.C.; Arey, J.; Atkinson, R. *Environ. Sci. Technol.* **1994**, *28*, 528.

Larson, S.E.; Edson, J.B.; Hummelshøj, P,; Jensen, N.O.; de Leeuw, G.; Mestayer, P.G. *Ophelia* **1995**, *42*, 193.

Lee, R.G.M.; Jones, K.C. *Environ. Sci. Technol*. **1999**, *33*, 3596.

Lindberg, S.E. *Atmos. Environ.* **1982**, *16*, 1701.

Mackay, D.; Paterson, S.; Schroeder, W.H. *Environ. Sci. Technol.* **1986**, *20*, 810.

Mackay, D.; Shiu, W.Y.; Ma, K.C. *Illustrated Handbook of Physical-Chemical Properties and Environmental Fate for Organic Chemicals Vol. 1.* Lewis Publishers: Chelsea, MI, 1992.

McCrady, J.K.; Maggard, S.P. *Environ. Sci. Technol.* **1993**, *27*, 343.

McCrady, J.K. *Chemosphere* **1994**, 28(1), 207.

Meylan, W.M.; Howard, P.H. *Chemosphere* **1993**, *26*, 2293.

Meylan, W.M.; Howard, P.H. *AOPWIN: Atmospheric Oxidation Program, v1.82 for Microsoft Windows 3.1.* Syracuse Research Corporation, Syracuse, NY, 1996b.

Meylan, W.M.; Howard, P.H. *User s Guide for AOPWIN: Atmospheric Oxidation Program.* Syracuse Research Corporation, Syracuse, NY, 1996a.

Nestrick, T.J.; Lamparski, L.L.; Townsend, D.I. *Anal. Chem.* **1980,** *52*, 1865.

Peters, K.; Eiden, R. *Atmos. Environ.* **1992**, *26A*, 2555.

Schwarzenbach, R.P.; Gschwend, P.M.; Imboden, D.M. *Environmental Organic Chemistry*, John Wiley and Sons: New York, NY, 1993.

Scire, J.A.; Moore, G.E.; Strimaitis, D. *Development and Testing of Dry Deposition Algorithms*. EPA-454/R-92-017, 1993 (NTIS PB94-183100).

Sivils, L.D.; Kapila, S.; Yan, Q.; Elseewi, A.A. *J. Chromatog., A* **1994**, *688*, 221.

Sivils, L.D.; Kapila, S.; Yan, Q.; Zhang, X.; Elseewi, A.A. *Organohalogen Compd.* **1995**, *24*, 167.

Slinn, W.G.N. *Water, Air, Soil Pollut.* **1977**, *7*, 513.

Slinn, S.A.; Slinn, W.G.N. *Atmos. Environ.* **1980**, *14*, 1013.

Thibodeaux, L.J.; Nadler, K.C.; Valsaraj, K.T.; Reible, D.D. *Atmos. Environ.* **1991**, *25A*, 1649.

Tsai, W.; Cohen, Y.; Sakugawa, H.; Kaplan, I.R. *Environ. Sci. Technol.* **1991**, *25*, 2012.

Tysklind, M.; Lundgren, K.; Rappe, C. *Chemosphere* **1993,** *27*, 535.

USEPA. *Estimating Exposure to Dioxin-Like Compounds. Vol. II: Properties, Sources, Occurrence and Background Exposures.* External Review Draft. EPA/600/6-88-005Cb, Office of Research & Development, Washington D.C., June 1994.

USEPA, *The Inventory of Sources of Dioxin in the United States*. External Review Draft. EPA/600/P-98/002Aa, April 1998, Office of Research & Development, Washington D.C., April, 1998

USEPA. *National Air Quality and Emissions Trends Report, 1996.* EPA 454/R-97-013. Office of Air Quality Planning and Standards, 1988.

USEPA. *Exposure and Human Health Reassessment of 2,3,7,8-TCDD and Related Compounds. Part 1: Estimating Exposure to Dioxin-Like Compounds. Vol. II: Sources of Dioxin-Like Compounds in the United States*. Draft Final Report. EPA/600/P-00/001Bb, Office of Research & Development, Washington D.C., September, 2000.

Van den Berg et al. *Environmental Health Perspectives* **1998**, *106*, 775

Voldner, E.C.; Schroeder, W.H. *Atmos. Environ.* **1989**, *23*, 1949.

Wesely, M. *Atmos. Environ.* **1989**, *23*, 1293.

Whitby, K.T. *Modeling of Atmospheric Aerosol Size Distributions, A Progress Report on EPA Research Grant No. R800971*", Rep. 253, Particle Technology Laboratory, Univ. Of Minnesota, Minneapolis, 1975 (as cited in: Prospero, J.M. *et al.*, *Rev. Geophys. Space Phys.* **1983**, *21*, 1607).

Williams, R.M. *Atmos. Environ.* **1982**, *16*, 1933.

Zufall, M.J.; Bergin, M.H.; Davidson, C.I. *Environ. Sci. Technol.* **1998**, *32*, 584.